Advanced Methods of Structural and Trajectory Analysis for Transport Aircraft

Final Report

Dr. Mark D. Ardema
Principal Investigator

June 15, 1994 - September 30, 1995

Santa Clara University
Santa Clara, CA 95053

NASA Ames Research Center Grant NCC 2-5068

Introduction

This report summarizes work accomplished under NASA Grant NCC2-5068, June 15, 1994 to September 30, 1995, entitled "Advanced Methods of Structural and Trajectory Analysis for Transport Aircraft," The effort was in two areas (1) development of advanced methods of structural weight estimation, and (2) development of advanced methods of trajectory optimization. The majority of the effort was spent in the structural weight area. During the course of the grant, there were slight deviations from the original work statement due to changing priorities of the sponsor. M. Chambers and H.-C. Chou were the graduate student research assistants assigned to the project.

Structural Weight Estimation

Analytically-based weight estimating subroutines for the fuselage and wing structures of transport aircraft were developed and integrated into the ACSYNT vehicle synthesis code. The subroutines were based on previously developed codes for hypersonic aircraft [Refs 1-3].

The methods of analysis used to develop the weight estimating routines are discussed in detail in a NASA TM, attached as an Appendix to this report. The TM also serves as a users manual for running the routines as an integral part of ACSYNT. The methods used and the resulting program will be only briefly reviewed here.

Preliminary weight estimates of aircraft traditionally have been made using empirical methods based on the actual weights of existing aircraft. The fuselage and wing designs of advanced aircraft, however, may be significantly different from those of existing aircraft. This means that an empirically based method of weight estimation may not be valid. On the other hand, finite-element methods of structural analysis, commonly used in aircraft detailed design, are not appropriate for conceptual and preliminary design, because of the large number of specific cases that need to be considered, and the large amount of input necessary for each case.

The body structural weight estimation method developed for ASCYNT is based on a third approach, beam theory structural analysis. This results in a weight estimate that is directly driven by material properties, load conditions, and vehicle size and shape, and is not confined to an existing data base. Since the analysis is done station-by-station along the vehicle longitudinal axis and along the wing structural chords, the distribution of loads and vehicle geometry is accounted for, giving an integrated weight that accounts for local conditions. Because of the beam assumption, the analysis is valid only for high aspect ratio wings and high fineness ratio fuselages.

Although the weight estimating routines are based on previously developed codes, there was substantial modification to the codes. Along the more significant changes were: (1) modeling the fuselage shell as a cylinder with two power-low ends (the previous program had two power low sections back-to-back); (2) changing the wing lift distribution from trapezoidal to elliptical; (3) allowing for linearly varying wing thickness ratio along the span; and (4) allowing

the engines to be mounted on either the fuselage or the wing, or a combination of both. The routines were integrated with ACSYNT and verified with test cases. The code was made more user friendly by streamlining and adding comment statements.

The structural weight routines were used to estimate the fuselage and wing weights of nine existing transport aircraft. This was necessary to assess the validity of the methods and to determine the "nonoptimum" weight. The nonoptimum weight is the portion of the weight not estimated by the structural analysis, such as fasteners, doublers, cutout reinforcement, uniform gage penalties, etc. The results show that the developed weight routines give statistically very good weight estimates.

Trajectory Optimization

In the trajectory area, the main task was to add a trajectory optimization routine to ACSYNT. The optimization is based on the energy-state dynamic model, and can be used to minimize time, fuel, or a weighted combination of the two.

The energy-state approximation has been used successfully many times to obtain guidance laws for a wide variety of aircraft and missions [Refs. 4-8]. In particular, in Ref. 5 this method is used to derive optimal guidance laws for minimizing direct operating costs (DOC) for transport aircraft. The guidance laws were found to be extremely accurate and have been implemented for on-board control of existing airplanes.

The starting point of the analysis is the equations of motion of an aircraft center of mass flying in a vertical plane above a flat, non-rotating earth:

$$\begin{aligned} \dot{h} &= \sin\gamma \\ \dot{v} &= \frac{T\cos\gamma - D - mg\sin\gamma}{m} \\ \dot{\gamma} &= \frac{T\sin\gamma + L - mg\cos\gamma}{mv} \\ \dot{m} &= -CT \end{aligned} \tag{1}$$

where the state variables are altitude, (h), speed (v), flight path angle (γ), and mass (m); the forces are thrust (T), lift (L), and drag (D); α, g and C are the angle of attack, the gravitational acceleration, and the specific fuel consumption, respectively. Next introduce a new state variable, the total mechanical energy per unit weight,

$$E = h + \frac{1}{2g}v^2 \tag{2}$$

Taking the time derivative of this, using eqns. (1), and replacing v by E as a state variable gives

$$\begin{aligned} \dot{E} &= \frac{v}{mg}(T\cos\alpha - D) = P \\ \dot{h} &= v\sin\gamma \\ \dot{\gamma} &= \frac{T\sin\alpha + L - mg\cos\gamma}{mv} \\ \dot{m} &= -CT \end{aligned} \tag{3}$$

where P is called the specific excess power.

The energy-state approximation consists of assuming that both γ and $\dot{\gamma}$ are small, and thus that $\dot{h}$ is small as well (these are very good approximations for transport aircraft flight). Neglecting these terms gives

$$\begin{aligned} \dot{E} &= P \\ \dot{m} &= -CT \\ o &= T\sin\alpha + L - mg \end{aligned} \tag{4}$$

which are the equations of the energy-state approximation.

The quantity to be minimized along the trajectory is a weighted sum of flight time and fuel mass consumed:

$$\phi = K_1 t + K_2 m_f \tag{5}$$

This allows minimum time trajectories to be computed ($K_1 = 1$, $K_2 = 0$), minimum fuel consumption ($K_1 = 0$, $K_2 = 1$), and minimum DOC (by proper weighting of K_1 and K_2). For a given energy gain along the trajectory, the quantity to be minimized is

$$J^1 = \int_{\phi_0}^{\phi_f} d\phi = \int_{t_0}^{t_f} \dot{\phi}\, dt = \int_{E_0}^{E_f} \frac{\dot{\phi}}{P} dE \tag{6}$$

where eqn. (4) was used. It is assumed that $\dot{\phi} >$, $P > 0$ and that E is monotonically increasing. For convenience, the integrand in eqn. (6) is inverted and we maximize

$$J = \int_{E_0}^{E_f} \frac{P}{\dot{\Phi}} dE = \int_{E_0}^{E_f} F dE \tag{7}$$

From eqns. (4), (5), and (7), the function F is:

$$F = \frac{v(T\cos\alpha - D)}{mg(K_1 + K_2 CT)}$$

The optimal trajectory guidance algorithm is then

$$v = \underset{v}{arg\,max}\,[F]_E \tag{9}$$

that is, at each energy level along the flight path, choose the v that maximizes F, subject to any relevant constraints. Once this v has been determined, the integration to the next step is done with eqns. (1) [or equivalently eqns. (3)], with two choices of approximation. One choice is with $\dot{\gamma} = 0$, and the other is with both $\dot{\gamma} = 0$ and $\dot{h} = 0$. The latter choice, corresponding to eqns. (4), is available in case severe jumps are present in the energy-state optimal path, making integration including the $\dot{h}$ term impossible. (The jumps which may occur are an important topic for future investigation.)

The first example of use of the trajectory optimization was the Boeing 747. Figure 1 shows the minimum time climb trajectory for this aircraft. Also shown are lines of constant E and the contours of the function F, illustrating that F is maximized at each value of E. Figure 2 shows the minimum fuel trajectory, and Figure 3 compares the two flight paths. It is seen that the minimum fuel path is somewhat higher than the minimum time path; the minimum DOC path would be between these two. Note that these paths have an acceleration at ground level to about M 0.5, which would not be operationally acceptable. All integrations were done with the $\dot{h}$ term included.

The algorithm was also used to determine optimal climb trajectories of two high speed (supersonic) civil transport designs, designated here as HSCT1 and HSCT 2. Figure 4 shows the minimum time path for HSCT1. Also shown are the contours of F (labeled P_s/B). The maximum dynamic pressure constraint (q max) has been set unrealistically high in order to better illustrate the nature of the path. The trajectory follows the terrain and q max limits, except for a transonic dive and a brief low supersonic jump to lower q. Figure 5 magnifies this behavior in the transonic/low supersonic region. The "trough" in the performance function $F(M, h)$, which causes this behavior, is clearly shown in Figure 6.

Figures 7, 8, and 9 show the same information for HSCT 1 for minimum fuel. As compared with minimum time paths, the minimum fuel paths have more jumps and are at lower q. Figure 9 shows that $F(M,h)$ is very "hilly" in the transonic region for this case, having multiple local maximums. This makes searching for the global maximum very difficult.

The elapsed time and weight of HSCT1 as a function of E are shown in Figures 10 and 11. It is seen that the minimum time path takes less time and has more fuel expenditure than the minimum fuel path, thus validating the calculations. As before, the minimum DOC path would lie between the two and would give intermediate time and weight.

The minimum time and minimum fuel trajectories for HSCT2 are displayed in Figures 12 - 15. The paths tend to follow the q max constraint, except for a transonic climb and dive; the dive is more severe for the minimum fuel path.

In order to execute the trajectory optimization routines in HAVOC, the following variables need to be set:

VIND	set to -2 for climb trajectory optimization
HDOTOP	set to .TRUE.: $\dot{h}$ included in integration .FALSE.: $\dot{h}$ not included in integration
NSTEP	number of search steps at each energy level (currently set to NELGCL, number of energy levels)
WGTFACK1	weighting parameter on fuel weight (also called FMNFUL)
WGTFACK2	weighting parameter on time (also called FMNTIM)

References

1. Ardema, M. D.: Body Weight of Hypersonic Aircraft: Part 1. NASA TM-101028, Oct. 1988.

2. Ardema, M. D.: and Chambers, M. C.: Body Weight of Hypersonic Aircraft: Part 2. NASA TM-102797, Aug. 1990.

3. Ardema, M. D.; Chambers, M.; Terjesen, E.; and Roberts, C.: Body Weight of Advanced Concept Hypersonic Aircraft. NASA TM-103893

4. Bryson, A. E.; Jr., Desai, M. N.; and Hoffman, W. C.: Energy-State Approximation in Performance Optimization of Supersonic Aircraft. *J. Aircraft*, vol. 6, 1969.

5. Lee, H. Q. and Erzberger, H.: Algorithm for Fixed-Range Optimal Trajectories, NASA TP 1565, July 1980.

6. Ardema, M. D.; Bowles, J. V.; and Whittaker, T.: Optimal Trajectories for Hypersonic Launch Vehicles. *Dynamics and Control*, 4, 337-347 (1994).

7. Ardema, M. D.; Bowles, J. V.; Terjesen, E. J.; and Whittaker, T.: Approximate Altitude Transitions for High-Speed Aircraft. AIAA *J. of Guidance, Control, and Dynamics*, Vol. 18, No. 3 (1995).

8. Ardema, M.; Bowles, J.; and Whittaker, T.: Near-Optimal Propulsion System Operation for Air-Breating Launch Vehicles. AIAA-94-3635, Proceedings of AIAA Guidance, Navigation, and Control Conference, Aug. 1-3, 1994, Scottsdale, AZ.

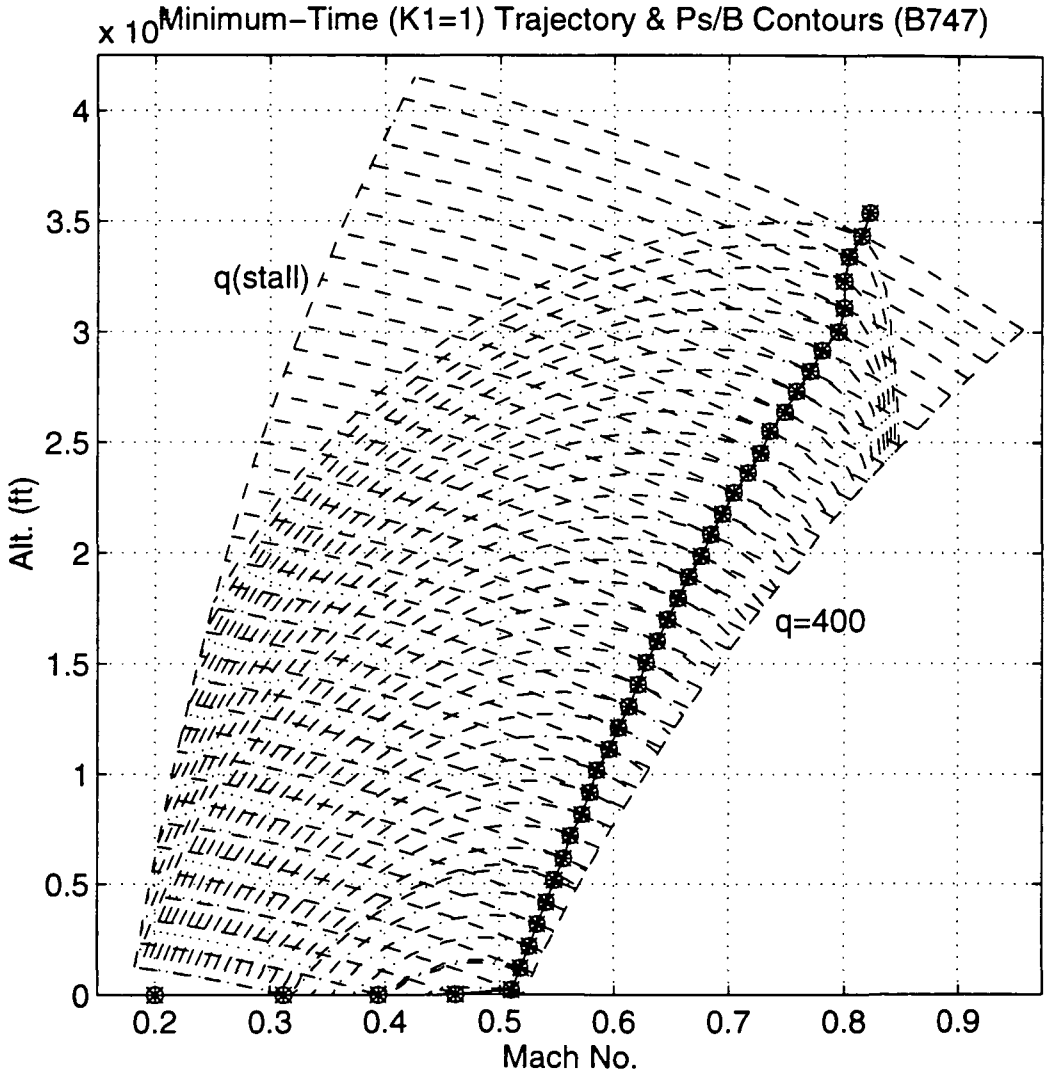

Figure 1. The optimized flight path of B747 in Min. Time.

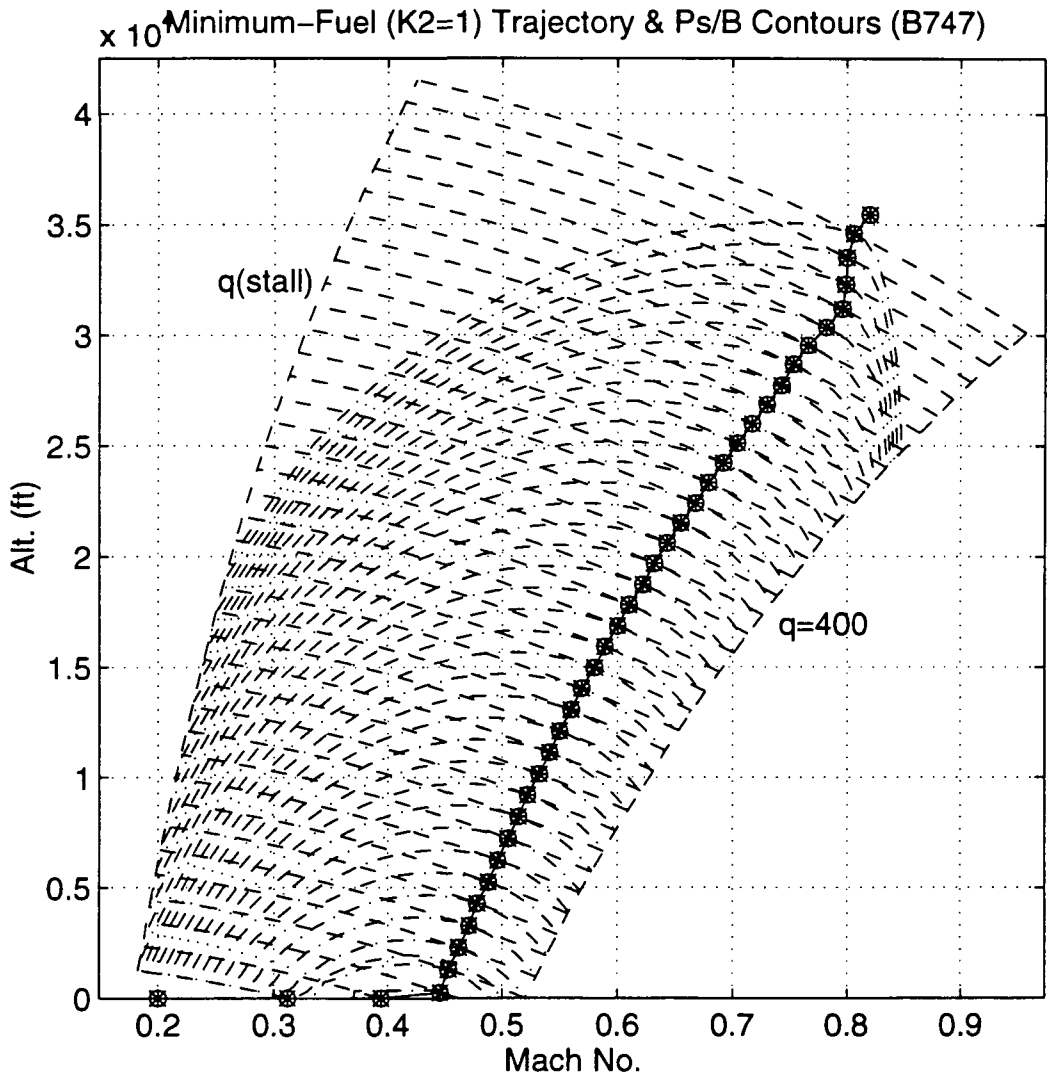

Figure 2. The optimized flight path of B747 in Min. Fuel.

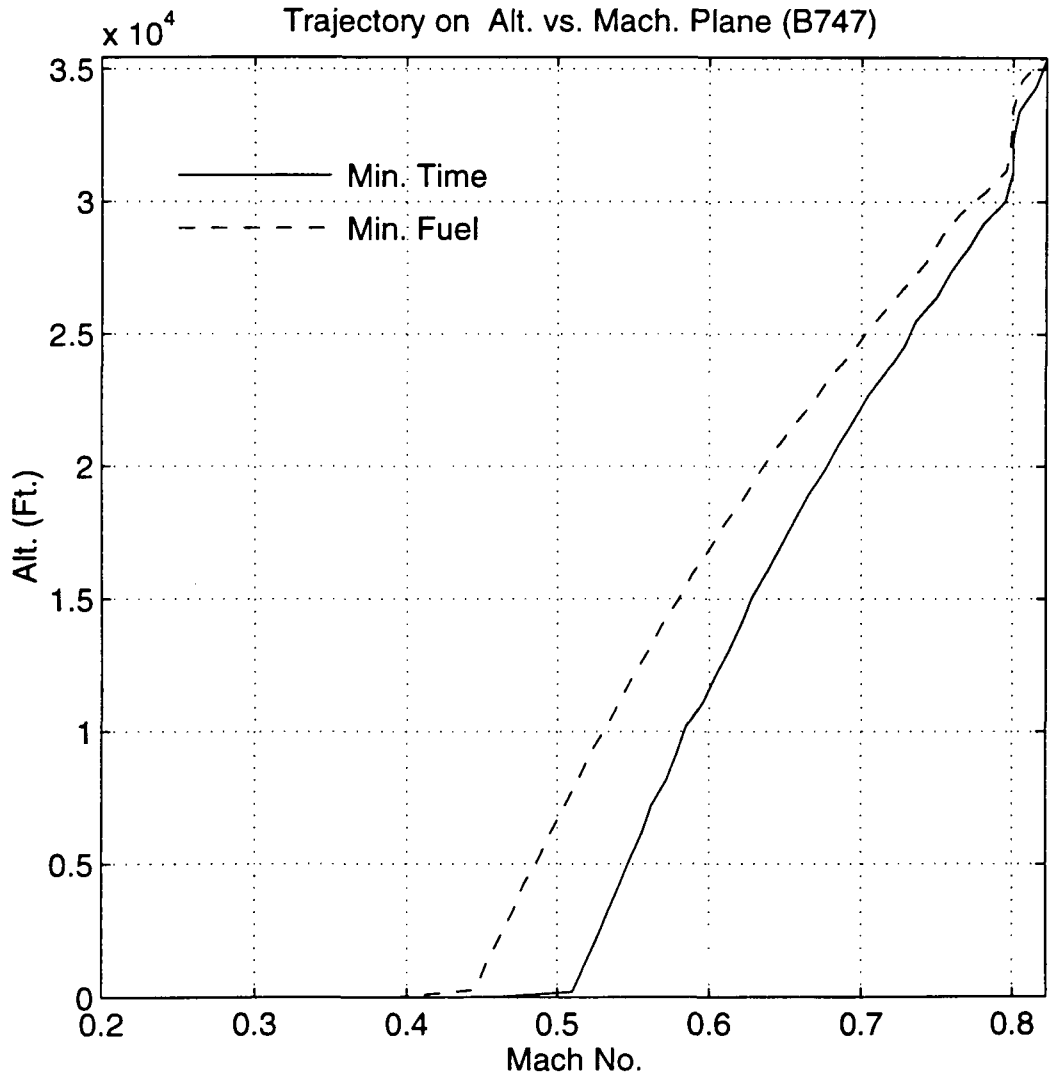

Figure 3. The optimized flight paths of B747.

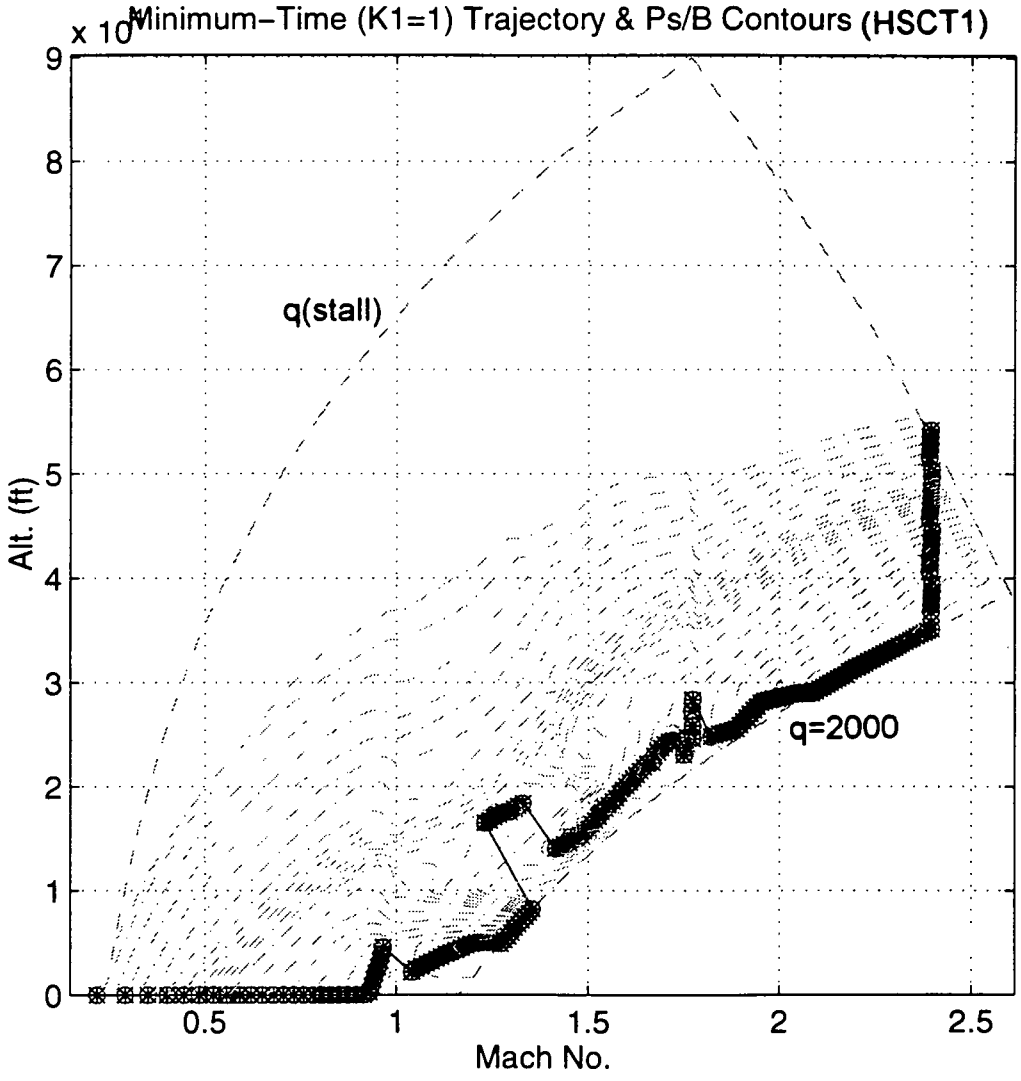

Figure 4. The optimized flight path of HSCT1 in Min. Time.

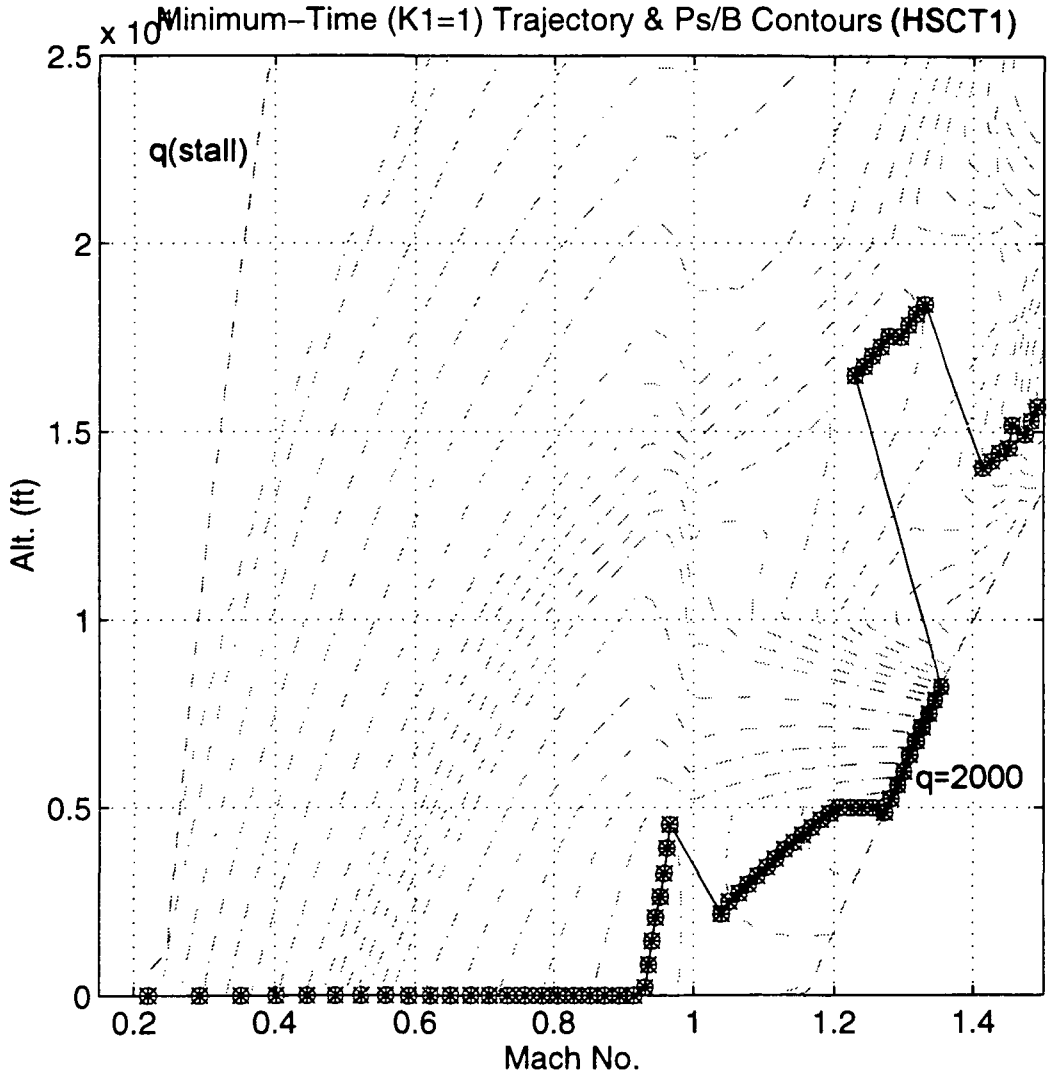

Figure 5. The optimized flight path, in min Time, and cost functional contours of HSCT1 in the transonic region.

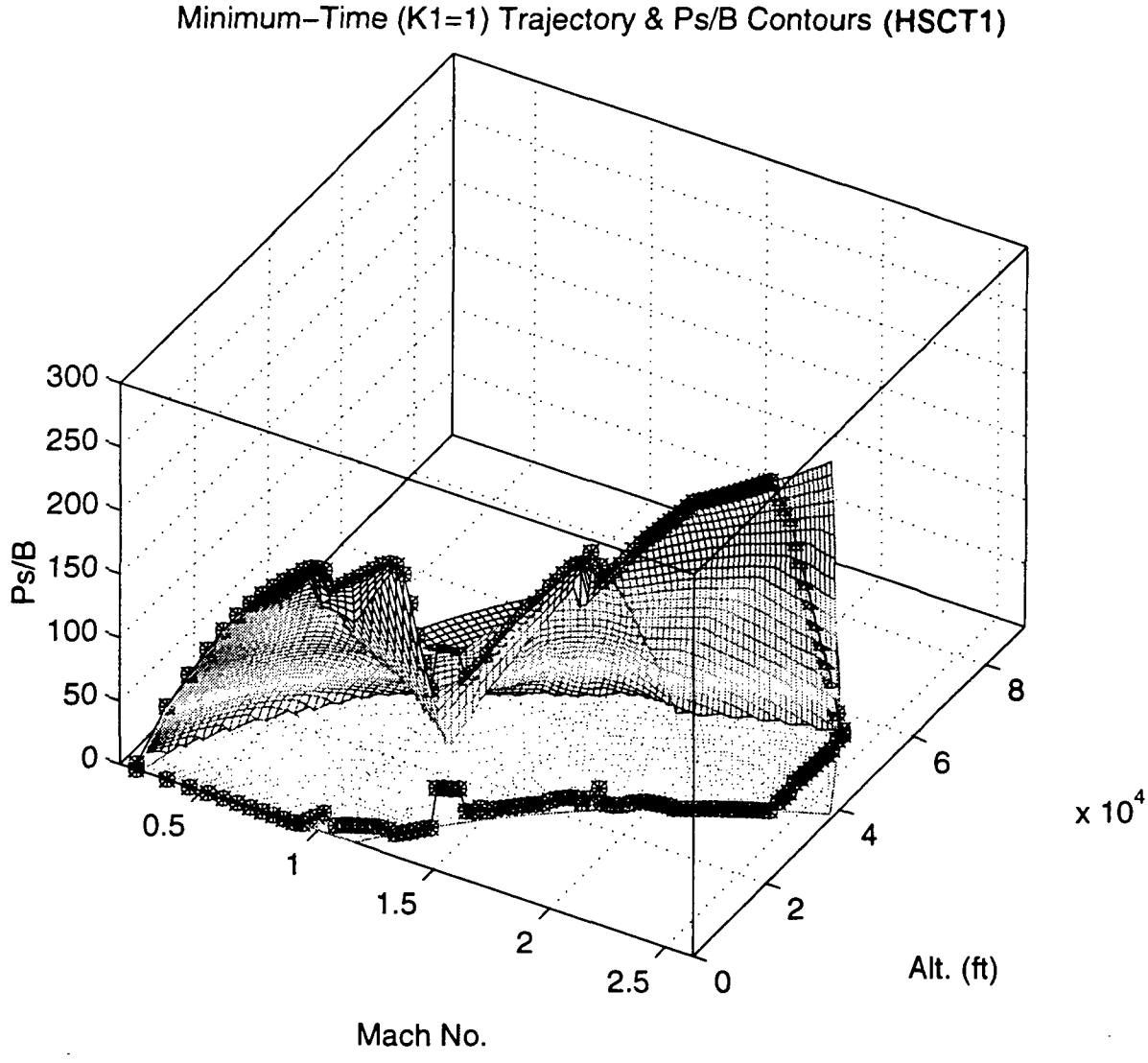

Figure 6. Cost functional mesh and ascent trajectory of HSCT1 in Min. Time.

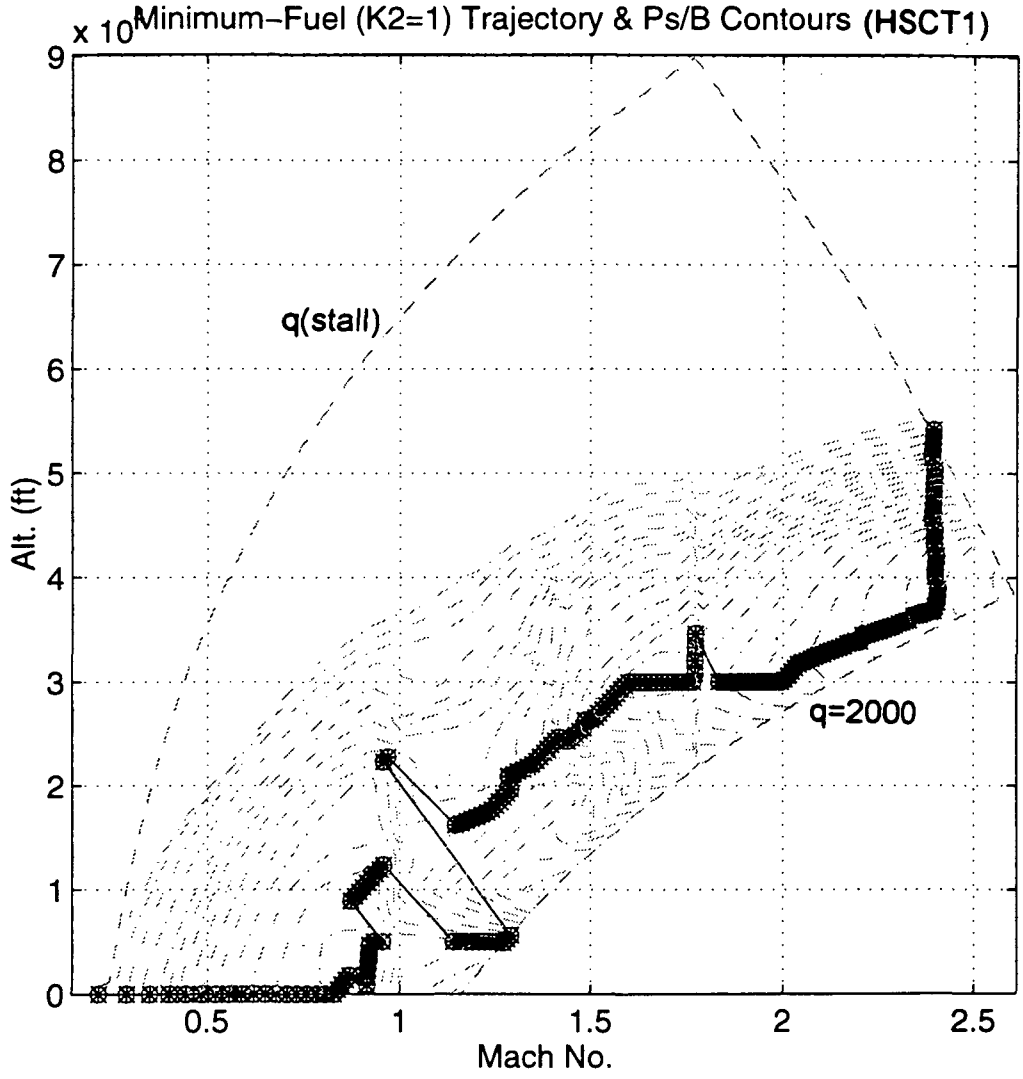

Figure 7. The optimized flight path of HSCT1 in Min. Fuel.

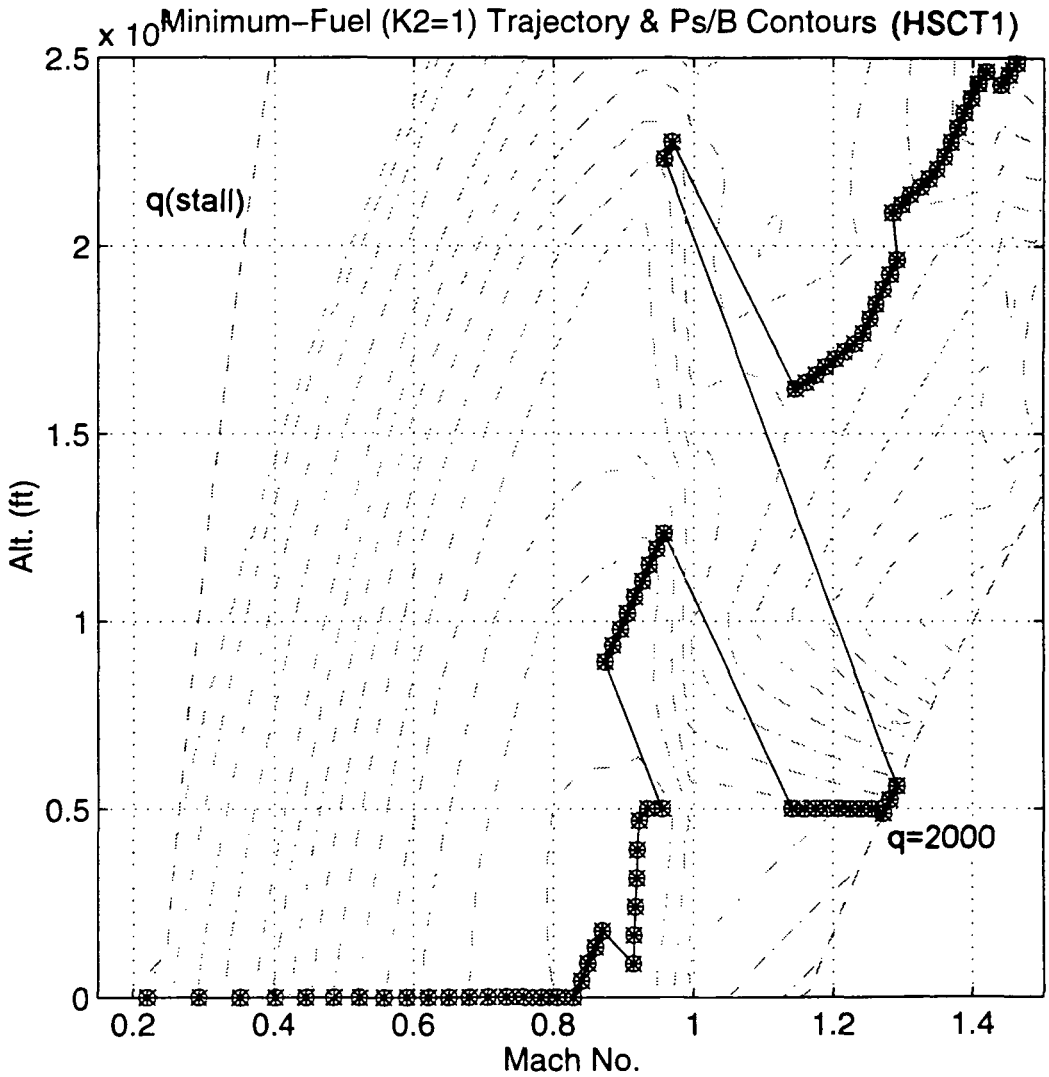

Figure 8. The optimized flight path, in Min. Fuel, and cost functional contours of HSCT1 in the transonic region.

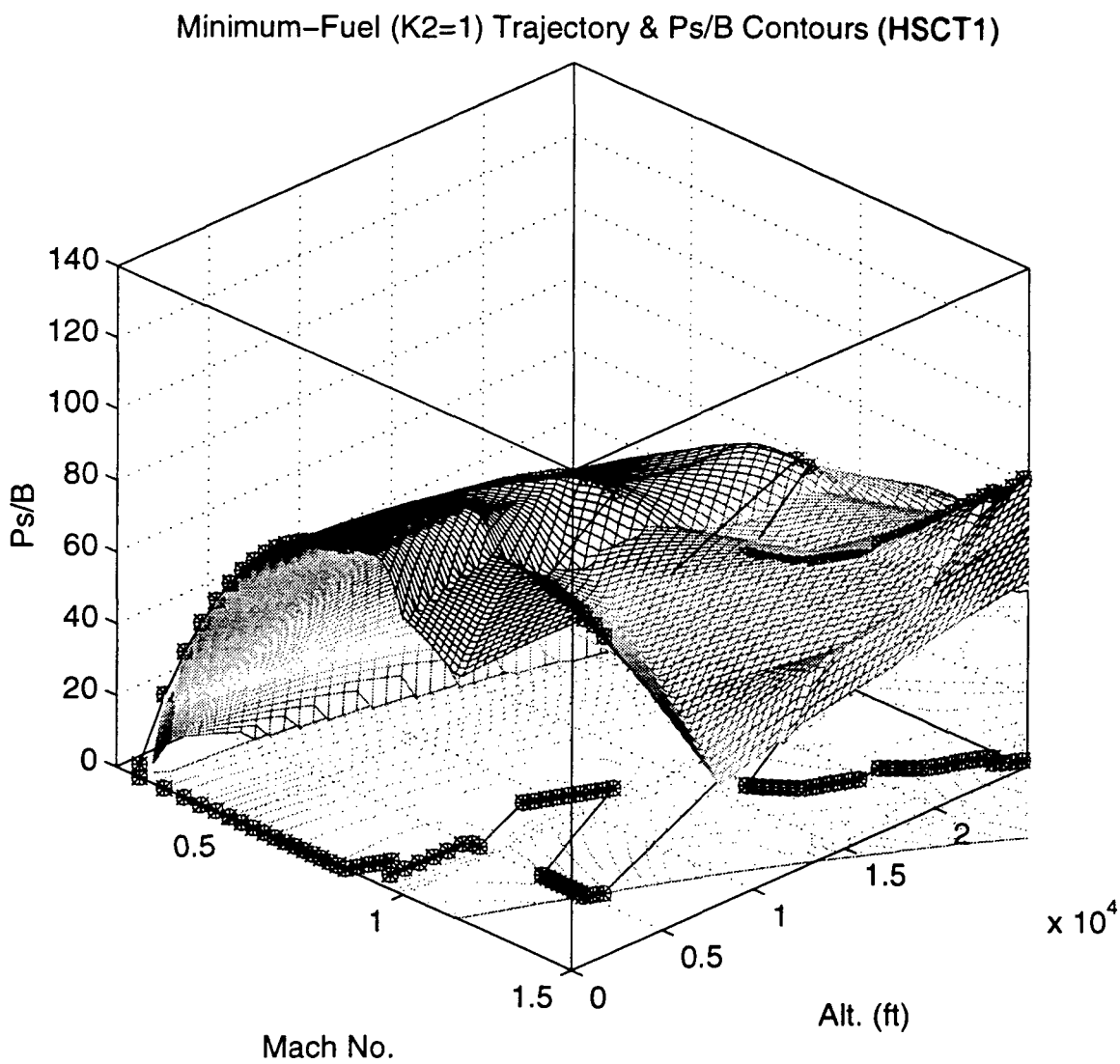

Figure 9. Cost functional mesh and ascent trajectory of HSCT1 in Min. Fuel in the transonic region.

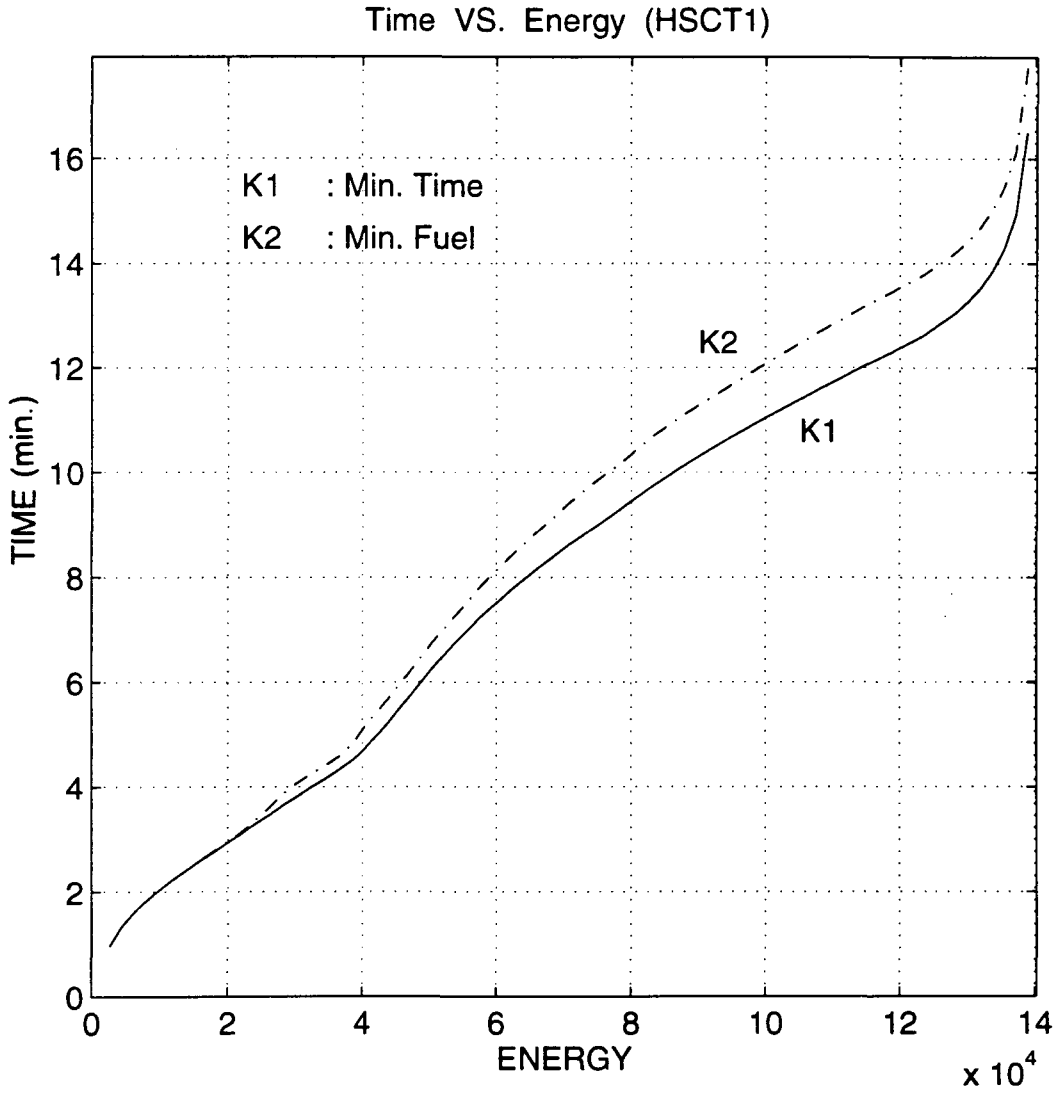

Figure 10. Time consumptions vs. energy level of HSCT1.

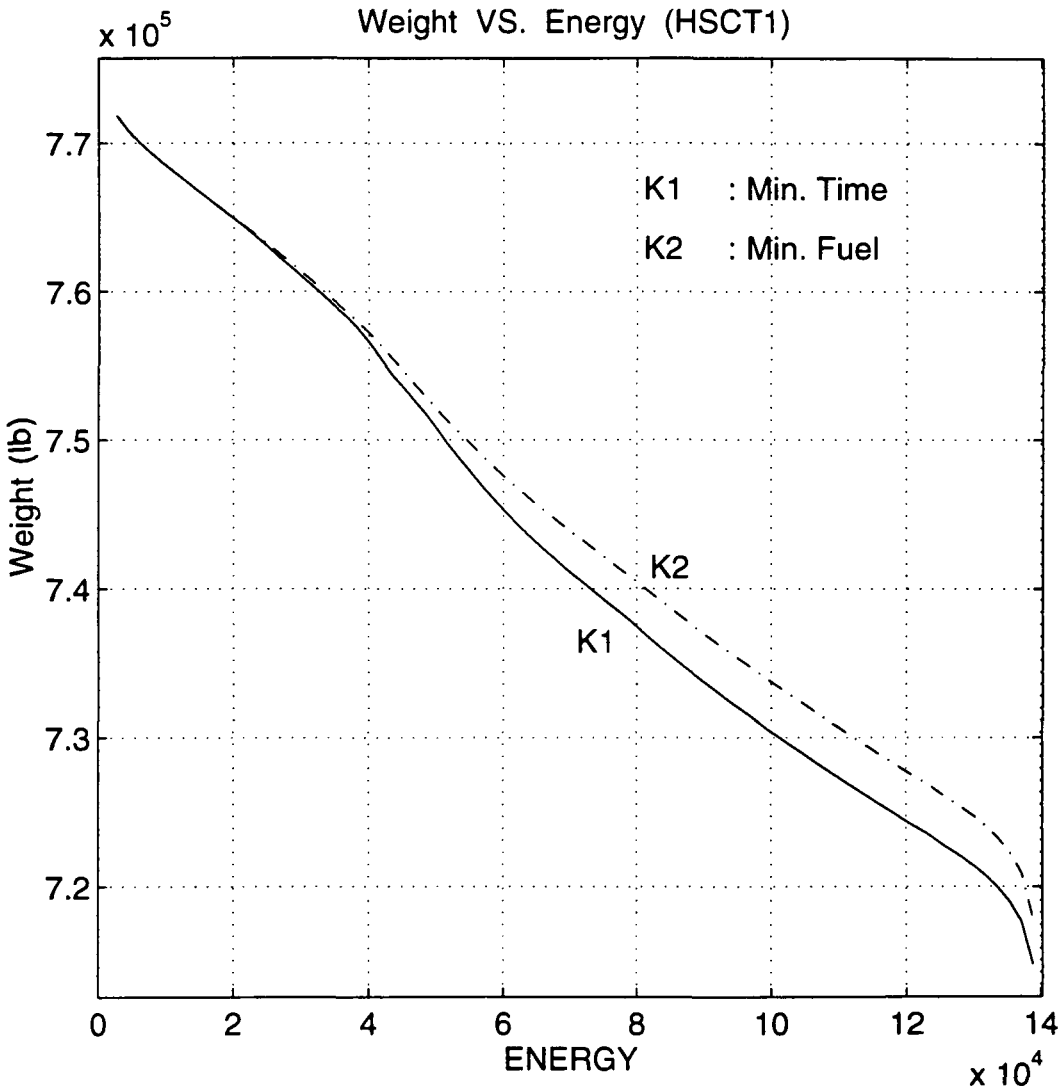

Figure 11. Weight status vs. energy level of HSCT1.

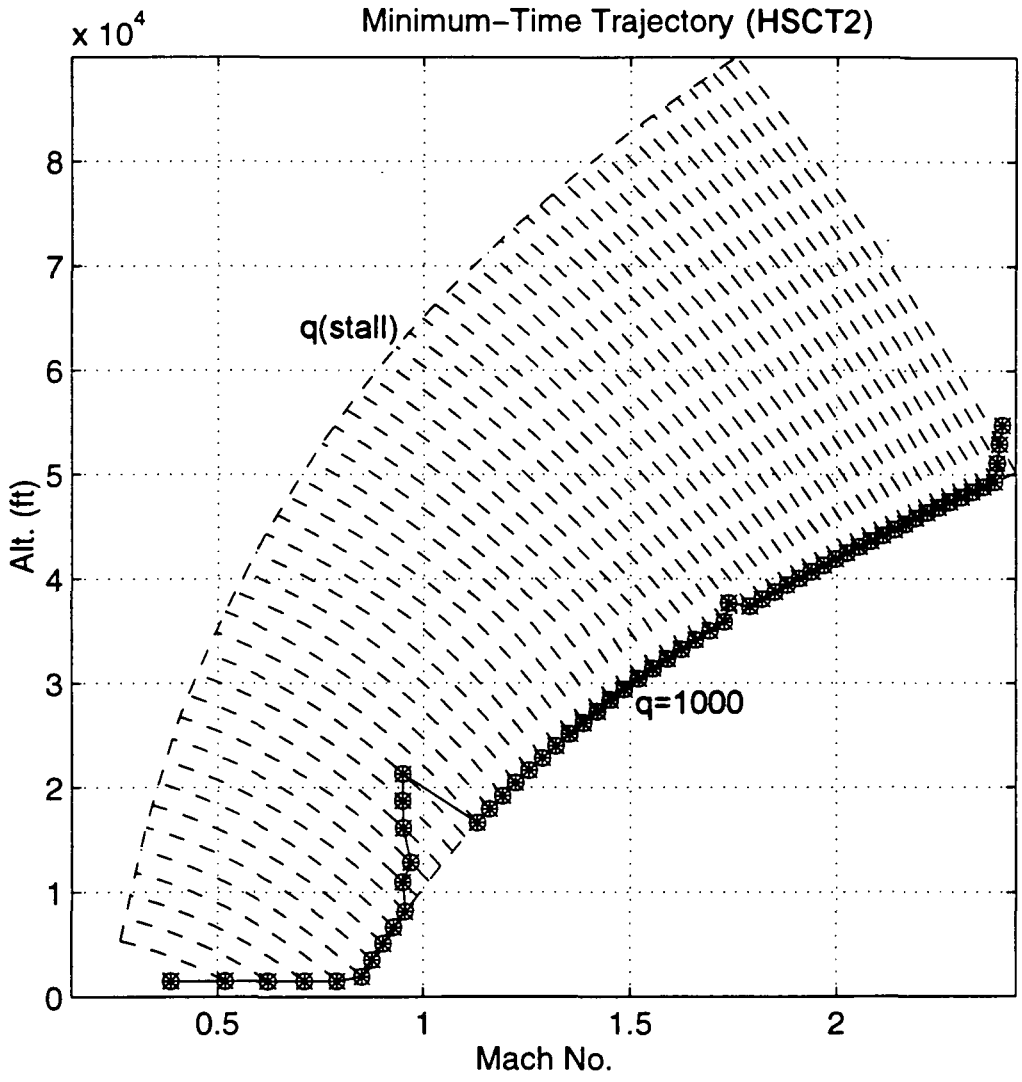

Figure 12. The optimized flight path of HSCT2 in Min. Time.

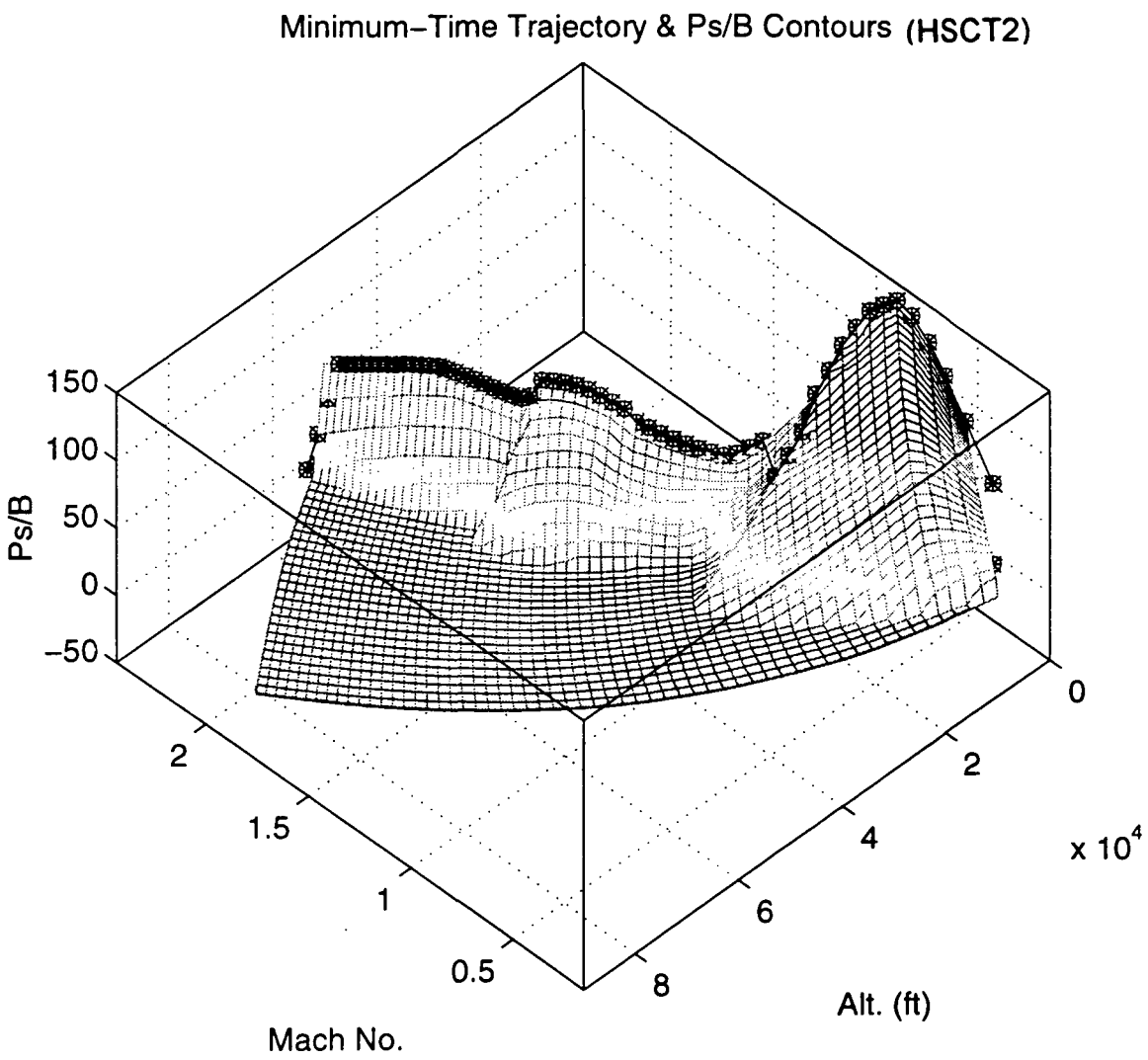

Figure 13. Cost functional mesh and ascent trajectory of HSCT2 in Min. Time.

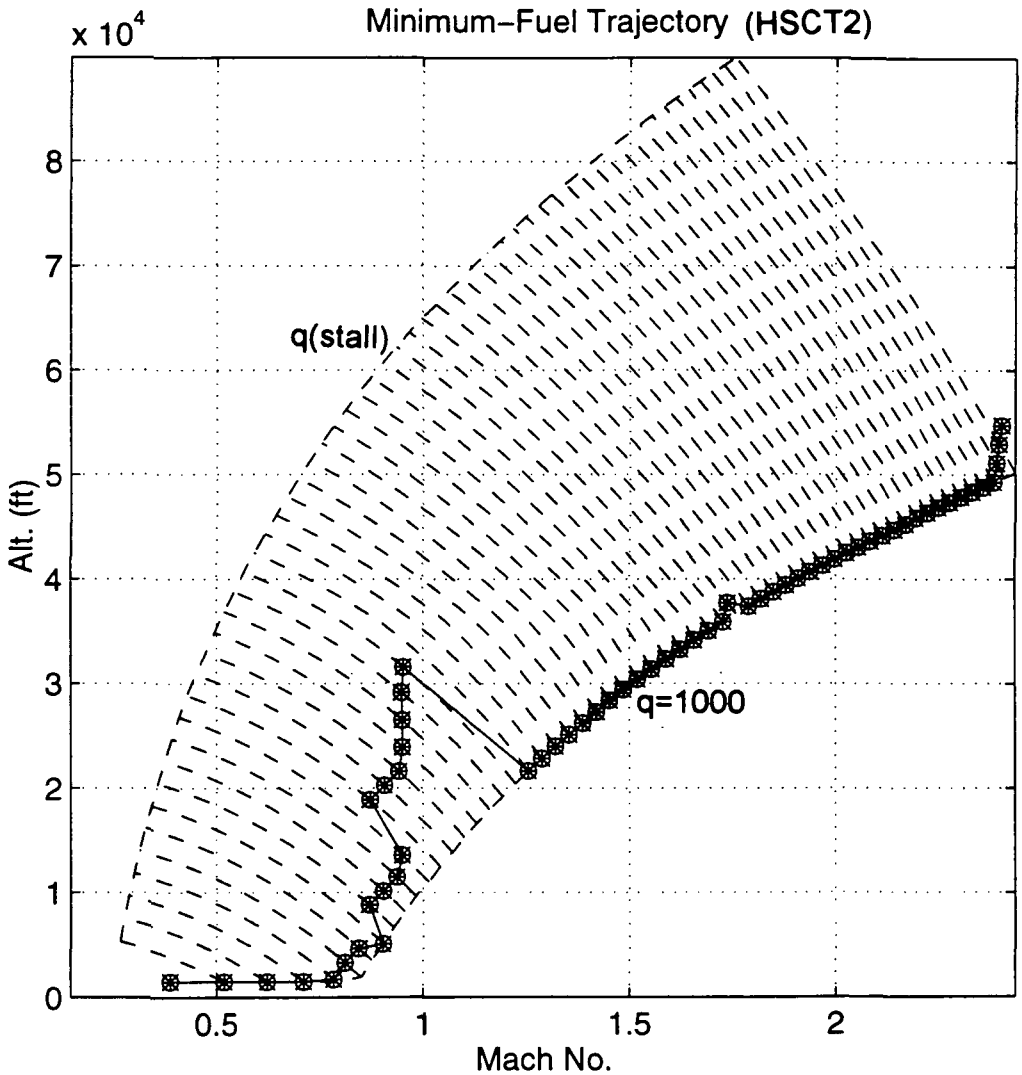

Figure 14. The optimized flight path of HSCT2 in Min. Fuel.

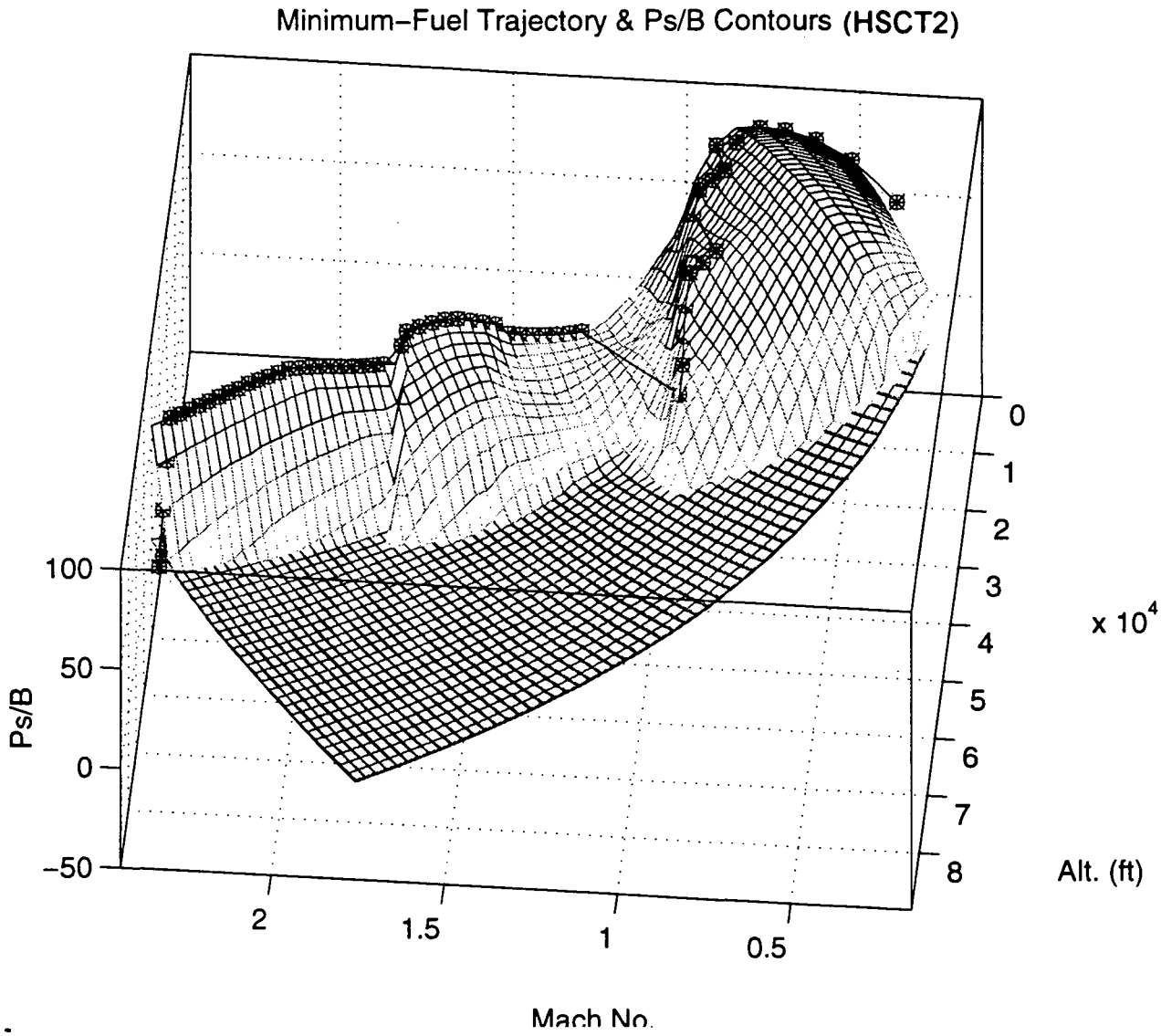

Figure 15. Cost functional mesh and ascent trajectory of HSCT2 in Min. Fuel.

Appendix

Analytical Fuselage and Wing Weight Estimation of Transport Aircraft

draft of proposed NASA TM

Analytical Fuselage and Wing Weight Estimation of Transport Aircraft

Ardema, Chambers, Patron
Santa Clara University

Moore, Hahn, Miura
NASA

October, 1995

SUMMARY

A method of estimating the load-bearing fuselage weight and wing weight of transport aircraft based on fundamental structural principals has been developed. This method of weight estimation represents a compromise between the rapid assessment of component weight using empirical methods based on actual weights of existing aircraft, and detailed, but time-consuming, analysis using the finite element method. The method was applied to nine existing subsonic transports for validation and correlation. Integration of the resulting computer program, PDCYL, has been made into the weights-calculating module of the ACSYNT computer program. ACSYNT has traditionally used only empirical weight estimation methods; PDCYL adds to ACSYNT a rapid, accurate means of assessing the fuselage and wing weights of unconventional aircraft. PDCYL also allows flexibility in the choice of structural concept, as well as a direct means of determining the impact of advanced materials on structural weight.

Using statistical analysis techniques, a relation between the load-bearing fuselage and wing weights calculated by PDCYL and corresponding actual weights was determined. A User's Manual, as well two sample outputs, one for a typical transport and another for an advanced concept vehicle, are given in the Appendices.

NOMENCLATURE

A	fuselage cross-sectional area
A_B	fuselage surface area
A_F	frame cross-sectional area
(AR)	aspect ratio of wing
b	wing span; intercept of regression line
b_s	stiffener spacing
b_S	structural semispan of wing, measured along quarter chord from fuselage
b_w	stiffener depth
C_F	Shanley's constant
C_P	center of pressure
$C_R^{'}$	theoretical root chord of wing
C_R	root chord of wing at fuselage intersection
C_{S_1}	portion of wing leading edge not used for structural box
C_{S_2}	portion of wing trailing edge not used for structural box
C_{SR}	structural root chord of wing
C_{ST}	structural tip chord of wing
C_T	tip chord length of wing
d	frame spacing
d_W	optimum web spacing of wing
D	maximum diameter of fuselage
e	wing buckling exponent
e_C	wing cover material factor
E	Young's modulus of shell material
E_F	Young's modulus of frame material
F_{cy}	compressive yield strength
F_{tu}	ultimate tensile strength
F_S	shear stress
h	thickness of sandwich shell
h_{e_i}	step function for i^{th} engine on wing

h_{lg_i} step function for i[th] landing gear on wing

I_F frame cross-section moment of inertia

I_y moment of inertia about y-axis

I_y' $I_y / \bar{t}_s$

K_{FI} frame stiffness coefficient, I_F / A_F^2

K_{mg} shell minimum gage factor

K_p shell geometry factor for hoop stress

K_S constant for shear stress in wing

K_{th} sandwich thickness parameter

l_B fuselage length

l_{LE} length from leading edge to structural box at theoretical root chord

l_{TE} length from trailing edge to structural box at theoretical root chord

l_{NG} length from nose to nose gear

l_{MG} length from nose to fuselage mounted main gear

l_1 nose length of fuselage

l_2 tail length of fuselage

l_π distance to breakpoint of fuselage

L lift

L_T maximum vertical tail lift

M longitudinal bending moment; wing longitudinal bending moment

m buckling equation exponent; slope of regression line

n normal load factor

N_{x_A} axial stress resultant

N_{x_B} bending stress resultant

N_{x_P} pressure stress resultant

N_x^+ tensile axial stress resultant

N_x^- compressive axial stress resultant

N_y hoop direction stress resultant

n_x longitudinal acceleration

P perimeter

P_g internal gage pressure

P_s perimeter of shell

P_w perimeter of walls

P_1 exponent of power law of nose of fuselage

P_2 exponent of power law of tail of fuselage

r radius of fuselage

$r(y)$ total wing chord as a function of position along quarter chord

$r_s(y)$ structural wing chord as a function of position along quarter chord

R correlation coefficient used for regression

R_{fin} fineness ratio

R_{HT} ratio of horizontal tail station to fuselage length

R_{LE} ratio of leading edge station of wing to fuselage length

R_{P_1} ratio of length to leading edge of fuselage propulsion to fuselage length

R_{P_2} ratio of length to trailing edge of fuselage propulsion to fuselage length

R_{NG} ratio of length to nose gear to fuselage length

R_{MG} ratio of length to fuselage mounted main gear to fuselage length

$R_t(y)$ thickness ratio of wing, linearly interpolated between root and tip thickness ratios

R_{TAP} taper ratio of wing

S_B plan area of the fuselage

S_{LG} stroke of landing gear

S_P plan area of wing

$t(y)$ thickness of wing box as a function of position along quarter chord

t_c core thickness

t_f face sheet thickness

t_s skin thickness

t_g material gage thickness, $\bar{t}_S/K_{mg}$

t_w stiffener thickness

t_{mg} material minimum gage thickness

$\bar{t}$ total equivalent isotropic thickness of shell and frames

$\bar{t}_B$ total equivalent isotropic thickness of fuselage structure

$\bar{t}_F$ smeared equivalent isotropic thickness of frames

$\bar{t}_S$	equivalent isotropic thickness of shell
$\bar{t}_{S_B}$	shell thickness required to preclude buckling failure
$\bar{t}_{S_C}$	shell thickness to preclude compressive failure
$\bar{t}_{S_G}$	shell thickness required to meet minimum gage constraint
$\bar{t}_{S_T}$	shell thickness required to preclude tensile failure
$\bar{t}_T$	smeared tension tie thickness
$\bar{t}_w$	smeared wall thickness
$\bar{t}_{w_G}$	thickness of wall to meet minimum gage constraint
$\bar{t}_{w_T}$	thickness of wall required to prevent tensile failure
T	torque on wing carrythrough structure
V_B	fuselage volume
V_W	volume of wing structural box, including structure
V_1	volume of fuselage nose
V_2	volume of fuselage tail
w_C	width of carrythrough structure of wing (usually same as D)
W	body structural weight
W'	weight of wing per unit span
W_I	ideal fuselage structural weight
W_{FT}	fuel weight
W_{NO}	weight of nonoptimum material
W_S	vehicle longitudinal weight distribution
W_{TO}	gross takeoff weight
W/S	shell structural weight per unit surface area
x	longitudinal fuselage coordinate
x_{ealc}	weight calculated by PDCYL
x_{HT}	distance from nose to theoretical quarter chord of horizontal tail
x_{LE}	distance from nose to leading edge of wing
x_{P_1}	distance from nose to leading edge of fuselage mounted propulsion
x_{P_1}	distance from nose to trailing edge of fuselage mounted propulsion
y	transverse fuselage coordinate; wing coordinate measured along 1/4 chord

y_{act}	actual weight
y_{est}	estimated weight after regression
z	vertical body coordinate
$Z(y)$	total width of wing box as a function of position along quarter chord
$Z_S(y)$	width of wing box structure as a function of position along quarter chord
δ	frame deflection
ε	shell buckling efficiency
ε_C	wing cover structural efficiency
ε_W	wing web structural efficiency
Λ	wing sweep
ρ	shell structural material density; wing structural material density
ρ_B	gross fuselage density
ρ_F	frame structural material density
μ	wing loading
σ_S	allowable shear stress for wing
Σ	sum over fuselage or wing length; solidity of wing
ψ	truss core angle

INTRODUCTION

A methodology based on fundamental structural principles has been developed to estimate the load-carrying weight of the fuselage and basic box weight of the wing for aircraft, and has been incorporated into the AirCraft SYNThesis Program (ACSYNT). This weight routine is also available to run independently of ACSYNT, and is a modification of a collection of previously developed structural programs (References 1-4). The main subroutine called by ACSYNT is PDCYL. This study has concentrated on modern transport aircraft because of the detailed weight information available, allowing the weights output from PDCYL to be compared to actual structural weights. The detailed weight statements also allow *non-optimum* factors to be computed which, when multiplied by the load-bearing structural weights calculated by PDCYL, will give good representative total structure weight estimates. These *non-optimum* factors will be computed through a regression analysis of a group of nine transport aircraft.

PDCYL is able to model both skin-stringer-frame and composite sandwich shell fuselage and wing box constructions. Numerous modifications were made to PDCYL and its associated collection of subroutines. These modifications include the addition of detailed fuselage shell geometry calculations; optional integration of a cylindrical fuselage midsection between the nose and tail sections; addition of landing and bump maneuvers to the load cases sizing the fuselage; ability to introduce an elliptical spanwise lift load distribution on the wing; variation of wing thickness ratio from tip to root; ability to place landing gear on the wing to relieve spanwise bending loads; distribution of propulsion system components between wing and fuselage; and the determination of maximum wingtip deflection.

Brief description of ACSYNT

The Aircraft Synthesis Computer program, ACSYNT, is an integrated design tool used in the modeling of advanced aircraft for conceptual design studies. ACSYNT development began at NASA-Ames Research Center in the 1970's and continues to this day. The ACSYNT program is quite flexible and can model a wide range of aircraft configurations and sizes, from remotely piloted high altitude craft to the largest transport.

The ACSYNT program uses the following modules, not necessarily in this order: Geometry, Trajectory, Aerodynamics, Propulsion, Stability, Weights, Cost, Advanced Aerodynamic Methods, and Take-off. An ACSYNT run would normally progress as follows: the Geometry module is called to define the aircraft shape and configuration; the Trajectory module then runs the vehicle through a specified mission; finally the Weight and Cost modules are executed. To determine the performance of the vehicle at each mission point, the Trajectory module will call the Aerodynamics and Propulsion modules.

After the mission is completed, the calculated weight of the aircraft may be compared with the initial estimate and an iteration scheme run to converge upon the

appropriate aircraft weight. This process is necessarily iterative as the aircraft weight ACSYNT calculates is dependent upon the initial weight estimate.

ACSYNT is able to perform a *sensitivity analysis* on any design variable, such as aspect ratio, thickness-to-chord ratio, fuselage length or maximum fuselage diameter. Sensitivity is defined as (change in objective function/value of objective function) divided by (change in design variable/design variable). As an example, if gross weight is the objective function and decreases when the wing thickness-to-chord ratio increases, then the sensitivity of thickness-to-chord ratio is negative. It is important to note that while this increase in thickness-to-chord ratio lowers the gross weight of the aircraft, it may also have a detrimental effect on aircraft performance, possibly violating performance constraints.

ACSYNT is also able to size multiple design variables by optimizing the *objective* function, subject to some preset limits or *constraints*. Objective functions such as gross weight, performance, or fuel weight, may be maximized or minimized subject to some upper or lower bounds. During the optimization process, lower and upper bounds may also be imposed on the design variables.

Three Methods of Weight Estimation

Two methods are commonly available to estimate both the load-bearing fuselage weight and wing box structure weight of aircraft. These methods, in increasing order of complexity and accuracy, are empirical regression and detailed finite element structural analysis. Each method has particular advantages and limitations which will be briefly discussed in the following sections. There is an additional method based on classical plate theory (CPT) which may be used to estimate the weight of the wing box structure.

Empirical

The empirical approach is the simplest weight estimation tool. It requires knowledge of fuselage and wing weights from a number of similar existing aircraft in addition to various key configuration parameters of these aircraft in order to produce a linear regression. This regression is a function of the configuration parameters of the existing aircraft and is then scaled to give an estimate of fuselage and wing weights for an aircraft under investigation. Obviously, the accuracy of this method is dependent upon the quality and quantity of data available for existing aircraft. Also, the accuracy of the estimation will depend on how closely the existing aircraft match the configuration and weight of the aircraft under investigation. All of the empirical regression functions currently in the ACSYNT program give total fuselage weight and total wing weight.

Finite Element

Finite element analysis is the matrix method of solution of a discretized model of a structure. This structure, such as an aircraft fuselage or wing, is modeled as a system of elements connected to adjacent elements at nodal points. An element is a discrete (or finite) structure that has a certain geometric makeup and set of physical characteristics. A nodal force acts at each nodal point, which is capable of displacement. A set of

mathematical equations may be written for each element relating its nodal displacements to the corresponding nodal forces. For skeletal structures, such as those composed of rods or beams, the determination of element sizing and corresponding nodal positioning is relatively straightforward. Placement of nodal points on these simple structures would naturally fall on positions of concentrated external force application or joints, where discontinuities in local displacement occur.

Continuum structures, such as an aircraft fuselage or wing, which would use some combination of solid, flat plate, or shell elements, are not as easily discretizable. An approximate mesh of elements must be made to model these structures. In effect, an idealized model of the structure is made , where the element selection and sizing is tailored to local loading and stress conditions.

The assembly of elements representing the entire structure is a large set of simultaneous equations that, when combined with the loading condition and physical constraints, can be solved to find the unknown nodal forces and displacements. The nodal forces and displacements are then substituted back into the each element to produce stress and strain distributions for the entire structural model.

Classical Plate Theory

CPT has been applied to wing structure design and weight estimation for the past 20 years. Using CPT a mathematical model of the wing based on an equivalent plate representation is combined with global Ritz analysis techniques to study the structural response of the wing. An equivalent plate model does not require detailed structural design data as required for finite element analysis model generation and has been shown to be a reliable model for low aspect ratio fighter wings. Generally, CPT will overestimate the stiffness of more flexible, higher aspect ratio wings, such as those employed on modern transport aircraft. Recently, transverse shear deformation has been included in equivalent plate models to account for this added flexibility. This new technique has been shown to give good representations of tip deflection and natural frequencies of higher aspect ratio wings. No fuselage weight estimation technique which corresponds to the equivalent plate model for wing structures is available.

Need for better, intermediate method

Preliminary weight estimates of aircraft are traditionally made using empirical methods based on the weights of existing aircraft, as has been described. These methods, however, are undesirable for studies of unconventional aircraft concepts for two reasons. First, since the weight estimating formulas are based on existing aircraft, their application to unconventional configurations (i.e., canard aircraft or area ruled bodies) is suspect. Secondly, they provide no straightforward method to assess the impact of advanced technologies and materials (i.e., bonded construction and advanced composite laminates).

On the other hand, finite-element based methods of structural analysis, commonly used in aircraft detailed design, are not appropriate for conceptual and preliminary design, as the idealized structural model must be built off-line. The solution of even a

moderately complex model is also computationally intensive and will become a bottleneck in the vehicle synthesis. Two approaches which may simplify finite-element structural analysis also have drawbacks. The first is to create detailed analyses at a few critical locations on the fuselage and wing, then extrapolate the results to the entire aircraft, but this can be misleading because of the great variety of structural, load, and geometric characteristics in a typical design. The second method is to create an extremely coarse model of the aircraft, but this scheme may miss key loading and stress concentrations in addition to suffering from the problems associated with a number of detailed analyses.

The fuselage and wing structural weight estimation method employed in PDCYL is based on a third approach, beam theory structural analysis. This results in a weight estimate that is directly driven by material properties, load conditions, and vehicle size and shape, and is not confined to an existing data base. Since the analysis is done station-by-station along the vehicle longitudinal axis, and along the wing structural chord, the distribution of loads and vehicle geometry is accounted for, giving an integrated weight that accounts for local conditions. An analysis based solely on fundamental principles will give an accurate estimate of structural weight only. Weights for fuselage and wing secondary structure, including control surfaces and leading and trailing edges, and some items from the primary structure, such as doublers, cutouts, and fasteners, must be estimated from examination of existing aircraft.

The equivalent plate representation, which is unable to model the fuselage structure, is not used in PDCYL.

METHODS

Overview

Since it is necessary in systems analysis studies to be able to rapidly evaluate a large number of specific designs, the methods employed in PDCYL are based on idealized vehicle models and simplified structural analysis. The analyses of the fuselage and wing structures are performed in different routines within PDCYL, and, as such, will be discussed separately. The PDCYL weight analysis program is initiated at the point where ACSYNT performs its fuselage weight calculation. PDCYL first performs a basic geometrical sizing of the aircraft in which the overall dimensions of the aircraft are determined and the propulsion system, landing gear, wing and lifting surfaces are placed.

Fuselage

The detailed fuselage analysis starts with a calculation of vehicle loads on a station-by-station basis; Three types of loads are considered – longitudinal acceleration (applicable to high-thrust propulsion systems), tank or internal cabin pressure, and longitudinal bending moment. All of these loads occur simultaneously representing a critical loading condition. For longitudinal acceleration, longitudinal stress resultants caused by acceleration are computed as a function of longitudinal fuselage station; these stress resultants are compressive ahead of the propulsion system and tensile behind the propulsion system. For pressure loads, the longitudinal distribution of longitudinal and circumferential (hoop) stress resultants is computed for a given shell gage pressure (generally 12 psig). There is an option to either use the pressure loads to reduce the compressive loads from other sources or not to do this; in either case, the pressure loads are added to the other tensile loads.

Longitudinal bending moment distributions from three load cases are examined for the fuselage. Loads on the fuselage are computed for a quasi-static pull-up maneuver, a landing maneuver, and travel over runway bumps. These three load cases occur at user-specified fractions of gross take-off weight. For pitch control there is an option to use either elevators mounted on the horizontal tail (the conventional configuration) or elevons mounted on the trailing edges of the wing. The envelope of maximum bending moments is computed for all three load cases and is then used to determine the net stress resultants at each fuselage station.

After the net stress resultants are determined at each fuselage station, a search is conducted at each station to determine the amount of structural material required to preclude failure in the most critical condition at the most critical point on the shell circumference. This critical point is assumed to be the outermost fiber at each station. Failure modes considered are tensile yield, compressive yield, local buckling, and gross buckling of the entire structure. A minimum gage restriction is also imposed as a final criteria. It is assumed that the material near the neutral fiber of the fuselage (with respect to longitudinal bending loads) is sufficient to resist the shear and torsion loads transmitted through the fuselage. For the shear loads this is a good approximation as the fibers

farthest from the neutral axis will carry no shear; also, for beams with large fineness ratios (fuselage length/maximum diameter) bending becomes the predominant failure mode.

The maximum stress failure theory is used for predicting yield failures. Buckling calculations assume stiffened shells behave as wide columns and sandwich shells behave as cylinders. The frames required for the stiffened shells are sized by the Shanley criterion. This criterion is based on the premise that, to a first-order approximation, the frames act as elastic supports for the wide column.

There are a variety of structural geometries available for the fuselage. There is a simply-stiffened shell concept using longitudinal frames. There are three concepts with Z-stiffened shells and longitudinal frames; one with structural material proportioned to give minimum weight in buckling, one with buckling efficiency compromised to give lighter weight in minimum gage, and one a buckling-pressure compromise. Similarly, there are three truss-core sandwich designs, two for minimal weight in buckling with and without frames, and one a buckling-minimum gage compromise.

It is assumed that the structural materials exhibit elasto-plastic behavior. Further, to account for the effects of creep, fatigue, stress-corrosion, thermal cycling and thermal stresses, options are available to scale the material properties of strength and Young's modulus of elasticity. In the numerical results of this study, all materials were considered elastic and the full room-temperature material properties were used.

Composite materials can be modeled with PDCYL by assuming them to consist of orthotropic lamina formed into quasi-isotropic (two-dimensionally, or planar, isotropic) laminates. Each of the lamina is assumed to be composed of filaments placed unidirectionally in a matrix material. Such a laminate has been found to give very nearly minimum weight for typical aircraft structures.

Wing

The wing structure is a multi-web box beam designed by spanwise bending and shear. The wing-fuselage carrythrough structure, defined by the wing-fuselage intersection, carries the spanwise bending, shear, and torsion loads introduced by the outboard portion of the wing.

The load case used for the wing weight analysis is the quasi-static pull-up maneuver. The applied loads to the wing include the distributed lift and inertia forces, and the point loads of landing gear and propulsion, if placed on the wing. Fuel may also be stored in the wing, which will relieve bending loads during the pull-up maneuver.

The wing weight analysis proceeds in a similar fashion to that of the fuselage. The weight of the structural box is determined by calculating the minimum amount of material required to satisfy static buckling and strength requirements at a series of spanwise stations. The covers of the multi-web box are sized by buckling due to local instability and the webs by flexure-induced crushing. Required shear material is computed independently of buckling material. Aeroelastic effects are not accounted for directly, although an approximation of the magnitude of the tip deflection during the pull-up

maneuver is made. For the carrythrough structure, buckling, shear, and torsion material are computed independently and summed.

As for the fuselage, there are a variety of structural geometries available. There are a total of six structural concepts, three with unstiffened covers and three with truss-stiffened covers. Both cover configurations use webs that are either Z-stiffened, unflanged, or trusses.

Geometry

Fuselage

The fuselage is assumed to be composed of a nose section, an optional cylindrical midsection, and a tail section. The gross density and fineness ratio are defined as

$$\rho_B = \frac{W_{TO}}{V_B} \tag{1}$$

$$R_{fin} = \frac{l_B}{D} \tag{2}$$

where W_{TO} is the gross take-off weight, V_B is the total fuselage volume, l_B is the fuselage length, and D is the maximum fuselage diameter. The fuselage outline is defined by two power-law bodies of revolution placed back-to-back, with an optional cylindrical midsection between them (Figure 1.) (For the present study, all nine transports used for validation of the analysis used the optional cylindrical midsection.)

With the cylindrical midsection, integration gives the fuselage volume, fuselage planform area, and fuselage surface area as

$$V_B = \frac{\pi D^2}{4}\left[\frac{l_1}{2P_1+1} + (l_B - l_2 - l_1) + \frac{l_2}{2P_2+1}\right] \tag{3}$$

$$S_B = D\left[\frac{l_1}{P_1+1} + (l_B - l_2 - l_1) + \frac{l_2}{P_2+1}\right] \tag{4}$$

$$A_B = \pi S_B \tag{5}$$

respectively, where l_1 and l_2 are the respective lengths to the start and end of the cylindrical midsection, and P_1 and P_2 are the respective powers that describe the nose and tail sections. P_1 and P_2, again for the case of the cylindrical midsection, are found by solving the power-law equations for the volumes of the nose and tail sections, which are input from ACSYNT. The solution of these equations gives the respective nose and tail powers as

$$P_1 = \frac{\pi D^2 l_1}{8V_1} - \frac{1}{2} \tag{6}$$

$$P_2 = \frac{\pi D^2 l_2}{8V_2} - \frac{1}{2} \tag{7}$$

where V_1 and V_2 are the corresponding nose and tail volumes.

The horizontal tail is placed according to its quarter chord location as a fraction of the fuselage length. The distance from the nose to the tail is

$$x_{HT} = l_B R_{HT} \tag{8}$$

where R_{HT} is the ratio of horizontal tail station to fuselage length.

Propulsion may be either mounted on the fuselage or placed on the wing. In the case of fuselage mounted propulsion, the starting and ending positions of the propulsion unit are again calculated from their respective fractions of fuselage length as

$$x_{P_1} = l_B R_{P1} \tag{9}$$

$$x_{P_2} = l_B R_{P2} \tag{10}$$

where R_{P1} and R_{P2} are the corresponding ratios of lengths to the leading and trailing edges of the fuselage engine pod to fuselage length.

Similarly, the nose landing gear is placed on the fuselage as a fraction of vehicle length; the main gear, on the other hand, may be placed either on the fuselage as a single unit, also as a fraction of fuselage length, or on the wing in multiple units as will be described below. The positions of the respective nose and optional fuselage-mounted main gear are

$$l_{NG} = l_B R_{NG} \tag{11}$$

$$l_{MG} = l_B R_{MG} \tag{12}$$

where R_{NG} and R_{MG} are the corresponding length ratios for the nose gear and main gear stations to vehicle length.

Wing

The lifting planforms are assumed to be tapered, swept wings with straight leading and trailing edges.

The wing loading is defined as

$$\mu = \frac{W_{TO}}{S_P} \tag{13}$$

where S_P is the wing planform area.

The wing is placed on the fuselage according to the location of the leading edge of its root chord, determined as a fraction of the fuselage length. The distance from the nose to the leading edge of the wing is

$$x_{LE} = l_B R_{LE} \tag{14}$$

where R_{LE} is the ratio of leading edge station to fuselage length.

The first step in computing the wing weight is the determination of the geometry of the structural wing box. In terms of the input parameters W_{TO}, (W/S_p), aspect ratio (AR), taper ratio (R_{TAP}), and leading edge sweep (Λ_{LE}), the dependent parameters wing area, span, root chord, tip chord, and trailing edge wing sweep are computed from

$$S_P = \frac{W_{TO}}{W/S} \tag{15}$$

$$b = \sqrt{(AR)\ S_P} \tag{16}$$

$$C_R' = \frac{2S_P}{b(1+R_{TAP})} \tag{17}$$

$$C_T = R_{TAP} C_R' \tag{18}$$

$$\tan(\Lambda_{TE}) = \tan(\Lambda_{LE}) + \frac{2C_R'}{b}(R_{TAP} - 1) \tag{19}$$

(Figure 2). It is assumed that specified portions of the streamwise (aerodynamic) chord are required for controls and high lift devices, leaving the remainder for the structural wing box. The portions of the leading and trailing edges that are left for non-structural use are specified as respective fractions C_{s_1} and C_{s_2} of the streamwise chord.

Determination of these chord fractions is accomplished through visual inspection of the wing planform. Measured at the theoretical root chord, the dimensions for the leading and trailing edges are

$$l_{LE} = C_{S_1} C'_R \tag{20}$$

$$l_{TE} = C_{S_2} C'_R \tag{21}$$

respectively. The intersection of this structural box with the fuselage contours determines the location of the rectangular carrythrough structure. The width of the carrythrough structure, w_C, is defined by the corresponding fuselage diameter.

The dimensions of the structural box and of the carrythrough structure are now determined (Figure 3). The structural semispan, b_S, is assumed to lie on the quarter-chord line, y, whose sweep is given by

$$\tan(\Lambda_S) = \frac{3}{4}\tan(\Lambda_{LE}) + \frac{1}{4}\tan(\Lambda_{TE}) \tag{22}$$

Thus,

$$b_S = \frac{b - D}{2\cos(\Lambda_S)} \tag{23}$$

The streamwise chord at any point on the wing is given by

$$r(\zeta) = C'_R - \frac{\zeta}{b/2}(C'_R - C_T) \tag{24}$$

where ζ is measured perpendicular to the vehicle longitudinal axis from the vehicle centerline toward the wingtip. Thus, the streamwise chord is the dimension of the wing parallel to the vehicle longitudinal axis. In particular, at the wing-fuselage intersection,

$$C_R = C'_R - \frac{D}{b}(C'_R - C_T) \tag{25}$$

The structural root and tip chords are

$$C_{SR} = (1 - C_{S_1} - C_{S_2})C_R \tag{26}$$

$$C_{ST} = (1 - C_{S_1} - C_{S_2})C_T \tag{27}$$

respectively. In terms of y, measured along the quarter chord from the wing-fuselage intersection toward the wingtip, the structural and total chords are given by

$$r_S(y) = C_{SR} - \frac{y}{b_S}(C_{SR} - C_{ST}) \tag{28}$$

$$r(y) = C_R - \frac{y}{b_S}(C_R - C_T) \tag{29}$$

where the structural chord is defined as the dimension of the rectangular wing box measured parallel to the vehicle longitudinal axis. Computation of the widths of the wing box and total wing structure, as shown in Figure 3, is relatively complicated due to the geometry at the wingtip and the wing-fuselage intersection. For the portion of the wing between the wingtip and the wing-fuselage intersection, the respective widths of the wing box and total wing structure at any spanwise station y are

$$Z_S(y) = r_S \cos(\Lambda_S) \tag{30}$$

$$Z(y) = r \cos(\Lambda_S) \tag{31}$$

where $Z_S(y)$ and $Z(y)$ are dimensions perpendicular to the structural semispan.

The thickness of the wing box at any spanwise station y is

$$t(y) = \begin{cases} rR_t(y), & 0 \le y \le b_S \quad \textit{(box structure)} \\ rR_t(0), & y < 0 \quad \textit{(carrythrough structure)} \end{cases} \tag{32}$$

where $R_t(y)$ is determined as a linear interpolation between the root and tip thickness ratios.

For the transports in the present study, all the fuel is carried within the wing structure. An option is also available to carry the fuel entirely within the fuselage, negating any bending relief in the wing. (The high altitude drone, described in Appendix C, was modeled with a fuselage fuel tank.) The volume of the rectangular wing box structure is found as follows:

$$V_W = 2\int_0^{b_S} r_S(y)t(y)dy = (C_R R_t)C_{SR}W_C$$

$$= 1.4R\int_0^{b_S}\left[C_R - \frac{y}{b_S}(C_R - C_T)\right]^2 dy + (1 - C_{S_1} - C_{S_2})R_t C_R{}^2 W_C$$

$$= 2R_t b_S\left[C_R{}^2 - C_R(C_R - C_T) + \frac{1}{3}(C_R - C_T)^2\right] \qquad (33)$$

This equation is based on flat upper and lower surfaces and neglects the volume taken up by the structure.

Loads

Fuselage

Fuselage loading is determined on a station-by-station basis along the length of the vehicle. Three types of fuselage loads are considered – longitudinal acceleration, tank pressure, and bending moment. In the present study, all three load types are assumed to occur simultaneously to determine maximum compressive and tensile loads at the outer shell fibers at each station.

Bending loads applied to the vehicle fuselage are obtained by simulating vehicle pitch-plane motion during a quasi-static pull-up maneuver; a landing; and movement over a runway bump. Simplified vehicle loading models are used where it is assumed that: (1) fuselage lift forces (nominally zero for subsonic transports) are distributed uniformly over the fuselage plan area, (2) wing loading, determined independently, is transferred by a couple of vertical force and torque through the wing carrythrough structure, (3) fuselage weight is distributed uniformly over fuselage volume, (4) control surface forces and landing gear reactions are point loads, and (5) the propulsion system weight, if mounted on the fuselage, is uniformly distributed. A factor of safety (nominally 1.5) is applied to each load case. The aircraft weight for each case is selected as a fraction of gross take-off weight. The resulting one-dimensional loading model is shown in Figure 4. All fuselage lift forces are assumed to be linear functions of angle of attack. Longitudinal bending moments are computed for each of the three loading cases and the envelope of the maximum values taken as the design loading condition. The bending moment computation is given in detail in Reference 4 and will only be summarized here.

Considering first the pull-up maneuver loading, the motion is assumed to be a quasi-static pitch-plane pull-up of given normal load factor n (nominally 2.5 for transport aircraft). The vehicle is trimmed with the appropriate control surface (a horizontal tail for all nine transport used for validation in the present study), after which the angle of attack is calculated.

Landing loads are developed as the aircraft descends at a given vertical speed, V_S, after which it impacts the ground; thereafter the main and nose landing gear is assumed to exert a constant, or optionally a $(1-\cos(\omega t))$, force during its stroke, S_{LG}, until the aircraft comes to rest. The vehicle weight is set equal to the nominal landing weight. Wing lift as a fraction of landing weight is specified, which reduces the effective load the landing gear carries. Likewise, the portion of total vehicle load the main gear carries is specified. No pitch-plane motion is considered during the landing.

Runway bump loads are handled by inputting the bump load factor into the landing gear. This simulates the vehicle running over a bump during taxi. In a similar fashion to the landing, the wing lift as a fraction of gross take-off weight is specified, as is the portion of effective load input through the main gear. No pitch-plane motion is considered during the bump.

Wing

For the wing, only a quasi-static pull-up maneuver condition at load factor n is considered for determining loads. At each spanwise station along the quarter chord, from the wingtip to the wing-fuselage intersection , the lift load, center of pressure, inertia load, center of gravity, shear force and bending moment are computed. For the inertia load, it is assumed that the fuel weight W_{FT} is distributed uniformly with respect to the wing volume so that the inertial load at y is $(W_{FT}/V_W)*V(y)$, where $V(y)$ is the volume outboard of y; this volume has centroid $C_g(y)$ with respect to station y. An estimate of the wing structural weight is included in W_{FT} for this calculation but the calculation is not redone when the actual structural weight has been computed.

There is an option for either a trapezoidal or a Schrenk (Reference 16) lift load distribution along the wingspan; the trapezoidal distribution represents a uniform lift over the wing area (which has a trapezoidal planform) while the Schrenk distribution is an average of the trapezoidal distribution with an elliptical distribution, where the lift is zero at the wingtip and maximum at the wing-fuselage intersection. Prandtl has shown that a true elliptical lift load distribution will have a minimum induced drag, but a combination of the elliptical and trapezoidal distributions will give a better representation of actual aircraft loading (Reference 16).

Plots of trapezoidal and Schrenk lift load distributions are shown in Figure 5. For the trapezoidal lift load distribution the lift load at y is $(W/S)A_{TRAP}(y)$, where $A_{TRAP}(y)$ is the area outboard of y; the centroid of this area is denoted $C_{P_{TRAP}}(y)$, where y is measured along the quarter chord. For the elliptical lift load distribution, the lift load matches the contour of an ellipse with the end of its major axis on the tip and the end of its minor axis directly above the wing-fuselage intersection. The area enclosed by the quadrant of the ellipse is set equal to the exposed area of the trapezoidal wing panel:

$$S_{ELL} = \frac{(b - w_C)}{4}(1 + R_{TAP})C_R \qquad (34)$$

Thus the value of lift at y, L_{ELL}, the area of ellipse outboard of y, A_{ELL}, and the center of pressure of lift outboard of y, $C_{P_{ELL}}$, for y measured along the structural box may be determined as

$$L_{ELL}(y) = \frac{4S_{ELL}}{\pi b_S}\left[1-\left(\frac{y}{b_S}\right)^2\right]^{\frac{1}{2}} \tag{35}$$

$$A_{ELL}(y) = S_{ELL} - \left\{\frac{2S_{ELL}}{\pi {b_S}^2}\left[y({b_S}^2 - y^2)^{\frac{1}{2}} + {b_S}^2 \sin^{-1}\left(\frac{y}{b_S}\right)\right]\right\} \tag{36}$$

$$C_{P_{ELL}}(y) = \frac{4}{3\pi}(b_S - y) \tag{37}$$

respectively.

For the Schrenk lift load distribution, the average of $A_{TRAP}(y)$ and $A_{ELL}(y)$ is used to represent the composite area, while the average of $C_{P_{TRAP}}(y)$ and $C_{P_{ELL}}(y)$ is used to represent the composite center of pressure.

Using the appropriate outboard area $A(y)$ and center of pressure $C_P(y)$, the shear force is

$$F_S(y) = nK_S\left[\frac{W}{S}A - \frac{W_{FT}}{V_W}V - \sum_{i=1}^{n_e} h_e(y_{e_i} - y)W_{e_i} - \sum_{i=1}^{n_{lg}} h_{lg}(y_{lg_i} - y)W_{lg_i}\right] \tag{38}$$

where n_e and n_{lg} are the number of engines and landing gear mounted on the semispan, respectively; W_{e_i} and W_{lg_i} are the weights of the i^{th} engine an i^{th} landing gear, respectively; y_{e_i} and y_{lg_i} are the locations of the i^{th} engine and i^{th} landing gear, respectively; and

$$h_e(y_{e_i} - y) = \begin{Bmatrix} 1, & y_{e_i} > y \\ 0, & y_{e_i} < y \end{Bmatrix} \tag{39}$$

$$h_{lg}(y_{lg_i} - y) = \begin{Bmatrix} 1, & y_{lg_i} > y \\ 0, & y_{lg_i} < y \end{Bmatrix} \tag{40}$$

The bending moment is

$$M(y) = nK_S\left[\frac{W}{S}AC_P - \frac{W_{FT}}{V_W}VC_g - \sum_{i=1}^{n_e} h_e(y_{e_i} - y)W_{e_i}(y_{e_i} - y) - \sum_{i=1}^{n_{lg}} h_{lg}(y_{lg_i} - y)W_{lg_i}(y_{lg_i} - y)\right] \tag{41}$$

Structural Analysis

Fuselage

Weight estimating relationships are now developed for the load-carrying fuselage structure. In addition, the volume taken up by the fuselage structure is also determined.

Considering first the circular shell, the stress resultants in the axial direction caused by longitudinal bending, axial acceleration, and pressure at a fuselage station x are

$$N_{x_B} = \frac{Mr}{I_y'} \tag{42}$$

$$N_{x_A} = \frac{N_x W_s}{P} \tag{43}$$

$$N_{x_P} = \frac{AP_g}{P} \tag{44}$$

respectively, where $r=D/2$ is the fuselage radius, $A=\pi r^2$ is the fuselage cross-sectional area, and $P=2\pi r$ is the fuselage perimeter. In Equation 42, $I_y'=\pi r^3$ is the moment of inertia of the shell divided by the shell thickness. In equation 43, for the case of fuselage-mounted propulsion, W_s is the portion of vehicle weight ahead of station x if x is ahead of the inlet entrance, or the portion of vehicle weight behind x if x is behind the nozzle exit. In equation 44, P_g is the limit gage pressure differential for the passenger compartment during cruise. The total tension stress resultant is then

$$N_x^+ = N_{x_B} + N_{x_P} \tag{45}$$

if x is ahead of the nozzle exit, and

$$N_x^+ = N_{x_B} + N_{x_P} + N_{x_A} \tag{46}$$

if x is behind it. Similarly, the total compressive stress resultant is

$$N_x^- = N_{x_B} + N_{x_A} - \begin{Bmatrix} 0, & \text{if not pressure stabilized} \\ N_{x_P}, & \text{if stabilized} \end{Bmatrix} \tag{47}$$

if x is ahead of the inlet entrance, and

$$N_x^- = N_{x_B} - \begin{Bmatrix} 0, & \text{if not pressure stabilized} \\ N_{x_P}, & \text{if stabilized} \end{Bmatrix} \tag{48}$$

if x is behind it. These relations are based on the premise that acceleration loads never decrease stress resultants, but pressure loads may relieve stress, if pressure stabilization is chosen as an option. The stress resultant in the hoop direction is

$$N_y = r\, P_g K_P \tag{49}$$

where K_p accounts for the fact that not all of the shell material (for example, the core material in sandwich designs) is available for resisting hoop stress.

The equivalent isotropic thicknesses of the shell are given by

$$\bar{t}_{S_C} = \frac{N_x^-}{F_{cy}} \tag{50}$$

$$\bar{t}_{S_T} = \frac{1}{F_{tu}} \max(N_x^+, N_y) \tag{51}$$

$$\bar{t}_{S_G} = K_{mg} t_{mg} \tag{52}$$

for designs limited by compressive yield strength (F_{cy}), ultimate tensile strength (F_{tu}), and minimum gage, respectively. In Equation 52, t_{mg} is a specified minimum material thickness and K_{mg} is a parameter relating $\bar{t}_{S_G}$ to t_{mg} which depends on the shell geometry.

A fourth thickness that must be considered is that for buckling critical designs, $\bar{t}_{S_B}$, which will now be developed. The nominal vehicles of this study have integrally stiffened shells stabilized by ring frames. In the buckling analysis of these structures, the shell is analyzed as a wide column and the frames are sized by the Shanley criteria (Reference 9). Expressions are derived for the equivalent isotropic thickness of the shell required to preclude buckling, $\bar{t}_{S_B}$, and for the *smeared* equivalent isotropic thickness of the ring frames required to preclude general instability, $\bar{t}_F$. The analysis will be restricted to the case of cylindrical shells. The major assumptions are that the structural shell behaves as an Euler beam and that all structural materials behave elastically.

For the stiffened shell with frames concept, the common procedure of assuming the shell to be a wide column is adopted. If the frame spacing is defined as d and Young's modulus of the shell material is defined as E, the buckling equation is then

$$\frac{\bar{N_x}}{dE} = \varepsilon\left(\frac{\bar{t}_{S_B}}{d}\right)^2 \tag{53}$$

or, solving for $\bar{t}_{S_B}$

$$\bar{t}_{S_B} = \sqrt{\frac{\bar{N_x} d}{E\varepsilon}} \tag{54}$$

Values of the shell efficiency ε for the various structural concepts are given in Table 2; the structural shell geometries available are simply stiffened, Z-stiffened, and truss-core sandwich. We next size the frames to prevent general instability failure. The Shanley criterion is based on the premise that the frames act as elastic supports for the wide column; this criterion gives the smeared equivalent thickness of the frames as

$$\bar{t}_{F_B} = 2r^2\sqrt{\frac{\pi C_F \bar{N_x}}{K_{FI} d^3 E_F}} \tag{55}$$

where C_F is Shanley's constant, K_{FI} is a frame geometry parameter, and E_F is Young's modulus for the frame material. (See Reference 3 for a discussion of the applicability of this criterion and for a detailed derivation of the equations presented here.) If the structure is buckling critical, the total thickness is

$$\bar{t} = \bar{t}_{S_B} + \bar{t}_{F_B} \tag{56}$$

Minimizing $\bar{t}$ with respect to d results in

$$\bar{t} = \frac{4}{27^{1/4}}\left(\frac{\pi C_F}{K_{F1}\varepsilon^3 E_F E^3}\right)^{1/8}\left(\frac{2r^2\rho_F\left(N_x^-\right)^2}{\rho}\right)^{1/4} \tag{57}$$

$$\bar{t}_{S_B} = \frac{3}{4}\bar{t} \tag{58}$$

$$\bar{t}_{F_B} = \frac{1}{4}\bar{t} \tag{59}$$

$$d = \left(6r^2\frac{\rho_F}{\rho}\sqrt{\frac{\pi C_F \varepsilon E}{K_{F1}E_F}}\right)^{1/2} \tag{60}$$

where ρ_F is the density of the frame material and ρ is the density of the shell material, so that the shell is three times as heavy as the frames.

Frame-less sandwich shell concepts may also be used. For these concepts, it is assumed that the elliptical shell buckles at the load determined by the maximum compressive stress resultant N_x^- on the cylinder. The buckling equation for this frame-less sandwich shell concepts is

$$\frac{N_x^-}{rE} = \varepsilon\left(\frac{\bar{t}_{S_B}}{r}\right)^m \tag{61}$$

where m is the buckling equation exponent. Or, solving for $\bar{t}_{S_B}$

$$\bar{t}_{S_B} = r\left(\frac{N_x^-}{rE\varepsilon}\right)^{\frac{1}{m}} \tag{62}$$

This equation is based on small deflection theory, which seems reasonable for sandwich cylindrical shells, although it is known to be inaccurate for monocoque cylinders. Values of m and ε may be found, for example in References 5 and 6 for many shell geometries. Table 2 gives values for sandwich structural concepts available in PDCYL, numbers 8 and 9, both of which are truss-core sandwich. The quantities N_x^-, r, and consequently $\bar{t}_{S_B}$, will vary with fuselage station dimension x.

At each fuselage station x, the shell must satisfy all failure criteria and meet all geometric constraints. Thus, the shell thickness is selected according to compression, tension, minimum gage and buckling criteria, or

$$\bar{t}_S = \max(\bar{t}_{S_C}, \bar{t}_{S_T}, \bar{t}_{S_G}, \bar{t}_{S_a}) \tag{63}$$

If $\bar{t}_S = \bar{t}_{S_a}$, the structure is buckling critical and the equivalent isotropic thickness of the frames, $\bar{t}_F$, is computed from Equation 59. If $\bar{t}_S > \bar{t}_{S_a}$, the structure is not buckling critical at the optimum frame sizing and the frames are re-sized to make $\bar{t}_S = \bar{t}_{S_a}$. Specifically, a new frame spacing is computed from Equation 54 as

$$d = \frac{E\varepsilon \bar{t}_S^{\,2}}{\bar{N}_x} \tag{64}$$

and this value is used in Equation 55 to determine $\bar{t}_F$.

The total thickness of the fuselage structure is then given by the summation of the smeared weights of the shell and the frames

$$\bar{t}_B = \bar{t}_S + \bar{t}_F \tag{65}$$

The shell gage thickness may be computed from $t_g = \bar{t}_S / K_{mg}$. The *ideal* fuselage structural weight is obtained by summation over the vehicle length

$$W_I = 2\pi\Sigma(\rho\bar{t}_{S_i} + \rho_F\bar{t}_{F_i})r_i\Delta x_i \tag{66}$$

where the quantities subscripted i depend on x.

We next discuss the derivation of the structural geometry parameters shown in Table 2. The Z-stiffened shell, typical of modern transport aircraft, will be used as an example of skin-stringer-frame construction. Using Reference 5 and Figure 6, the equivalent isotropic thickness of the smeared skin and stringers is

$$\bar{t}_S = t_s + \frac{2b_f f_f}{b_s} + \frac{b_w t_w}{b_s} = \left[1 + 1.6\left(\frac{b_w}{b_s}\right)\left(\frac{t_w}{t_s}\right)\right] t_s \tag{67}$$

Since only the skin is available for resisting pressure loads,

$$K_p = 1 + 1.6\left(\frac{b_w}{b_s}\right)\left(\frac{t_w}{t_s}\right) \tag{68}$$

For minimum gage designs, if $t_s > t_w$ then $t_w = t_{mg}$ and

$$\bar{t}_S = \left[\left(\frac{t_s}{t_w}\right) + 1.6\left(\frac{b_w}{b_s}\right)\right] t_{mg} \tag{69}$$

so that

$$K_{mg} = \left(\frac{t_s}{t_w}\right) + 1.6\left(\frac{b_w}{b_s}\right) \tag{70}$$

On the other hand, if $t_s<t_w$ then $t_s=t_{mg}$ and

$$\bar{t}_S = \left[1 + 1.6\left(\frac{b_w}{b_s}\right)\left(\frac{t_w}{t_s}\right)\right] t_{mg} \tag{71}$$

so that

$$K_{mg} = 1 + 1.6\left(\frac{b_w}{b_s}\right)\left(\frac{t_w}{t_s}\right) \tag{72}$$

Equations 68, 70, and 72 show that for both pressure loading critical and minimum gage limited structure, (b_w/b_s) and (t_w/t_s) should be as small as possible (i.e. no stringers). As an option in PDCYL, all of the detailed shell dimensions shown in Figure 6 are computed and output at each fuselage station.

In practice, a typical design will be influenced by bending and pressure loads and by the minimum gage constraint, and thus a compromise is necessary. If buckling is of paramount importance, then a good choice is (b_w/b_s)=0.87 and (t_w/t_s)=1.06 because this gives the maximum buckling efficiency for this concept, namely ε=0.911 (Reference 5). From Equations 68 and 72,

$$K_p = K_{mg} = 1 + (1.6)(0.87)(1.06) = 2.475 \tag{73}$$

This is concept 3 in Tables 1 and 2. If pressure dominates the loading condition, then (b_w/b_s)=0.6 and (t_w/t_s)=0.6 is a reasonable choice, giving ε=0.76, K_p=1.576, and K_{mg}=2.628; this is concept 5. For minimum gage dominated structure, the geometry (b_w/b_s)=0.58 and (t_w/t_s)=0.90 gives concept 6.

The geometry of the truss-core sandwich shell concept is shown in Figure 7. The equivalent isotropic shell thickness of this concept is

$$\bar{t}_s = \left(2 + \frac{t_c}{t_f}\frac{1}{\cos(\psi)}\right) t_f \tag{74}$$

Reference 5 shows that the optimum buckling efficiency is obtained for (t_c/t_f)=0.65 and ψ=55°. This gives ε=0.4423, K_{mg}=4.820, and K_p=3.132, concept 8 in Tables 1 and 2. To get a design that is lighter for minimum gage dominant structure, a geometry is chosen that places equal thickness material in the face sheets and the core; the choice of (t_c/t_f)=1.0 and ψ=45° gives structural concept 9. These calculations assume that the face sheets and core are composed of the same material and are subject to the same minimum gage constraint.

Since the preceding analysis gives only the ideal weight, W_I, the *non-optimum* weight, W_{NO}, (including fasteners, cutouts, surface attachments, uniform gage penalties, manufacturing constraints, etc.) has yet to be determined. The method used will be explained in a later section.

Wing

Using the geometry and loads applied to the wing developed above, the structural dimensions and weight of the structural box may now be calculated. The wing structure is assumed to be a rectangular multi-web box beam with the webs running in the direction of the structural semispan. Reference 5 indicates that the critical instability mode for miltiweb box beams is simultaneous buckling of the covers due to local instability and of the webs due to flexure induced crushing. This reference gives the solidity (ratio of volume of structural material to total wing box volume) of the least weight multi-web box beams as

$$\Sigma = \varepsilon\left(\frac{M}{Z_S t^2 E}\right)^e \tag{75}$$

where ε and e depend on the cover and web geometries (Table 3), M is the applied moment, t is the thickness, E is the elastic modulus, and Z_S is obtained from Reference 5. The solidity is therefore

$$\Sigma = \frac{W'_{BEND}(y)}{\rho Z_S t} \tag{76}$$

where W'_{BEND} is the weight of bending material per unit span and ρ is the material density. W'_{BEND} is computed from Equations 75 and 76. The weight per unit span of the shear material is

$$W'_{SHEAR}(y) = \frac{\rho F_S}{\sigma_S} \tag{77}$$

where F_S is the applied shear load and σ_S is the allowable shear stress. The optimum web spacing (Figure 8) is computed from (Reference 2)

$$d_W = t\left[\frac{(1-2e_C)}{(1-e_C)\sqrt{2\varepsilon_W}}\left(\frac{M}{Z_S t^2 E}\right)^{\frac{2e_C-3}{2e_C}} \varepsilon_C^{\frac{3}{2e_C}}\right]^{\frac{2e_C}{4e_C-3}} \tag{78}$$

where subscripts W and C refer to webs and covers, respectively. The equivalent isotropic thickness of the covers and webs are

$$\bar{t}_C = d_W\left(\frac{M}{Z_S\, t\, E\varepsilon_C d_W}\right)^{\frac{1}{e_C}} \tag{79}$$

$$\bar{t}_W = t\sqrt{\left(\frac{M}{Z_S t^2 E}\right)^{\left(2-\frac{1}{e_C}\right)}\left(\frac{\varepsilon_C d_W}{t}\right)^{\frac{1}{e_C}}\left(\frac{2}{\varepsilon_W}\right)} \tag{80}$$

respectively, and the gage thicknesses are

$$t_{gc} = K_{gc}\bar{t}_C \tag{81}$$

$$t_{gw} = K_{gw}\bar{t}_W \tag{82}$$

Values of ε, e, ε_C, E_C, ε_W, K_{g_w}, and K_{g_c}, are found in Table 3 for various structural concepts (Reference 5). If the wing structural semispan is divided into N equal length segments, the total *ideal* weight is the wing box structure is

$$W_{BOX} = \frac{2b_S}{N}\sum_{i=1}^{N}\left(W'_{BEND_i} + W'_{SHEAR_i}\right) \tag{83}$$

The wing carrythrough structure consists of torsion material in addition to bending and shear material. The torsion material is required to resist the twist induced due to the sweep of the wing. The bending material is computed in a similar manner as that of the box except that only the longitudinal component of bending moment contributes. Letting $t_0=t(y=0)$ and $M_0=M(y=0)$,

$$\Sigma_C = \varepsilon\left(\frac{M_0\cos(\Lambda_S)}{t_0^2 C_{SR} E}\right)^e \tag{84}$$

The weight of the bending material is then

$$W_{BEND_C} = \rho\Sigma_C C_{SR} t_0 w_C \tag{85}$$

where w_C is the width of the carrythrough structure. (When the wing-fuselage intersection occurs entirely within the cylindrical midsection, as is the case with all nine transport used for validation in the present study, $w_C=D$.) The quantities d_W, t_W, and t_C, are computed in the same manner as for the box. The weight of the shear material is

$$W_{SHEAR_C} = \rho\frac{F_{S_0}}{\sigma_S} w_C \tag{86}$$

where $F_{S_0} = F_S(0)$.

The torque on the carrythrough structure is

$$T = M_0\sin(\Lambda_S) \tag{87}$$

and the weight of the torsion material is then

$$W_{TORSION_C} = \frac{\rho T(t_0 + C_{SR})w_C}{t_0 C_{SR}\sigma_S} \tag{88}$$

Finally, the *ideal* weight of the carrythrough structure is computed from a summation of the bending shear and torsion material, or

$$W_C = W_{BEND_C} + W_{SHEAR_C} + W_{TORSION_C} \tag{89}$$

As in the case of the fuselage structural weight, *non-optimum* weight must be added to the ideal weight to obtain the true wing structural weight. The method used will be discussed below.

The static deflection of the wingtip under the pull-up maneuver is also determined. Using the moment-area method applied to an Euler beam (Reference 14), the deviation of point B on the deflected surface from the tangent drawn from another point A on the surface is equal to the area under the $M/(EI)$ diagram between A and B multiplied by the distance to the centroid of this area from B,

$$t_{BA} = \int_B^A y\, d\theta = \int_B^A \frac{M}{EI}\, y\, dy \tag{90}$$

where θ is the angular displacement of the beam and y is the longitudinal axis of the beam. For the case of a wing with trapezoidal planform, the longitudinal axis, y, will lie along the quarter-chord line (Figure 3). For a wing with a horizontal unloaded configuration, the tangential deviation, t_{BA}, will equal the true vertical tip displacement (assumed to be the case). Only the wing cover contributes to the bending resistance, while the webs offer similar shear stiffness. The wing area moment of inertia, I, at any structural semispan station y is determined with the Parallel Axis theorem, as cover thickness is small when compared with total wing thickness.

Regression Analysis

Overview

Using fuselage and wing weight statements of nine subsonic transports, a relation between the calculated load-bearing structure weights obtained through PDCYL and the actual load-bearing structure weights, primary structure weights, and total weights is determined using statistical analysis techniques. A basic application which is first described is linear regression, wherein the estimated weights of the aircraft are related to the weights calculated by PDCYL with a straight line, $y=mx+b$, where y is the value of the estimated weight, m is the slope of the line, x is the value obtained through PDCYL, and b is the y-intercept. This line is termed a *regression* line, and is found by using the *method of least squares*, in which the sum of the squares of the residual errors between actual data points and the corresponding points on the regression line is minimized. Effectively, a straight line is drawn through a set of ordered pairs of data (in this case nine weights obtained through PDCYL and the corresponding actual weights) so that the aggregate deviation of the actual weights above or below this line is minimized. The estimated weight is therefore dependent upon the independent PDCYL weight.

As an example, if the form of the regression equation is linear, the estimated weight is

$$y_{est} = m\,x_{calc} + b \tag{91}$$

where m is the slope, b is the intercept, and x_{calc} is the weight PDCYL calculates. The resulting residual to be minimized is

$$E = \sum_{i=1}^{n} (y_{actual_i} - y_{est_i})^2 \tag{92}$$

or

$$E = \sum_{i=1}^{n} (y_{actual_i} - m\,x_{calc_i} - b)^2 \tag{93}$$

where y_{actual} is the actual component weight and n is the number of aircraft whose data is to be used in the fit. By taking partial derivatives of the residual error with respect to both m and b, equations for the values of these two unknown variables are found to be

$$m = \frac{n\sum_{i=1}^{n} x_{calc_i} y_{act_i} - \sum_{i=1}^{n} x_{calc_i} \sum_{i=1}^{n} y_{act_i}}{n\sum_{i=1}^{n} x_{calc_i}^2 - (\sum_{i=1}^{n} x_{calc_i})^2} \tag{94}$$

$$b = \bar{y}_{act} - n\,\bar{x}_{calc} \qquad \bar{x}, \bar{y} = \textit{mean values of } x \textit{ and } y \tag{95}$$

Of key importance is the degree of accuracy to which the prediction techniques are able to estimate actual aircraft weight. A measure of this accuracy, the correlation coefficient, denoted R, represents the reduction in residual error due to the regression technique. R is defined as

$$R = \sqrt{\frac{E_i - E_r}{E_r}} \tag{96}$$

where E_i and E_r refer to the residual errors associated with the regression before and after analysis is performed, respectively. A value of R=1 denotes a perfect fit of the data with the regression line. Conversely, a value of R=0 denotes no improvement in the data fit due to regression analysis.

There are two basic forms of equations which are implemented in this study. The first is of the form

$$y_{est} = m\,x_{calc} \tag{97}$$

The second general form is

$$y_{est} = m\,x_{calc}^{a} + b \tag{98}$$

The first form is a simplified version of the linear example as discussed above, with the y-intercept term set to zero. However, because the second general equation is not linear, nor can it be transformed to a linear equation, an alternative method must be employed. In order to formulate the resulting *power-intercept* regression equation, an iterative approach developed by D. W. Marquardt is utilized (Reference 15). This algorithm starts at a certain point in space, and, by applying the method of steepest descent, a gradient is obtained which indicates the direction in which the most rapid decrease in the residual errors will occur. In addition, the Taylor Series method produces a second similar vector. Interpolation between these two vectors yields a direction in which to move the point in order to minimize the associated error. After several iterations, the process converges to a minimum value. It should be noted that there may be several local minimums and there is no guarantee that the method converges to the global one.

Fuselage

The analysis above is used to develop a relationship between weight calculated by PDCYL and actual wing and fuselage weights. The data was obtained from detailed weight break-downs of nine transport aircraft (References 12, 13, 17-19) and is shown in Table 4 for the fuselage. Because the theory used in the PDCYL analysis only predicts the load-carrying structure of the aircraft components, a correlation between the predicted weight and the actual load-carrying structural weight, primary weight, as well as the total weight of the fuselage was made.

Structural weight consists of all load-carrying members including bulkheads and frames, minor frames, covering, covering stiffeners, and longerons. For the linear curve-fit, the resulting regression equation is

$$W_{actual} = 1.3313 W_{calc} \qquad R=0.99624 \qquad (99)$$

This shows that the *non optimum* factor for fuselage structure is 1.3313; in other words, the calculated weight must be increased by about 33% to get the actual structural weight. For the alternative power-intercept curve fitting analysis, the resulting load-carrying regression equation is

$$W_{actual} = 4019.9 + 0.01952 W_{calc}^{1.4073} \qquad R=0.99624 \qquad (100)$$

To use either of these equations to estimate total fuselage weight, non-structural weight items must be estimated independently and added to the structural weight.

Primary weight consists of all load-carrying members as well as any secondary structural items such as joints fasteners, keel beam, fail-safe straps, flooring, flooring structural supplies, and pressure web. It also includes the lavatory structure, galley support, partitions, shear ties, tie rods, structural firewall, torque boxes, and attachment fittings. The linear curve fit for this weight yields the following primary regression equation

$$W_{actual} = 1.8493 W_{calc} \qquad R=0.98471 \qquad (101)$$

The primary power-intercept regression equation is

$$W_{actual} = 5531.9 + 0.019094 W_{calc}^{1.4407} \qquad R=0.98934 \qquad (102)$$

The total fuselage weight accounts for all members of the body, including the structural weight and primary weight. It does not include passenger accommodations, such as seats, lavatories, kitchens, stowage, and lighting; the electrical system; flight and navigation systems; alighting gear; fuel and propulsion systems; hydraulic and pneumatic

systems; the communication system; cargo accommodations; flight deck accommodations; air conditioning equipment; the auxiliary power system; and emergency systems. Linear regression results in the following total fuselage weight equation

$$W_{actual} = 2.5178 W_{calc} \qquad R=0.98549 \qquad (103)$$

The total fuselage weight power-intercept regression equation is

$$W_{actual} = 6877.8 + 0.099541 W_{calc}^{1.308} \qquad R=0.9878 \qquad (104)$$

Plots of actual fuselage component weight verses PDCYL-calculated weight, as well as the corresponding linear regressions, is shown in Figures 9-11.

Wing

The same analysis was performed on the wing weight for the sample aircraft and is shown in Table 5. The wing box, or load-carrying structure, consists of spar caps, interspar coverings, spanwise stiffeners, spar webs, spar stiffeners, and interspar ribs. The wing box linear regression equation is

$$W_{actual} = 1.0379 W_{calc} \qquad R=0.98482 \qquad (105)$$

so that the nonoptimum factor, is 1.0379. Power-intercept regression results in

$$W_{actual} = -930.36 + 1.131 W_{calc}^{0.99472} \qquad R=0.98537 \qquad (106)$$

Wing primary structural weight includes all wing box items in addition to auxiliary spar caps and spar webs, joints and fasteners, landing gear support beam, leading and trailing edges, tips, structural firewall, bulkheads, jacket fittings, terminal fittings, and attachments. Linear regression results in

$$W_{actual} = 1.4217 W_{calc} \qquad R=0.99285 \qquad (107)$$

Power-intercept regression yields

$$W_{actual} = -908.14 + 1.8928 W_{calc}^{0.97461} \qquad R=0.9929 \qquad (108)$$

The total wing weight includes wing box and primary weight items in addition to high-lift devices, control surfaces and access items. It does not include the propulsion system, fuel system, and thrust reversers; the electrical system; alighting gear; hydraulic and pneumatic systems; anti-icing devices; and emergency systems. The resulting total weight linear regression equation is

$$W_{actual} = 1.8353 W_{calc} \qquad R=0.98857 \qquad (109)$$

The power-intercept equation for total wing weight is

$$W_{actual} = 657.33 + 1.6624 W_{calc}^{1.0083} \qquad R=0.98862 \qquad (110)$$

Plots of actual wing component weight verses PDCYL-calculated weight, as well as the corresponding linear regressions, is shown in Figures 12-14.

Discussion

Both fuselage and wing weight linear regressions give excellent correlation with the respective weights of existing aircraft, as evidenced by the high values of the correlation coefficient, R.

There are, however, two results of the correlations which are somewhat puzzling. First, the constant term in two of the wing power-intercept equations is negative; this will usually numerically insignificant. Second, the exponents in the fuselage power-intercept equations are significantly different than one; this may be due to convergence to a local, rather than the global, minimum.

Because estimates of non-load-bearing primary structure are generally not available at the conceptual design stage, and because non-primary structure is probably not well-estimated by a non-optimum factor, Equation 101 and Equation 107 are recommended for estimating the primary structural weights of the respective transport fuselage and wing structures (Figure 10; Figure 13).

REFERENCES

1. Ardema, M. D., *Body Weight of Hypersonic Aircraft: Part 1.* NASA TM 101028, Oct. 1988.

2. Ardema, M. D. and Williams, L. J., *Transonic Transport Study – Structures and Aerodynamics,* NASA TM X-62,157, May 1972.

3. Ardema, M. D., *Structural Weight Analysis of Hypersonic Aircraft,* NASA TN D-6692, Mar. 1972.

4. Ardema, M. D., *Analysis of Bending Loads of Hypersonic Aircraft,* NASA TM X-2092, 1970.

5. Crawford, R. F. and Burns, A. B., *Strength, Efficiency, and Design Data for Beryllium Structures,* ASD-TR-61-692, Feb. 1962.

6. Crawford, R. F. and Burns, A. B., *Minimum Weight Potentials for Stiffened Plates and Shells,* AIAA Journal, vol. 1, no. 4, Apr. 1963, pp. 879-886.

7. Vinson, J. R. and Shore, S., *Minimum Weight Web Core Sandwich Panels Subjected to Uniaxial Compression,* Journal of Aircraft, vol. 8, no. 11, Nov. 1971, pp. 843-847.

8. Vinson, J. R., *Optimum Design of Composite Hex-Cell and Square Cell Honeycomb Sandwich Panels Subjected to Uniaxial Compression,* AIAA Journal, vol. 24, no. 10, Oct. 1987, pp. 1690-1696.

9. Shanley, F. R., *Weight-Strength Analysis of Aircraft Structures, Second Edition,* Dover, New York, 1960.

10. Timoshenko, S. P. and Young, D. H., *Theory of Structures,* McGraw-Hill, 1945.

11. Moore, M. and Samuels, J., *ACSYNT Aircraft Synthesis Program – User's Manual,* Systems Analysis Branch, NASA-Ames Research Center, Sep. 1990.

12. Niu, M. C.-Y., *Airframe Structural Design: Practical Design Information and Data on Aircraft Structures*, Conmilit Press, 1991.

13. York, P. and Labell, R. W., *Aircraft Wing Weight Build-Up Methodology with Modification for Materials and Construction Techniques*, NASA CR 166173, Sep. 1980.

14. Popov, E. P., *Mechanics of Materials, Second Edition*, Prentice-Hall, New Jersey, 1976.

15. Marquardt, D. W., *Least Squares Estimation of Nonlinear Parameters, a Computer Program in FORTRAN IV Language*, IBM SHARE Library, Distribution Number 309401, August 1966.

16. McCormick, B. W., *Aerodynamics, Aeronautics, and Flight Mechanics*, John Wiley & Sons, 1979.

17. The Boeing Company, Commercial Airplane Division, Weight Research Group, Thomas, R. B. and Parsons, S. P., *Weight Data Base*, Doc. No. D6-23204 TN, 1968.

18. McDonnell Douglas Aircraft Company, Detailed weight statement for MD-11 transport aircraft, June 1987.

19. McDonnell Douglas Aircraft Company, Detailed weight statement for MD-80 transport aircraft, July 1991.

20. Megson, T. H. G., *Aircraft Structures for Engineering Students, Second Edition*, Halsted Press, 1990.

TABLE 1. FUSELAGE STRUCTURAL GEOMETRY CONCEPTS.

(KCON Sets Concept Number)

2. Simply Stiffened Shell, Frames, Sized for Minimum Weight in Buckling
3. Z-Stiffened Shell, Frames, Best Buckling
4. Z-Stiffened Shell, Frames, Buckling-Minimum Gage Compromise
5. Z-Stiffened Shell, Frames, Buckling-Pressure Compromise
6. Truss-Core Sandwich, Frames, Best Buckling
8. Truss-core Sandwich, No Frames, Best Buckling
9. Truss-Core Sandwich, No Frames, Buckling-Minimum Gage -Pressure Compromise

TABLE 2. FUSELAGE STRUCTURAL GEOMETRY PARAMETERS.

STRUCTURAL CONCEPT (KCON)	m	ε	K_{mg}	K_p	K_{th}
2	2	0.656	2.463	2.463	0.0
3	2	0.911	2.475	2.475	0.0
4	2	0.760	2.039	1.835	0.0
5	2	0.760	2.628	1.576	0.0
6	2	0.605	4.310	3.965	0.459
8	1.667	0.4423	4.820	3.132	0.405
9	1.667	0.3615	3.413	3.413	0.320

TABLE 3. WING STRUCTURAL COEFFICIENTS AND EXPONENTS.

COVERS	WEBS	ε	e	ε	e_c	ε_w	K_{gc}	K_{gw}
UNSTIFF	TRUSS	2.25	0.556	3.62	3	0.605	1.000	0.407
UNSTIFF	UNFLANGED	2.21	0.556	3.62	3	0.656	1.000	0.505
UNSTIFF	Z-STIFF.	2.05	0.556	3.62	3	0.911	1.000	0.405
TRUSS	TRUSS	2.44	0.600	1.108	2	0.605	0.546	0.407
TRUSS	UNFLANGED	2.40	0.600	1.108	2	0.656	0.546	0.505
TRUSS	Z-STIFF.	2.25	0.600	1.108	2	0.911	0.546	0.405

TABLE 4. FUSELAGE WEIGHT BREAKDOWNS FOR NINE TRANSPORT AIRCRAFT.

	Weight, lb.			
Aircraft	PDCYL	Load-Carrying Structure	Primary Structure	Total Structure
720	6622	9013	13336	19383
727	5848	8790	12424	17586
737	3425	5089	7435	11831
747	28507	39936	55207	72659
880	8612	8705	9452	13507
DC-8	9517	13312	18584	24886
MD-11	20608	25970	34999	54936
MD-83	7488	9410	11880	16432
L-1011	21762	28352	41804	52329

TABLE 5. WING WEIGHT BREAKDOWNS FOR NINE TRANSPORT AIRCRAFT.

	Weight, lb.			
Aircraft	PDCYL	Load-Carrying Structure	Primary Structure	Total Structure
720	13588	11747	18914	23528
727	8336	8791	12388	17860
737	5706	5414	7671	10687
747	49285	50395	68761	88202
880	12319	9241	14144	17585
DC-8	21892	19130	27924	35330
MD-11	30561	35157	47614	62985
MD-83	6888	8720	11553	15839
L-1011	24234	28355	36101	46233

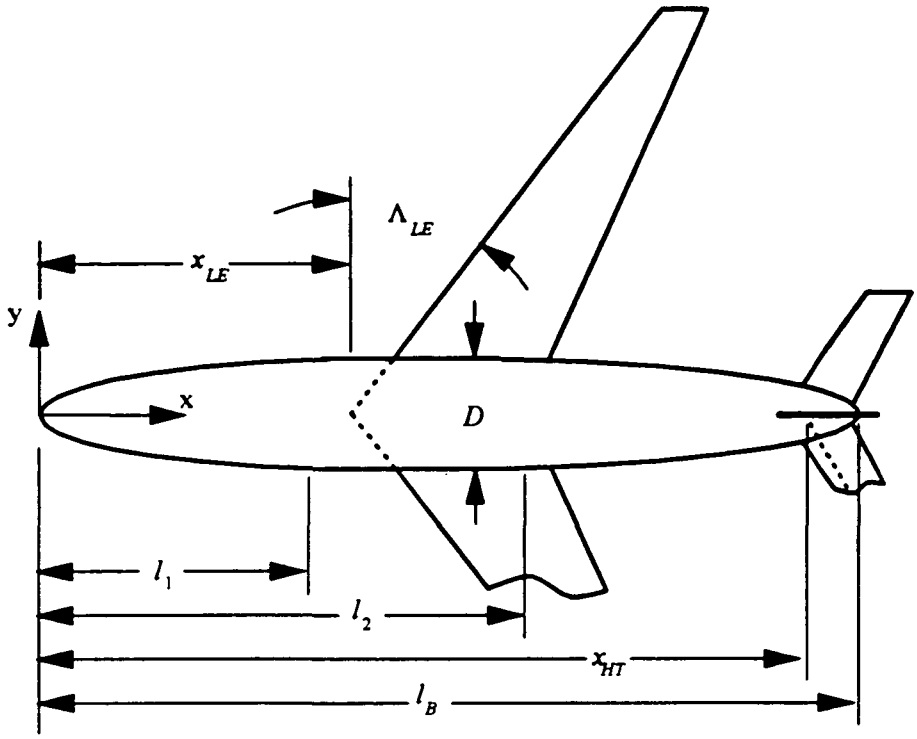

Figure 1. The Body Geometry, Including Cylindrical Midbody.

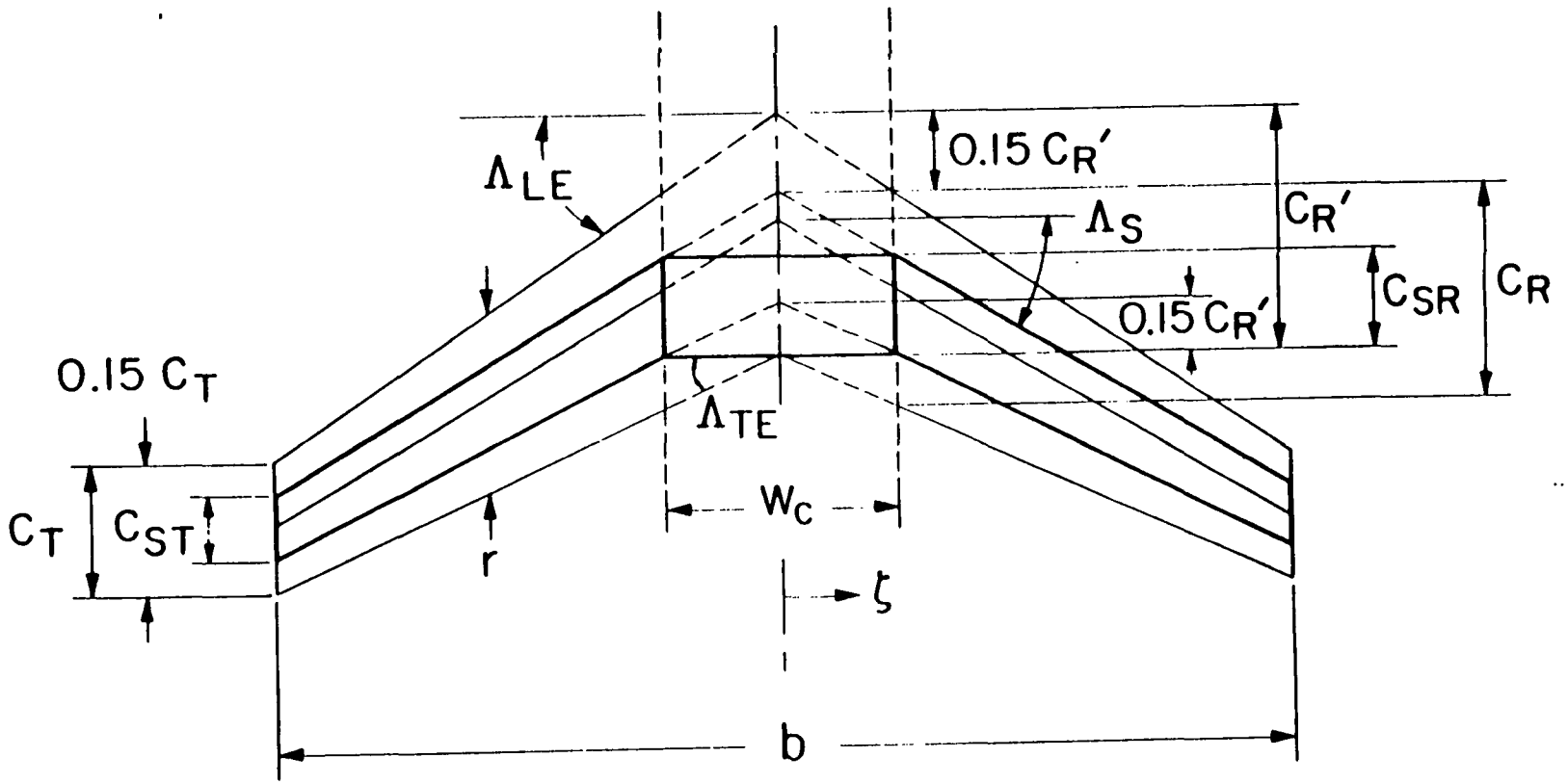

Figure 2. Wing Structural Planform Geometry.

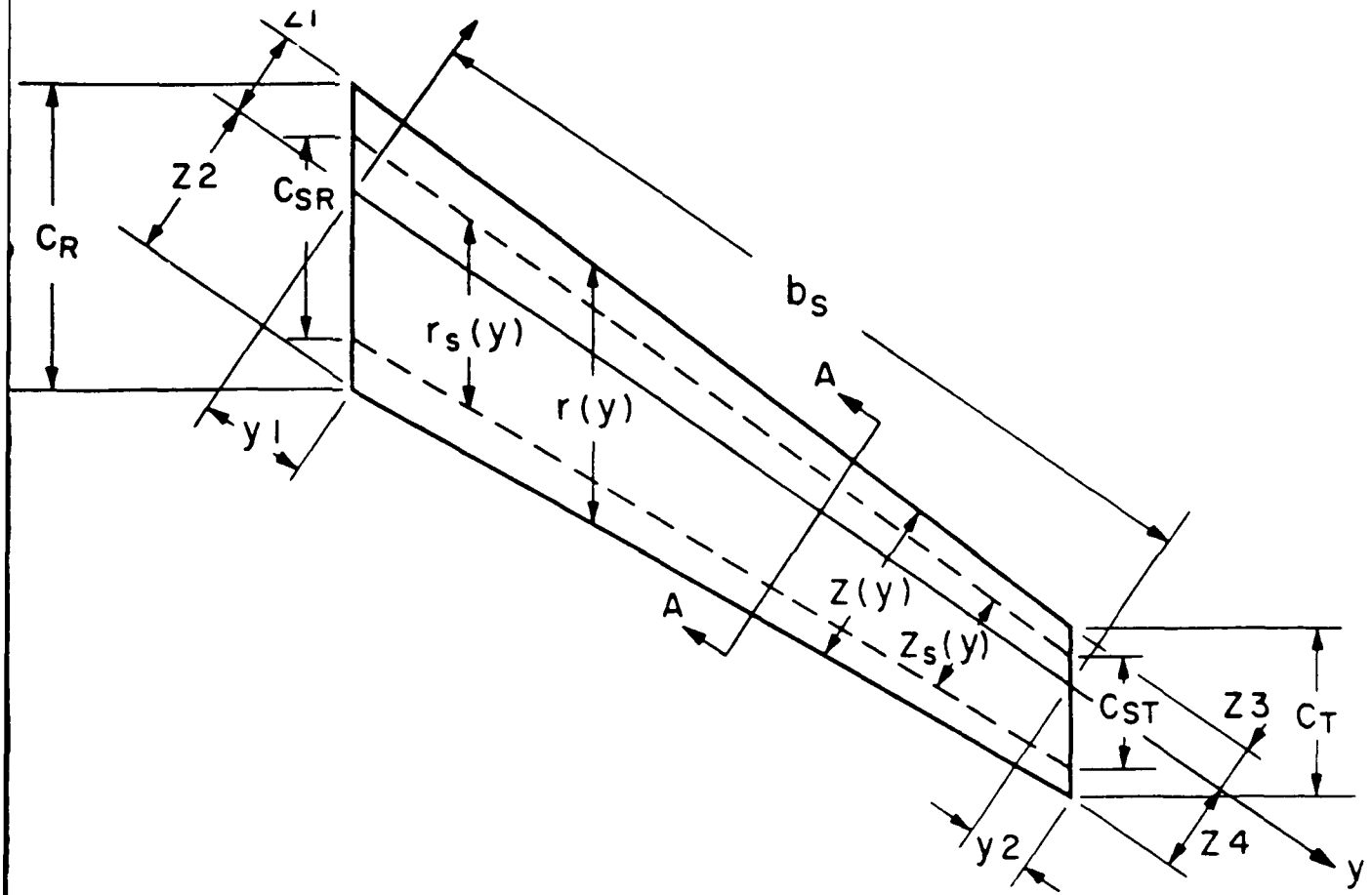

Figure 3. Wing Coordinate System.

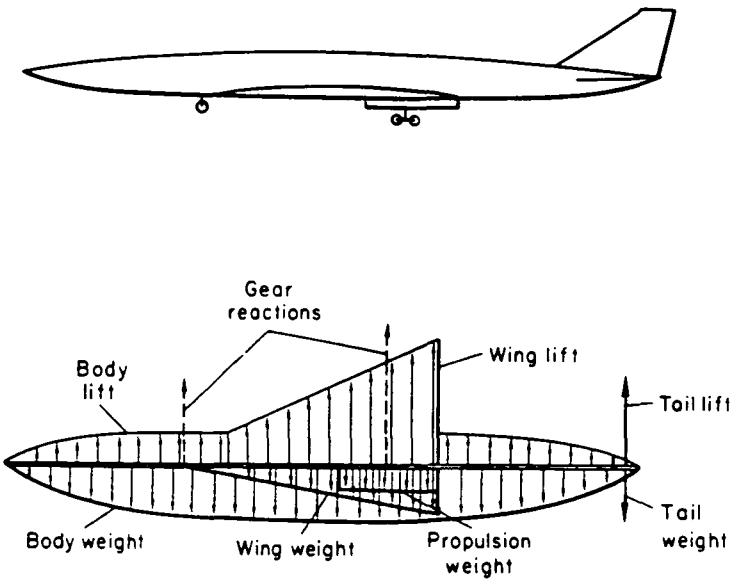

Figure 4. Loading Model.

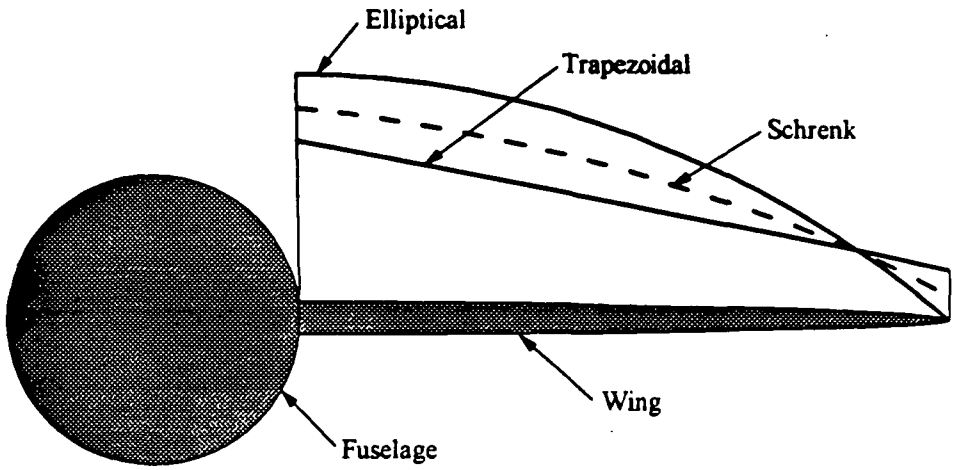

Figure 5. Spanwise Wing Lift-load Distributions.

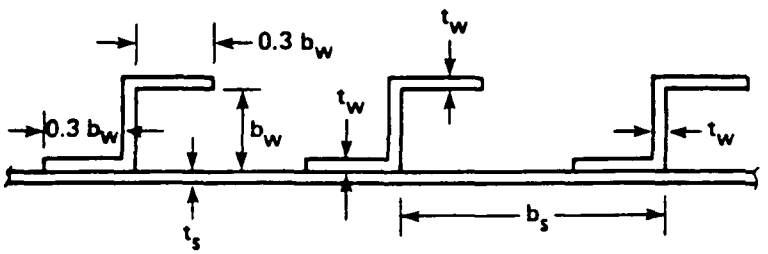

Figure 6. Typical Z-Stiffened Shell Geometry.

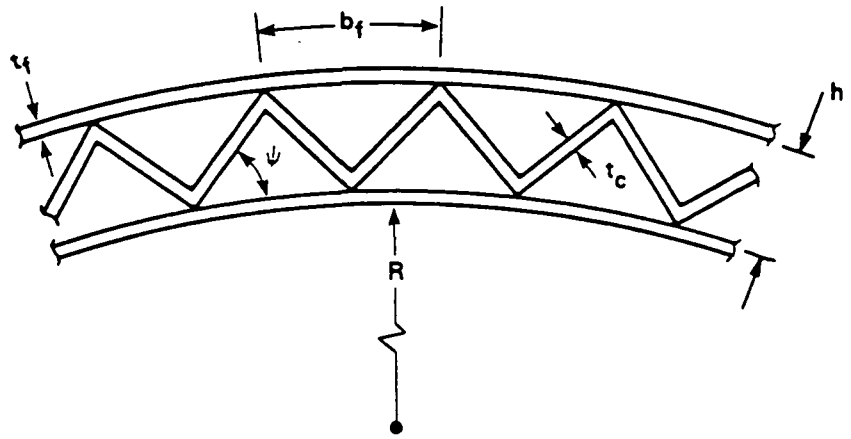

Figure 7. Truss-Core Sandwich Geometry.

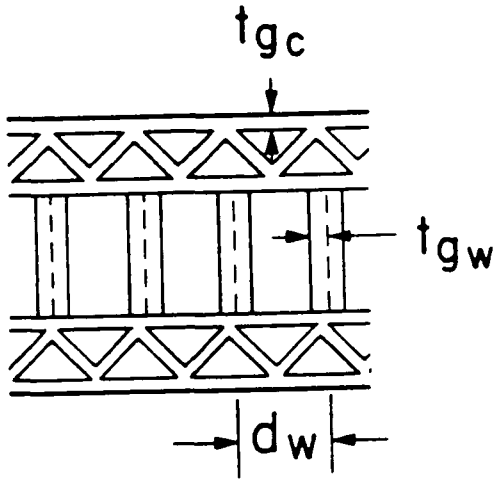

Figure 8. Wing Structural Concept.

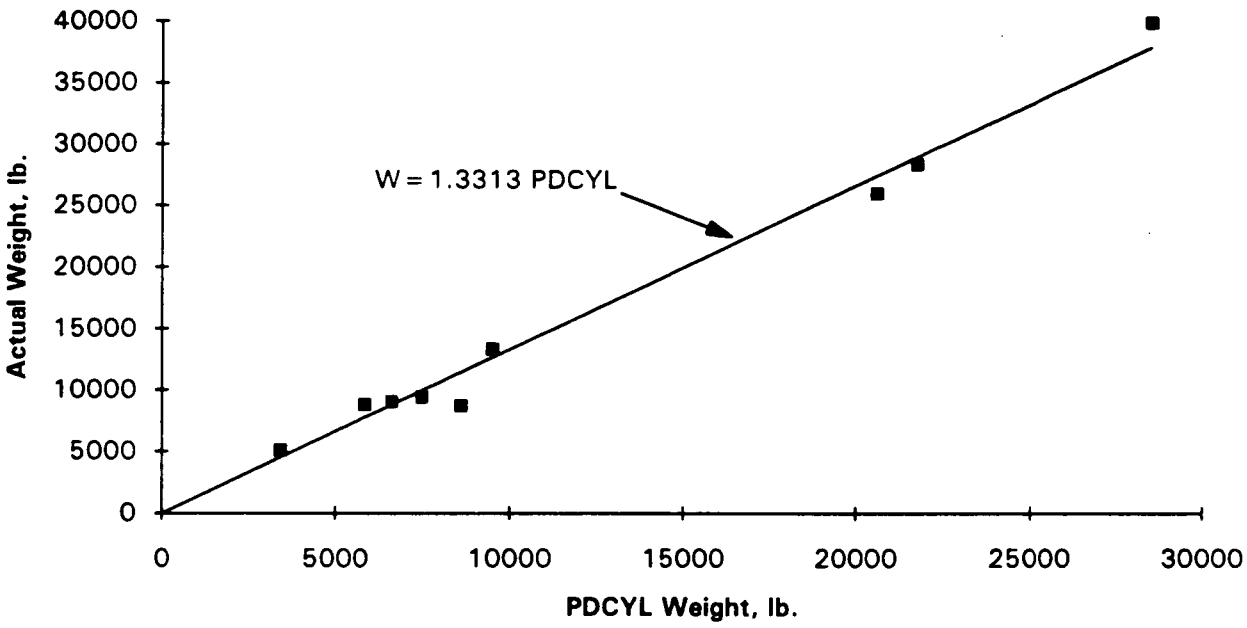

Figure 9. Fuselage Load-Carrying Structure and Linear Regression.

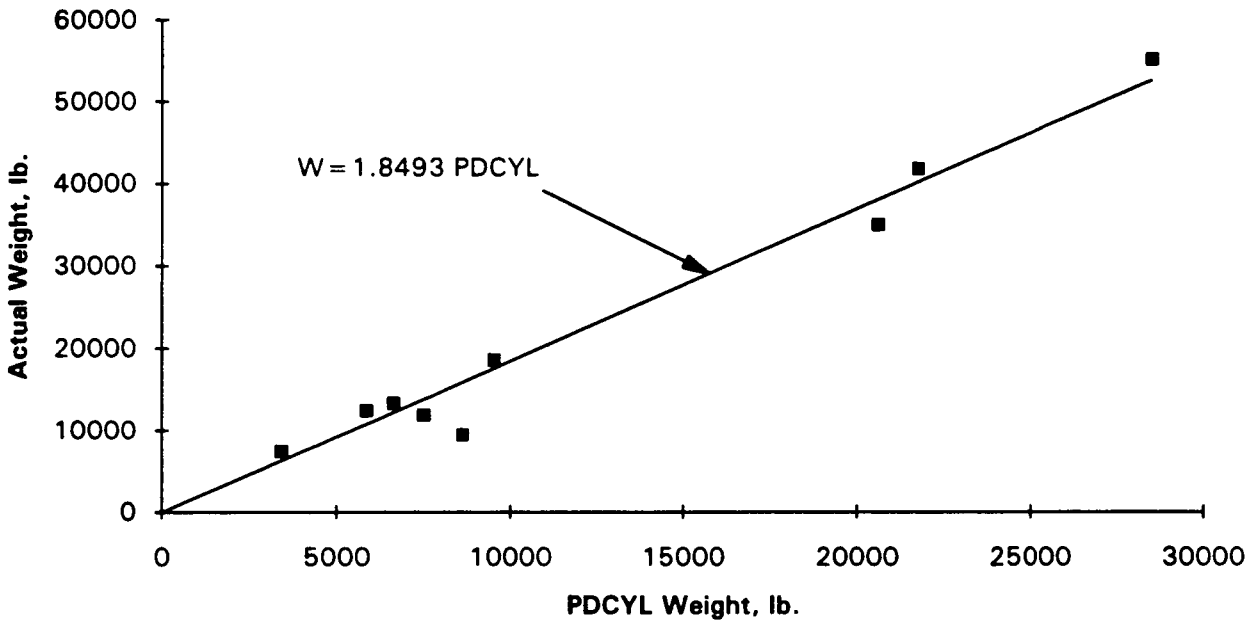

Figure 10. Fuselage Primary Structure and Linear Regression.

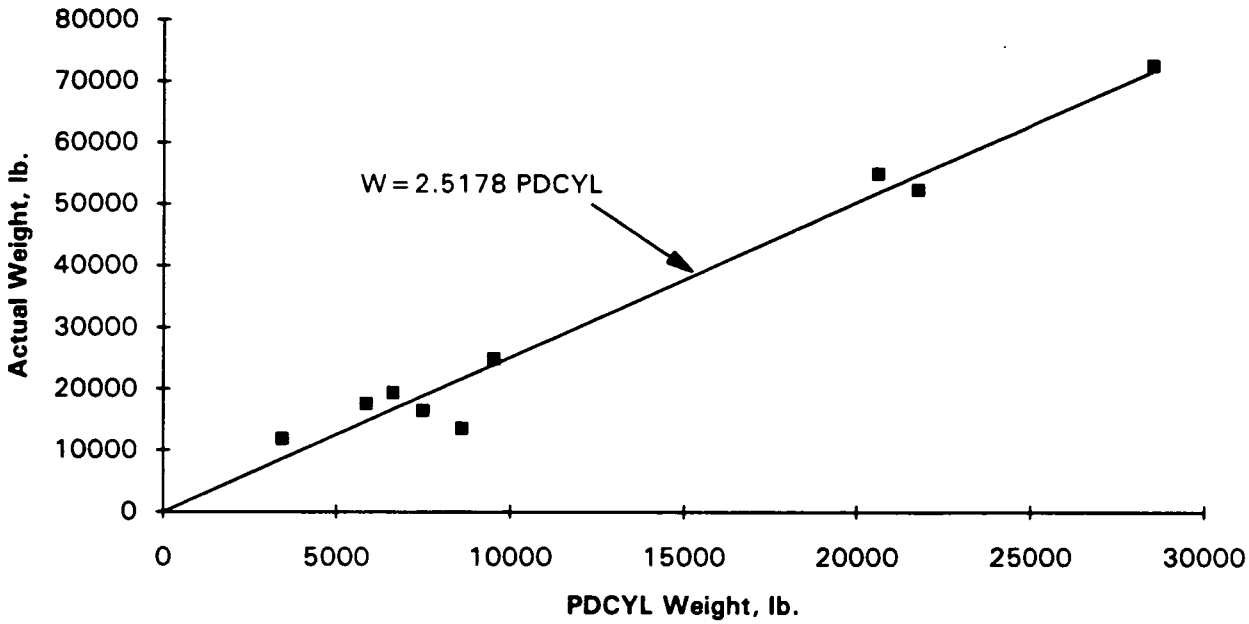

Figure 11. Fuselage Total Structure and Linear Regression.

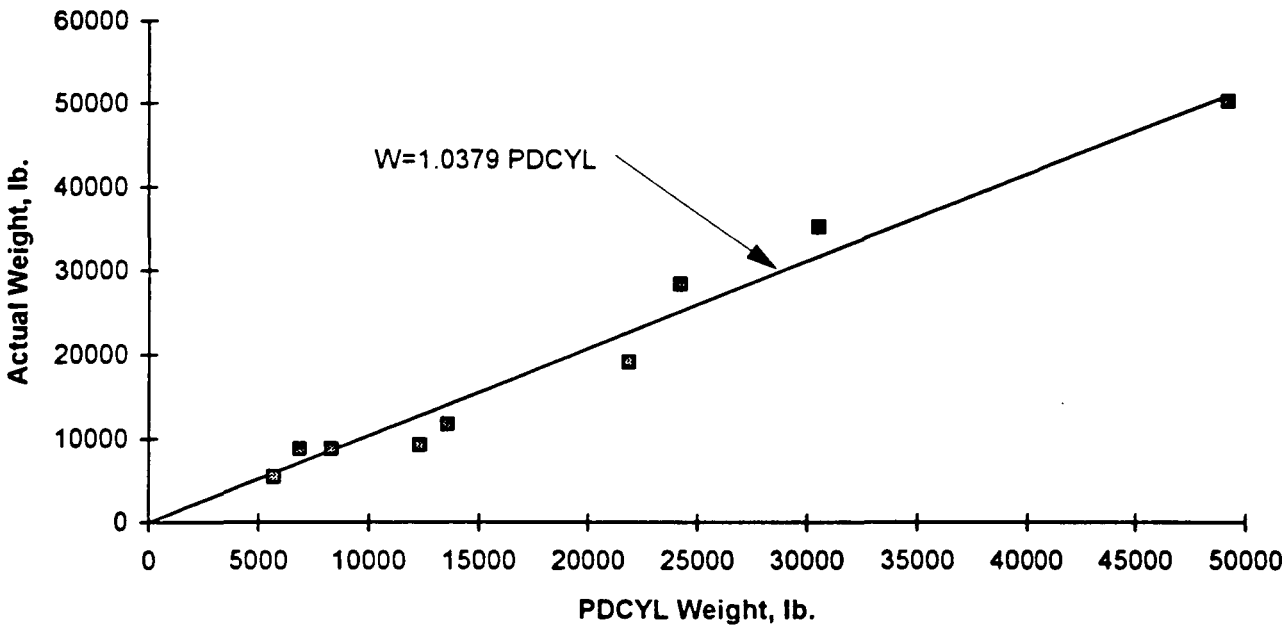

Figure 12. Wing Load-Carrying Structure and Linear Regression.

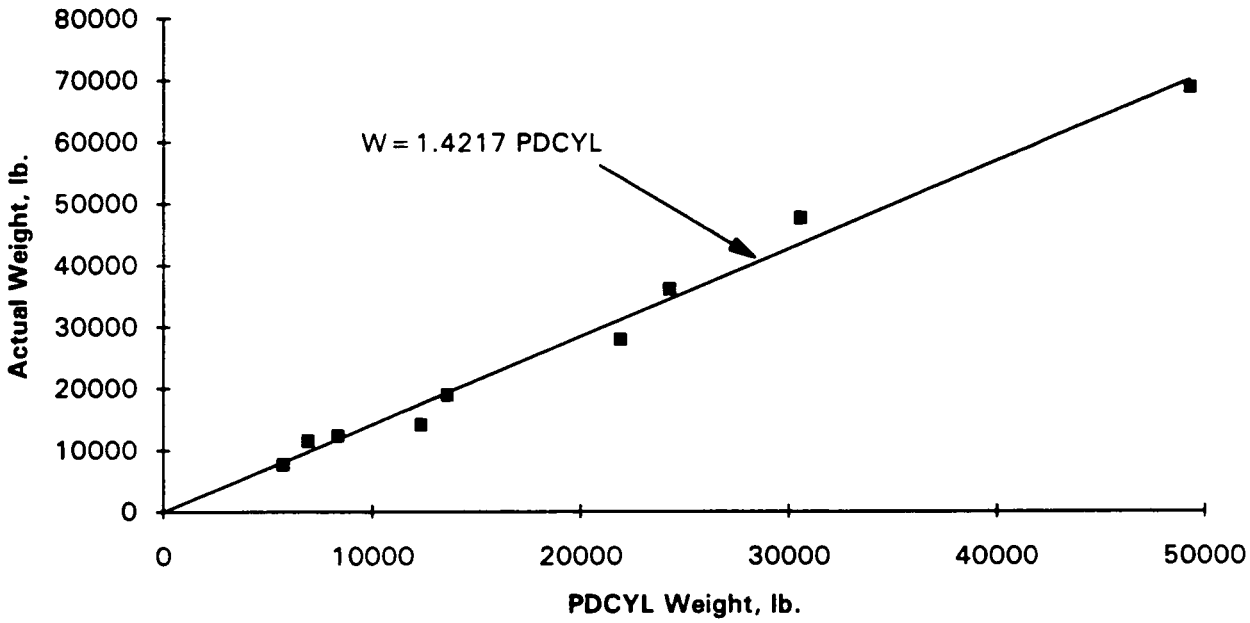

Figure 13. Wing Primary Structure and Linear Regression.

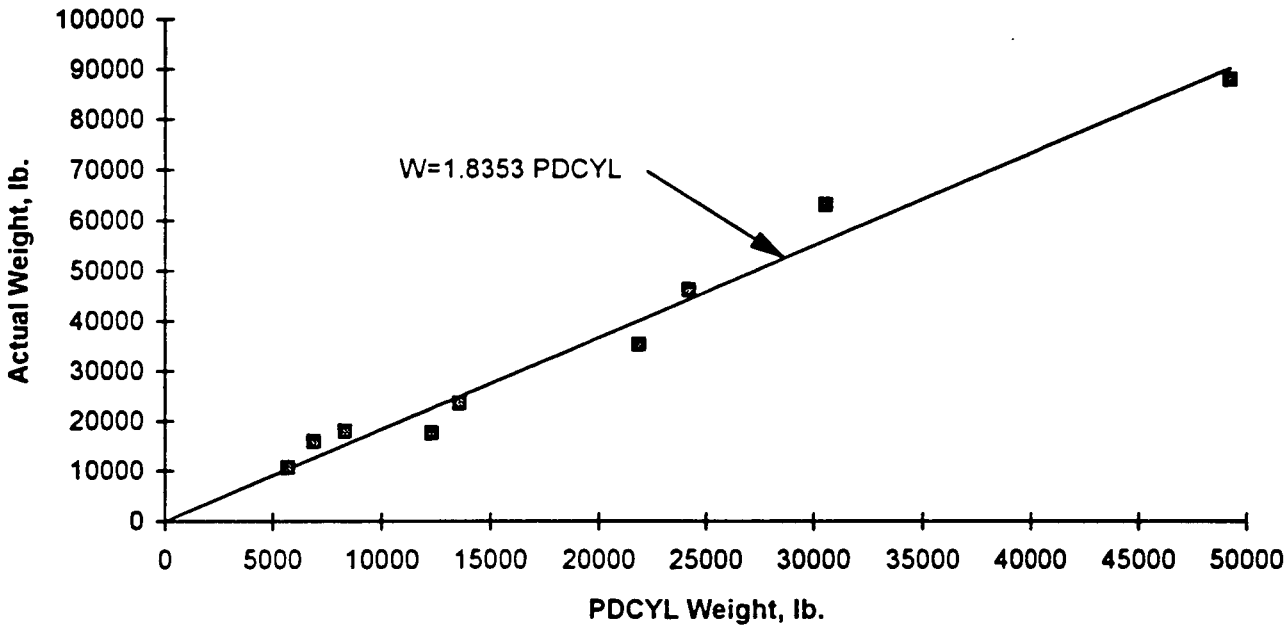

Figure 14. Wing Total Structure and Linear Regression.

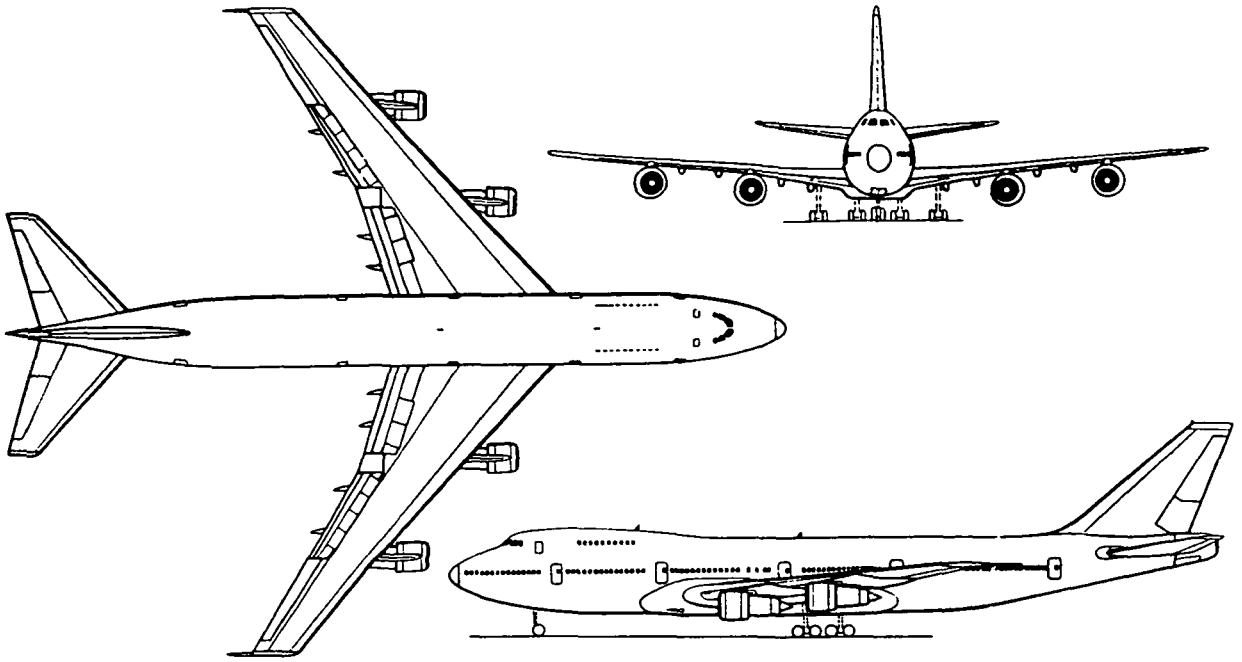

Figure 15. 747 Configuration.

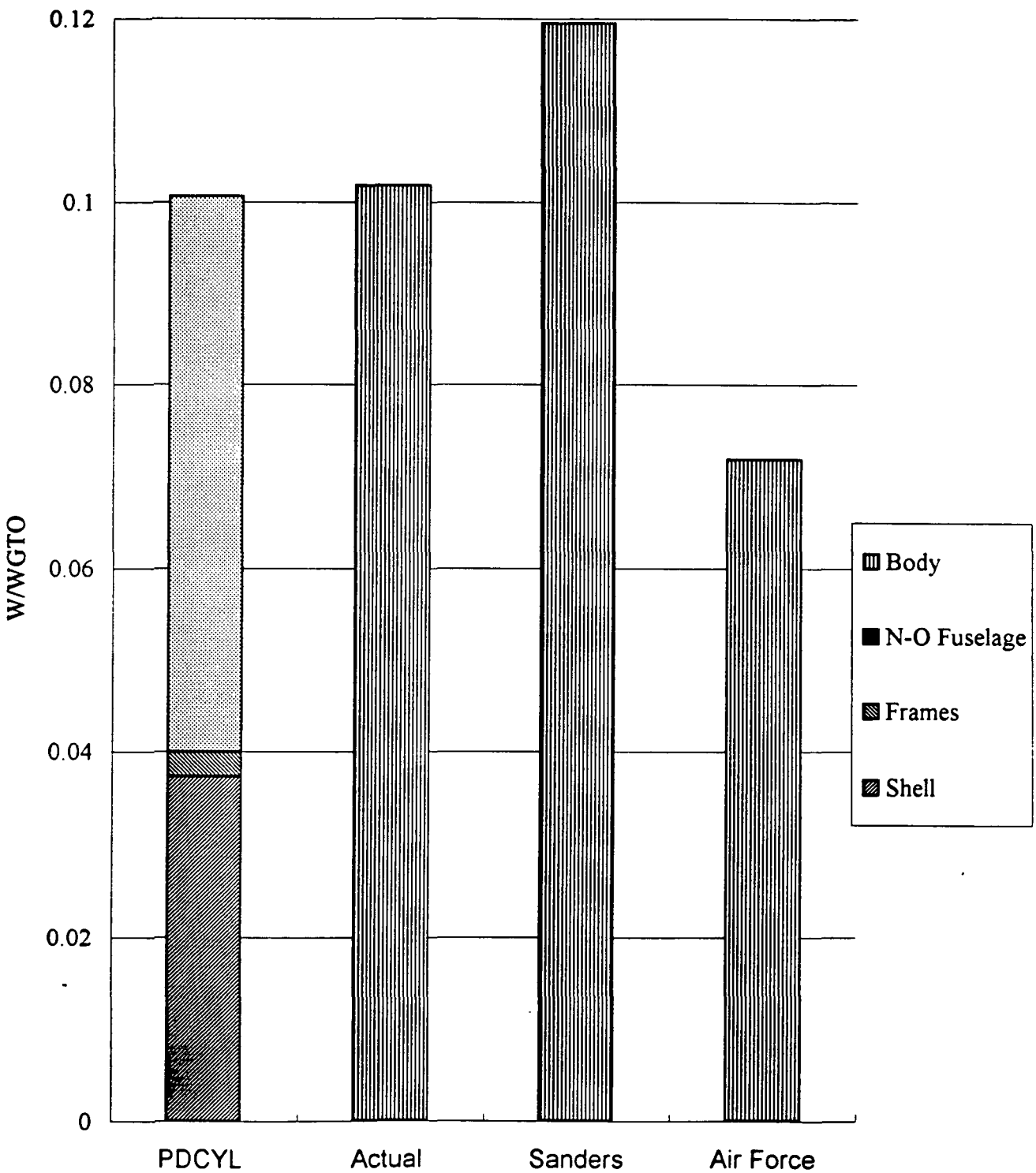

Figure 16a. 747-21P FUSELAGE Unit Weights.

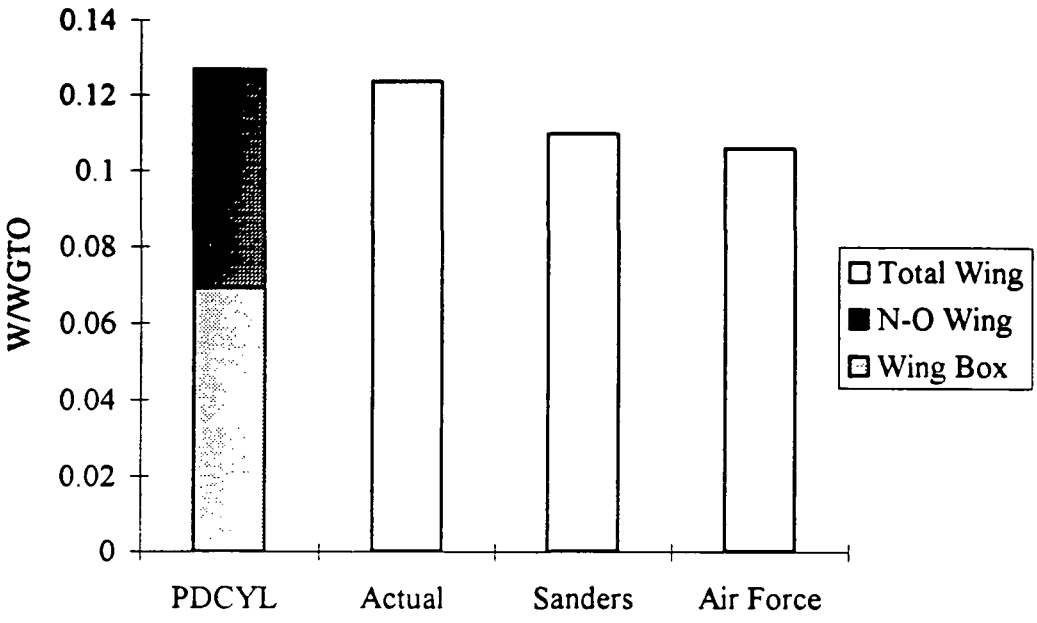

Figure 16b. 747-21P Wing Unit Weights.

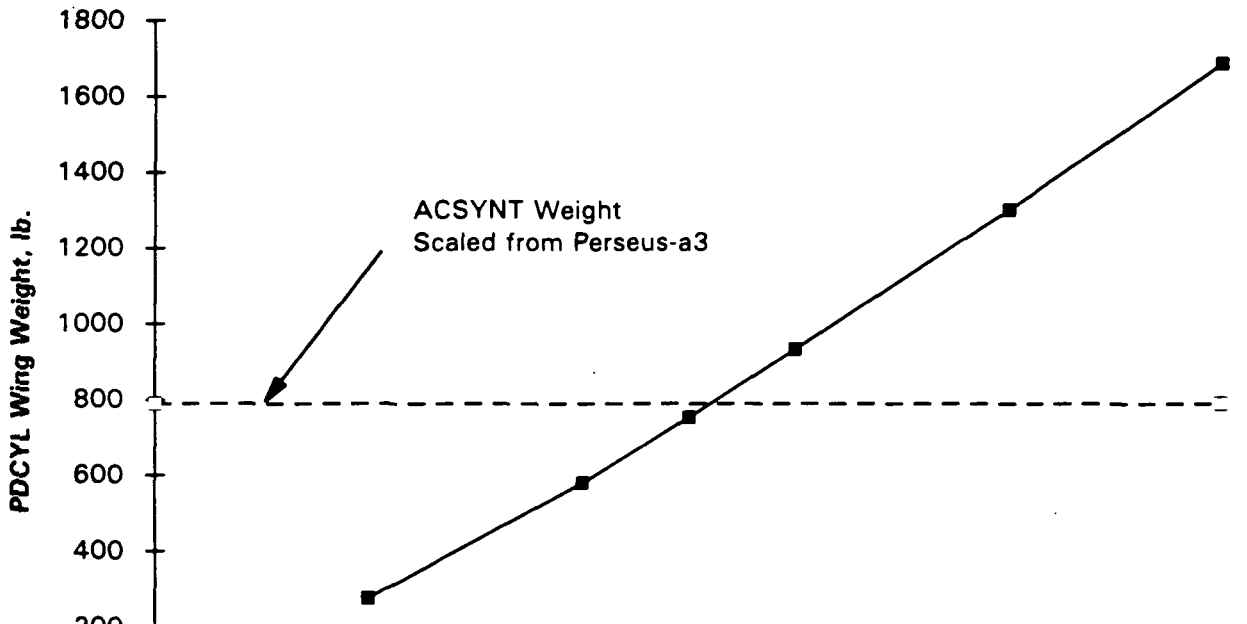

Figure ~~18~~ 17. Variation in wing weight as a function of structural box length.

APPENDIX A: User's Manual, Example

Description

The purpose of this appendix is to give a detailed example of the input procedure used to allow PDCYL to calculate fuselage and wing weights for a sample transport aircraft during an ACSYNT run. A sample output from PDCYL will also be given. The Boeing 747-21P will be used for the example. The layout of the 747-21P is shown in Figure 15. The weights of the load-carrying portions of the fuselage and wing box for the 747-21P will be calculated by PDCYL and scaled by the respective nonoptimum factors developed earlier to give estimates for the weights of the fuselage and wing. A comparison between methods currently used by ACSYNT to estimate fuselage and wing weights and PDCYL output will be made with the corresponding actual weights of the 747-21P.

Input

PDCYL requires input from both the existing ACSYNT data structure and an additional namelist containing data required by PDCYL which are not contained within the current ACSYNT format. There are three steps to run PDCYL within ACSYNT. First, the aircraft type is specified in the ACSYNT Control input. Currently the Transport Aircraft type is used. Second, data within ACSYNT module namelists is required. The ACSYNT Geometry, Trajectory, and Weights modules supply data for PDCYL execution. PDCYL uses the WING, HTAIL, VTAIL, FUS, WPOD, and FPOD namelists from the Geometry module. From the Trajectory module, the TRDATA namelist is used. From the Weights module the OPTS namelist is used. Third, data from the PDCYLIN namelist is used.

Variables used from ACSYNT namelists and the PDCYLIN namelist are given in Table 6 and Table 7, respectively. Default values for all variables are also given. These default values match the Boeing 747-21P. Key configuration parameters are given for each of the nine aircraft used in the validation study in Table 8. An example of the PDCYLIN namelist input for the 747-21P is shown in Figure 16.

Output

PDCYL weights output begins with the wing box and carrythrough structure analysis. The wing is sized during a quasi-static pull-up maneuver where the load factor is set equal to the ultimate load factor (nominally 3.75). Wing output contains three parts. First is the overall geometrical configuration. Second is a detailed station-by-station bending, shear, and torsion analysis and corresponding geometrical sizing along the span. Third is the detailed geometrical layout, loading, and weight breakdown of the carrythrough structure, weight breakdown of the wing components and deflection of the wingtip. This wing weight is multiplied by the non-optimum factor and returned to

ACSYNT. An example of the PDCYL wing weight output for the 747-21P is shown in Figure 17.

Next, the fuselage is analyzed. Fuselage output contains four parts. First is the overall geometrical layout and weight breakdown. Second is a station-by-station bending, shear and axial stress analysis. Up to three load cases are investigated. In order they are a quasi-static pull-up maneuver, a landing maneuver, and travel over runway bumps. Third, the envelope of worst case loading is shown for each station, from which the shell and frames are sized. Corresponding unit weight breakdowns are also given. As an option, the detailed geometric configuration at each station may be output. Fourth, weights summaries are given for the top and bottom sections of the fuselage (nominally the same). These summaries are then averaged to give the weight summary of the entire fuselage. The fuselage weight, including the corresponding non-optimum factor, is returned to ACSYNT. An example of the PDCYL fuselage weight output for the 747-21P is shown in Figure 18.

Figure 19a shows a comparison between fuselage weight estimates from the Sanders equation, the Air Force equation, and PDCYL with the actual fuselage weight of the 747-21P. Figure 19b shows a similar comparison for the wing weight. SLOPE and TECH factors were set to one for the comparisons in Figures 19a and 19b.

TABLE 6. ACSYNT VARIABLES.

1. Geometry module

Namelist WING

Variable	Type	Dimensio	Description	Units/Comment	Default (747)
SWEEP	float	1	Sweep of wing.	Degrees	37.17
KSWEEP	integer	1	1->Referenced to the leading edge. 2 -> Referenced to the quarter chord. 3-> Referenced to the trailing edge.		2
AR	float	1	Aspect Ratio of wing.		6.96
TAPER	float	1	Taper Ratio of wing.		0.2646
TCROOT	float	1	Thickness-to-chord ratio at the root		0.1794
TCTIP	float	1	Thickness-to-chord ratio at the tip		0.078
ZROOT	float	1	Elevation of MAC above fuselage reference plane, measured as a fraction of the local fuselage radius.		-0.1
AREA	float	1	Planform Area of wing.	ft^2	5469
DIHED	float	1	Dihedral angle of wing.	Degrees	7
XWING	float	1	Ratio of distance measured from nose to leading edge of wing to total fuselage length.		0.249

Namelist HTAIL (horizontal tail)

Variable	Type	Dimensio	Description	Units/Comment	Default (747)
SWEEP	float	1	Sweep of tail	Degrees	34.29
KSWEEP	integer	1	1->Referenced to the leading edge. 2 -> Referenced to the quarter chord. 3-> Referenced to the trailing edge.		2
AR	float	1	Aspect Ratio of the horizontal wing.	(span)^2/Area	3.625
TAPER	float	1	Taper Ratio of the horizontal wing.	tip chord/root chord	0.25
TCROOT	float	1	Thickness-to-chord ratio at the root		0.11
TCTIP	float	1	Thickness-to-chord ratio at the tip.		0.08
ZROOT	float	1	Elevation of MAC above fuselage reference plane, measured as a fraction of the local fuselage radius.		0.69
AREA	float	1	Planform Area of the horizontal win	ft^2	1470
XHTAIL	float	1	Position for trailing edge of tail root chord. If ZROOT .LE. 1, then XHTAIL is given as a fraction of body length. Else, XHTAIL is given as a fraction of the local vertical tail chord.		1

Namelist VTAIL (vertical tail)

Variable	Type	Dimensio	Description	Units/Comment	Default (747)
SWEEP	float	1	Sweep of vertical tail	Degrees	45.73
KSWEEP	integer	1	1-> Referenced to the leading edge. 2 ->Referenced to the quarter chord. 3-> Referenced t the trailing edge		2
AR	float	1	Aspect Ratio of vertical tail.	(span)^2/Area	1.247
TAPER	float	1	Taper Ratio of vertical tail.	tip chord/root chord	0.34
TCROOT	float	1	Thickness-to-Chord ratio at root.		0.1298
TCTIP	float	1	Thickness-to-Chord ratio at tip.		0.089
ZROOT	float	1	Elevation of MAC above fuselage reference plane, measured as a fraction of the local fuselage radius.		0.6
AREA	float	1	Planform Area of vertical tail.	ft.^2	830

Namelist FUS (fuselage)

Variable	Type	Dimensio	Description	Units/Comment	Default (747)
FRN	float	1	Fineness Ratio of the nose section.	(Length/Diameter)	2.13
FRAB	float	1	Fineness Ratio of after-body section	(Length/Diameter)	3.29
BODL	float	1	Length of fuselage	ft.	225.167
BDMAX	float	1	Maximum diameter of fuselage	ft.	20.2

Namelist WPOD (wing-mounted propulsion pod)

Variable	Type	Dimensio	Description	Units/Comment	Default (747)
DIAM	float	1	Engine Diameter.	ft.	6.2
LENGTH	float	1	Length of engine pod.	ft.	15
X	float	1	X location of nose of pod relative to leading edge of wing, given as a fraction of local chord of wing. (>0 if face of pod is behind leading edge of wing.)		-0.631
Y	float	1	Y location of center of pod, given as a fraction of semispan, measured from body centerline.		0.241
Z	float	1	Z location of center of pod above wing local chord, given as fraction of maximum pod diameter.		-0.83
SWFACT	float	1	Wetted Area multiplier.		

Namelist FPOD (fuselage-mounted propulsion pod)

Variable	Type	Dimensio	Description	Units/Comment	Default (747)
DIAM	float	1	Engine Diameter.	ft.	N/A
LENGTH	float	1	Length of engine pod.	ft.	N/A
SOD	float	1	Stand-off-distance, the distance from the pod wall to the fuselage wall, given as a fraction of maximum pod radius.		N/A
THETA	float	1	Angular orientation of pod, THETA measured positive up from the horizontal reference plane.	Degrees	N/A
X	float	1	X location of nose relative to nose of pod, given as a fraction of body length.		N/A

2. Trajectory module

Namelist TRDATA (used for load factors)

Variable	Type	Dimensio	Description	Units/Comment	Default (747)
DESLF	float	1	Design load factor	N/A	2.5
ULTLF	float	1	Ultimate load factor, usually 1.5*DESLF	N/A	3.75

3. Weights module

Namelist OPTS

Variable	Type	Dimensio	Description	Units/Comment	Default (747)
WGTO	float	1	Gross-take-off-weight.	lb.	713000
WE	float	1	Total Weight of propulsion system. (includes both wing and fuselage mounted engines.)	lb	44290

TABLE 7. PDCYL VARIABLES.

Namelist PDCYLIN

Wing

Material Properties

Variable	Type	Dimensio	Description	Units/Comment	Default (747)
PS	float	1	Plasticity Factor.		1
TMGW	float	1	Min. gage thickness for the wing	inches	0.2
EFFW	float	1	Buckling efficiency of the web.		0.656
EFFC	float	1	Buckling efficiency of the covers		1.03
ESW	float	1	Young's Modulus for wing material	psi	1.07E+07
FCSW	float	1	Ult. compressive strength of wing	psi	54000
DSW	float	1	Density of the wing material.	lb./in^3	0.101
KDEW	float	1	Knock-down-factor for Young's Modulus.		1
KDFW	float	1	Knock-down-factor for Ultimate strength.		1

Geometric Parameters

Variable	Type	Dimensio	Description	Units/Comment	Default (747)
ISTAMA	integer	1	1 -> the position of the wing is unknown. 2 -> the position of the wing is known		2
CS1	float	1	Position of structural wing box from leading edge as % of root chord.		0.088
CS2	float	1	Position of structural wing box from trailing edge as % of root chord.		0.277

Structural Concept

Variable	Type	Dimensio	Description	Units/Comment	Default (747)
CLAQR	float	1	Ratio of body lift to wing lift	For subsonic aircraf CLAQR ~ 0.0	0.001
IFUEL	integer	1	1 -> no fuel is stored in the wing 2 -> fuel is stored in the wing		2
CWMAN	float	1	Design maneuver load factor	6.25E+05	1
CF			Shanley's const. for frame bending		6.25E-05

Fuselage

Structural Concept

Variable	Type	Dimensio	Description	Units/Comment	Default (747)
CKF	float	1	Frame stiffness coefficient.		5.24
EC	float	1	Power in approximation equation for buckling stability.		2.36
KGC	float	1	Buckling coefficient for component general buckling of stiffener web panel.		0.368
KGW	float	1	Buckling coefficient for component local buckling of web panel.		0.505

KCON(T/B)	STRUCTURAL GEOMETRY CONCEPT	Default (747)
2	Simply stiffened shell, frames, sized for minimum weight in buckling	4
3	Z-stiffened shell, frames, best buckling	
4	Z-stiffened shell, frames, buckling-minimum gage compromise	
5	Z-stiffened shell, frames, buckling-pressure compromise	
6	Truss-core sandwich, frames, best buckling	
8	Truss-core sandwich, no frames, best buckling	
9	Truss-core sandwich, no frames, buckling-minimum gage-pressure compromise	

Material Properties

Variable	Type	Dimensio	Description	Units/Comment	Default (747)
FTS(T/B)	float	4	Tensile Strength on (top/bottom)		58500
FCS(T/B)	float	4	Compressive Strength		54000
ES(T/B)	float	4	Young's Modulus for the shells		1.07E+07
EF(T/B)	float	4	Young's Modulus for the frames		1.07E+07
DS(T/B)	float	4	Density of shell material on (t/b)		0.101
DF(T/B)	float	4	Density of frame material		0.101
TMG(T/B)	float	4	Minimum Gage thickness		0.071
KDE	float	1	Knock-down-factor for modulus		1
KDF	float	1	Knock-down-factor for strength		1

Geometric Parameters

Variable	Type	Dimensio	Description	Units/Comment	Default (747)
CLBR1	float	1	Fuselage break point as a fraction of total fuselage length		1.1
ICYL	integer	1	1 -> modeled with a mid-body cylinder. Else uses two power-law bodies back-to-back		1

Loads

Variable	Type	Dimensio	Description	Units/Comment	Default (747)
AXAC	float	1	Axial Acceleration.	g's	0
CMAN	float	1	Weight fraction at maneuver.		1
ILOAD	integer	1	1 -> analyze maneuver only. 2 -> analyze maneuver and landing only. 3 -> analyze bump, landing, and maneuver.		3
PG(T/B)	float	12	Fuselage gage pressure on (top/bot)		13.65
WFBUMP	float	1	Weight fraction at bump.		0.001
WFLAND	float	1	Weight fraction at landing.		0.9

Landing Gear

Variable	Type	Dimensio	Description	Units/Comment	Default (747)
VSINK	float	1	Design sink velocity at landing.		10
STROKE	float	1	Stroke of landing gear.		2.21
CLRG1	float	1	Length fraction of nose landing gear.		0.1131
CLRG2	float	1	Length fraction of main landing gear measured as a fraction of total fuselage length.		0.466
WFGR1	float	1	Weight fraction of nose landing gear.		0.0047
WFGR2	float	1	Weight fraction of main landing gear.		0.0398
IGEAR	integer	1	1 -> main landing gear located on fuselage 2 -> main landing gear located on wing		2
GFRL	float	1	Ratio of force taken by nose landing gear to force taken by main gear at landing.		0.001
CLRGW1 CLRGW2	float float	1 1	Position of wing gear as a fraction structural semispan.	If only 1 wing gear, set CLRGW2 = 0.0	0.064 0.1844

Tails

Variable	Type	Dimensio	Description	Units/Comment	Default (747)
ITAIL	integer	1	1 -> control surfaces mounted on tail. 2 -> control surfaces mounted on wing.		1

Weights

Variable	Type	Dimensio	Description	Units/Comment	Default (747)
WTFF	float	1	Weight fraction of fuel.		0.262
CBUM	float	1	Weight fraction at bump.		1
CLAN	float	1	Weight fraction at landing.		0.791

Factors

Variable	Type	Dimensio	Description	Units/Comment	Default (747)
ISCHRENK	integer	1	1 -> use Schrenk load distribution on wing else -> use trapezoidal distribution.		1
ICOMND	integer	1	1 -> print gross shell dimensions envelope 2 -> print detailed shell geometry.		1
WGNO	float	1	Non-optimal factor for wing (including the secondary structure.)		1
SLFMB	float	1	Static load factor for bumps.		1.2
WMIS	float	1	Volume component of secondary structure.		0
WSUR	float	1	Surface area component of secondary structure.		0
WCW	float	1	Factor in weight equation for non-optimal weights.		1
WCA	float	1	Factor in weight equation multiplying surface areas for non-optimal weights.		0
NWING	integer	1	Number of wing segments for analysis.		40

TABLE 8. KEY CONFIGURATION PARAMETERS FOR NINE TRANSPORT AIRCRAFT.

ACSYNT INPUT PARAMETERS

1. Geometry module

Namelist WING

Variable	720	727	737	747	880	dc8	md11	md83	l-1011
SWEEP	35	32	25	37.17	33.5	30.6	35	24.16	35
KSWEEP	2	2	2	2	2	2	2	2	2
AR	6.958	7.67	8.21	6.96	7	7.52	7.5	9.62	6.98
TAPER	0.333	0.2646	0.2197	0.2646	0.2494	0.1974	0.255	0.156	0.3
TCROOT	0.1551	0.154	0.126	0.1794	0.08	0.1256	0.167	0.138	0.13
TCTIP	0.0902	0.09	0.112	0.078	0.121	0.105	0.093	0.12	0.09
ZROOT	-1	-1	-0.25	-0.1	-1	-1	-0.79	-1	-1
AREA	2460	1587	1005	5469	2000	2927	3648	1270	3590
DIHED	3	3	6	7	7	3	6	3	3
XWING	0.2963	0.376	0.35	0.249	0.301	0.302	0.218	0.468	0.359

Namelist HTAIL

Variable	720	727	737	747	880	dc8	md11	md83	l-1011
SWEEP	35	31.05	30.298	34.29	33.44	35	35.5	30.8	3.5
KSWEEP	2	2	2	2	2	2	2	2	2
AR	3.15	3.4	4.04	3.625	3.87	4.04	3.43	4.88	4
TAPER	0.457	0.383	0.3974	0.25	0.286	0.329	0.412	0.357	0.33
TCROOT	0.11	0.11	0.132	0.11	0.095	0.095	0.143	0.107	0.095
TCTIP	0.09	0.0894	0.108	0.08	0.08	0.08	0.1067	0.08	0.08
ZROOT	0.5	2	0.67	0.69	0.805	0.25	0.6875	2	0.5
AREA	500	376	312	1470	1470	559	920	314	1282
XHTAIL	1	0.95	0.8532	0.974	0.84	1	0.96	0.98	0.9265

Namelist VTAIL

Variable	720	727	737	747	880	dc8	md11	md83	l-1011
SWEEP	35	48.4	34.16	45.73	33.4	35	38	39.4	35
KSWEEP	2	2	2	2	2	2	2	2	2
AR	1.45	1.09	1.814	1.247	1.524	1.905	1.73	1.48	1.6
TAPER	0.484	0.641	0.3024	0.34	0.333	0.292	0.343	0.844	0.3
TCROOT	0.11	0.11	0.1322	0.1298	0.1	0.096	0.105	0.127	0.11
TCTIP	0.0896	0.09	0.1081	0.089	0.08	0.101	0.125	0.103	0.0896
ZROOT	0.95	0.2	0	0.6	0	0.95	0.85	0.9	0.95
AREA	312.4	356	225	830	295	352	605	550	550

Namelist FUS

Variable	720	727	737	747	880	dc8	md11	md83	l-1011
FRN	1.81	2	1.915	2.13	1.93	2	1.67	1.15	1.76
FRAB	2.86	2.831	2.361	3.29	2.57	2.9375	2.27	2.73	2.96
BODL	130.5	116.67	90.58	225.167	124.167	153	192.42	135.5	177.67
BDMAX	14.21	14.2	13.167	20.2	15	13.5	19.75	11.44	19.583

Namelist WPOD (inboard)

Variable	720	727	737	747	880	dc8	md11	md83	l-1011
DIAM	3.24	N/A	3.542	6.2	2.633	4.42	9.04	N/A	3.24
LENGTH	12.15	N/A	10	15	12.147	12.15	18.08	N/A	12.15
X	0.917	N/A	-0.22	-0.631	-1.09	-0.4	-0.558	N/A	-0.639
Y	0.386	N/A	0.343	0.241	0.697	0.352	0.33125	N/A	0.461
Z	-1	N/A	-0.548	-0.83	-0.78	-1.2	-0.5	N/A	-1
SWFACT	1	N/A	1	1	1	1	1	N/A	1

Namelist WPOD (outboard)

Variable	720	727	737	747	880	dc8	md11	md83	l-1011
DIAM	3.24	N/A	N/A	6.2	2.633	4.42	N/A	N/A	N/A
LENGTH	12.15	N/A	N/A	15	1.147	12.15	N/A	N/A	N/A
X	0.917	N/A	N/A	-0.631	-0.78	-0.955	N/A	N/A	N/A
Y	0.674	N/A	N/A	0.441	0.371	0.61	N/A	N/A	N/A
Z	-1	N/A	N/A	-0.83	-0.78	-1.2	N/A	N/A	N/A
SWFACT	1	N/A	N/A	1	1	1	N/A	N/A	N/A

Namelist FPOD

Variable	720	727	737	747	880	dc8	md11	md83	l-1011
DIAM	N/A	3.542	N/A	N/A	N/A	N/A	9.04	6.6	3.24
LENGTH	N/A	10	N/A	N/A	N/A	N/A	40.68	20.34	12.15
SOD	N/A	0	N/A	N/A	N/A	N/A	0	0	0
THETA	N/A	90	N/A	N/A	N/A	N/A	90	0	90
X	N/A	0.699	N/A	N/A	N/A	N/A	0.812	0.746	0.725
SYMCO	N/A	1	N/A	N/A	N/A	N/A	1	0	-1

Namelist FPOD (third engine)

Variable	720	727	737	747	880	dc8	md11	md83	l-1011
DIAM	N/A	3.542	N/A	N/A	N/A	N/A	N/A	N/A	N/A
LENGTH	N/A	10	N/A	N/A	N/A	N/A	N/A	N/A	N/A
SOD	N/A	0.2	N/A	N/A	N/A	N/A	N/A	N/A	N/A
THETA	N/A	14.8	N/A	N/A	N/A	N/A	N/A	N/A	N/A
X	N/A	0.699	N/A	N/A	N/A	N/A	N/A	N/A	N/A
SYMCO	N/A	0	N/A	N/A	N/A	N/A	N/A	N/A	N/A

2. Trajectory module

Namelist TRDATA

Variable	720	727	737	747	880	dc8	md11	md83	l-1011
CLBR1	. 1.1	1.1	1.1	1.1	1.1	1.1	1.1	1.1	1.1
ICYL	1	1	1	1	1	1	1	1	1

3. Weights module

Namelist OPTS

Variable	720	727	737	747	880	dc8	md11	md83	l-1011
WGTO	202000	160000	100800	713000	185000	335000	602500	140000	409000
WE	18202	12759	8165	44290	15158.2	27058	40955	10340	34797

PDCYL INPUT PARAMETERS

Wing

Geometric Parameters

Variable	720	727	737	747	880	dc8	md11	md83	l-1011
ISTAMA	2	2	2	2	2	2	2	2	2
CS1	0.1	0.2125	0.0724	0.088	0.1	0.0818	0.168	0.181	0.093
CS2	0.27	0.25	0.238	0.277	0.264	0.136	0.2835	0.271	0.296

Structural Concept

Variable	720	727	737	747	880	dc8	md11	md83	l-1011
CLAQR	0.001	0.001	0.001	0.001	0.001	0.001	0.001	0.001	0.001
IFUEL	2	2	2	2	2	2	2	2	2
CWMAN	1	1	1	1	1	1	1	1	1
CF	6.25E-05	6.25E-05	6.25E-05	6.25E-05	6.25E-05	6.25E-05	6.25E-05	6.25E-05	6.25E-05

Material Properties

Variable	720	727	737	747	880	dc8	md11	md83	l-1011
PS	1	1	1	1	1	1	1	1	1
TMGW	0.2	0.2	0.2	0.2	0.2	0.2	0.2	0.2	0.2
EFFW	0.656	0.656	0.656	0.656	0.656	0.656	0.656	0.656	0.656
EFFC	1.03	1.03	1.03	1.03	1.03	1.03	1.03	1.03	1.03
ESW	1.08E+07	1.08E+07	1.08E+07	1.07E+07	1.07E+07	1.08E+07	1.07E+07	1.07E+07	1.06E+07
FCSW	63500	56000	56000	54000	54000	56000	56000	56000	67000
DSW	0.101	0.101	0.101	0.101	0.101	0.101	0.101	0.101	0.101
KDEW	1	1	1	1	1	1	1	1	1
KDFW	1	1	1	1	1	1	1	1	1

Fuselage

Geometric Parameters

Variable	720	727	737	747	880	dc8	md11	md83	l-1011
CLBR1	1.1	1.1	1.1	1.1	1.1	1.1	1.1	1.1	1.1
ICYL	1	1	1	1	1	1	1	1	1

Structural Concept

Variable	720	727	737	747	880	dc8	md11	md83	l-1011
CKF	5.24	5.24	5.24	5.24	5.24	5.24	5.24	5.24	5.24
EC	2.36	2.36	2.36	2.36	2.36	2.36	2.36	2.36	2.36
KGC	0.368	0.368	0.368	0.368	0.368	0.368	0.368	0.368	0.368
KGW	0.505	0.505	0.505	0.505	0.505	0.505	0.505	0.505	0.505

Material Properties

Variable	720	727	737	747	880	dc8	md11	md83	l-1011
FTS(T/B)	58500	58500	58500	58500	58500	64000	58500	58500	58500
FCS(T/B)	54000	54000	54000	54000	54000	39000	54000	54000	54000
ES(T/B)	1.07E+07	1.07E+07	1.07E+07	1.07E+07	1.07E+07	1.07E+07	1.07E+07	1.07E+07	1.07E+07
EF(T/B)	1.07E+07	1.07E+07	1.07E+07	1.07E+07	1.07E+07	1.07E+07	1.07E+07	1.07E+07	1.07E+07
DS(T/B)	0.101	0.101	0.101	0.101	0.101	0.101	0.101	0.101	0.101
DF(T/B)	0.101	0.101	0.101	0.101	0.101	0.101	0.101	0.101	0.101
TMG(T/B	0.04	0.04	0.036	0.071	0.067	0.05	0.055	0.055	0.075
KDE	1	1	1	1	1	1	1	1	1
KDF	1	1	1	1	1	1	1	1	1

Loads

Variable	720	727	737	747	880	dc8	md11	md83	l-1011
AXAC	0	0	0	0	0	0	0	0	0
CMAN	1	1	1	1	1	1	1	1	1
ILOAD	3	3	3	3	3	3	3	3	3
PG(T/B)	12.9	12.9	11.25	13.65	12.9	13.155	11.5	12.5	12.6
WFBUM	0.001	0.001	0.001	0.001	0.001	0.001	0.001	0.001	0.001
WFLAN	0.9	0.9	0.9	0.9	0.9	0.9	0.9	0.9	0.9

Landing Gear

Variable	720	727	737	747	880	dc8	md11	md83	l-1011
VSINK	10	10	10	10	10	10	10	10	10
STROKE	1.67	1.167	1.167	2.21	1.33	1.375	1.9	1.67	2.17
CLRG1	0.133	0.1306	0.145	0.1131	0.095	0.108	0.141	0.055	0.161
CLRG2	0.51	0.5896	0.5254	0.466	0.437	0.499	0.57	0.597	0.56
WFGR1	0.00389	0.00725	0.0052	0.0047	0.0057	0.0311	0.0031	0.004	0.005
WFGR2	0.036	0.0738	0.0382	0.0398	0.0322	0.0742	0.0058	0.035	0.044
IGEAR	2	2	2	2	2	2	2	2	2
GFRL	0.001	0.001	0.001	0.001	0.001	0.001	0.001	0.001	0.001
CLRGW1	0.1675	0.1736	0.1846	0.064	0.1574	0.14	0.2	0.148	0.232
CLRGW2	0	0	0	0.1844	0	0	0	0	0

Tails

Variable	720	727	737	747	880	dc8	md11	md83	l-1011
ITAIL	1	1	1	1	1	1	1	1	1

Weights

Variable	720	727	737	747	880	dc8	md11	md83	l-1011
WTFF	0.3263	0.2625	0.156	0.262	0.366	0.418	0.336	0.2795	0.246
CBUM	1	1	1	1	1	1	1	1	1
0.813	0.813	0.859	0.972	0.791	0.716	0.7164	0.7137	0.9143	0.851

Factors

Variable	720	727	737	747	880	dc8	md11	md83	l-1011
ISCHRE	1	1	1	1	1	1	1	1	1
ICOMND	1	1	1	1	1	1	1	1	1
WGNO	1	1	1	1	1	1	1	1	1
SLFMB	1.2	1.2	1.2	1.2	1.2	1.2	1.2	1.2	1.2
WMIS	0	0	0	0	0	0	0	0	0
WSUR	0	0	0	0	0	0	0	0	0
WCW	1	1	1	1	1	1	1	1	1
WCA	0	0	0	0	0	0	0	0	0
NWING	40	40	40	40	40	40	40	40	40

```
$PDCYLIN

      PS=1.,          TMGW=.02,       EFFW=.656,
      EFFC=1.03,      ESW=10.7E06,    FCSW=54000.,    DSW=0.101,
      KDEW=1.0,       KDFW=1.0,

      ISTAMA=2,       CS1=0.088,      CS2=0.277,

      CLAQR=.001,     IFUEL=2,        CWMAN=1.0,      CF=6.25E-05,

      CKF=5.24,       EC=2.36,        KGC=.368,       KGW=.505,

      FTST = 4*58500.,8*0.,           FTSB = 4*58500.,8*0.,
      FCST = 4*54000.,8*0.,           FCSB = 4*54000.,8*0.,
      EST = 4*10.70E06,8*0.,          ESB = 4*10.70E06,8*0.,
      EFT = 4*10.70E06,8*0.,          EFB = 4*10.70E06,8*0.,
      DST = 4*.101,8*0.,              DSB = 4*.101,8*0.,
      DFT = 4*.101,8*0.,              DFB = 4*.101,8*0.,
      TMGT = 4*.071,8*0.,             TMGB = 4*.071,8*0.,
      KDE = 0.9,                      KDF = 0.9,

      CLBR1=1.1,      ICYL = 1,

      KCONT = 12*4,   KCONB = 12*4,

      AXAC=0.,        CBUM=1.0,       CLAN=0.791,
      CMAN=1.0,       ILOAD=3,        PGB = 12*13.65, PGT = 12*13.65,
      WFBUMP=0.001,   WFLAND=0.9,

      WTFF=0.262,

      VSINK=10.0,     STROKE=2.21,    CLRG1=.1131,    CLRG2=0.466,
      WFGR1=0.0047,   WFGR2=0.0398,   IGEAR=2,        GFRL=0.001,
      CLRGW1=0.064,   CLRGW2 =0.1844,

      ITAIL=1,

      ISCHRENK=1,     ICOMND=1,       WGNO=1.00,      SLFMB=1.2,
      WMIS=0.,        WSUR=0.,        WCW=1.0,        WCA=0.0,
      NWING=40,

$END
```

Figure 16. PDCYLIN Namelist for 747-21P.

FT	FT	FT	FT				DEG.	DEG.	DEG.	FT3	LBS	LB/FT3
195.1006	114.493	41.4649	11.0904	0.247	0.179	0.078	42.98067	30.30835	40.200	28673.285	186806.00	8.504

WING STATION FT	CHORD FT	LENGTH FT	LENGTH PRIME FT	BEND MOM FT-LBS	WEB SPACE IN	COVER THICK IN	WEB THICK IN	CGAGE THICK IN	WGAGE THICK IN	UNITWT COVERS LB/FT2	UNITWT WEBS LB/FT2	NJW
114.493	11.0904	5.4566	5.4566	4288.	0.4491	0.0543	0.03960	0.0200	0.02000	0.7904	0.5760	3
111.631	11.8497	5.8733	5.8733	27040.	0.7538	0.0543	0.03960	0.0200	0.02000	0.7904	0.5760	3
108.769	12.6091	6.2901	6.2901	77741.	1.0248	0.0543	0.03960	0.0200	0.02000	0.7904	0.5760	3
105.906	13.3684	6.7069	6.7069	161942.	1.2771	0.0543	0.03960	0.0200	0.02000	0.7904	0.5760	3
103.044	14.1278	7.1236	7.1236	283938.	1.5186	0.0543	0.03960	0.0200	0.02000	0.7904	0.5760	3
100.182	14.8872	7.5404	7.5404	447297.	1.7534	0.0678	0.03960	0.0250	0.02000	0.9863	0.5760	5
97.319	15.6465	7.9572	7.9572	655095.	1.9840	0.0871	0.03960	0.0321	0.02000	1.2670	0.5760	5
94.457	16.4059	8.3739	8.3739	910018.	2.2119	0.1068	0.03960	0.0393	0.02000	1.5528	0.5760	5
91.595	17.1653	8.7907	8.7907	1214473.	2.4381	0.1264	0.03960	0.0465	0.02000	1.8380	0.5760	5
88.732	17.9246	9.2075	9.2075	1570601.	2.6633	0.1457	0.03960	0.0536	0.02000	2.1186	0.5760	5
85.870	18.6840	9.6242	9.6242	1980293.	2.8879	0.1644	0.03960	0.0605	0.02000	2.3916	0.5760	5
83.008	19.4434	10.0410	10.0410	2445268.	3.1124	0.1825	0.03960	0.0672	0.02000	2.6549	0.5760	5
80.145	20.2027	10.4578	10.4578	2967051.	3.3370	0.1999	0.03960	0.0736	0.02000	2.9072	0.5760	5
77.283	20.9621	10.8745	10.8745	3546989.	3.5618	0.2164	0.03960	0.0796	0.02000	3.1476	0.5760	5
74.421	21.7215	11.2913	11.2913	4186258.	3.7870	0.2321	0.03960	0.0854	0.02000	3.3755	0.5760	5
71.558	22.4808	11.7081	11.7081	4885885.	4.0127	0.2469	0.03960	0.0909	0.02000	3.5909	0.5760	5
68.696	23.2402	12.1248	12.1248	5646725.	4.2390	0.2608	0.03960	0.0960	0.02000	3.7936	0.5760	5
65.834	23.9996	12.5416	12.5416	6469509.	4.4658	0.2739	0.03960	0.1008	0.02000	3.9838	0.5760	5
62.971	24.7589	12.9584	12.9584	7354798.	4.6933	0.2861	0.03960	0.1053	0.02000	4.1617	0.5760	5
60.109	25.5183	13.3751	13.3751	8303019.	4.9214	0.2976	0.03960	0.1095	0.02000	4.3277	0.5760	5
57.247	26.2776	13.7919	13.7919	9314444.	5.1502	0.3082	0.03960	0.1134	0.02000	4.4821	0.5760	5
54.384	27.0370	14.2087	14.2087	10389186.	5.3796	0.3180	0.03960	0.1170	0.02000	4.6252	0.5760	5
51.522	27.7964	14.6254	14.6254	11527247.	5.6095	0.3271	0.03960	0.1204	0.02000	4.7575	0.5760	5
48.660	28.5557	15.0422	15.0422	12728482.	5.8400	0.3355	0.03960	0.1235	0.02000	4.8794	0.5760	5
45.797	29.3151	15.4590	15.4590	13992557.	6.0711	0.3432	0.03960	0.1263	0.02000	4.9914	0.5760	5
42.935	30.0745	15.8757	15.8757	15312193.	6.3018	0.3501	0.03960	0.1288	0.02000	5.0915	0.5760	5
40.073	30.8338	16.2925	16.2925	16581607.	6.5214	0.3540	0.03960	0.1303	0.02000	5.1479	0.5760	5
37.210	31.5932	16.7093	16.7093	17912086.	6.7424	0.3576	0.03960	0.1316	0.02000	5.2003	0.5760	5
34.348	32.3526	17.1260	17.1260	19302712.	6.9648	0.3609	0.03960	0.1328	0.02000	5.2485	0.5760	5
31.486	33.1119	17.5428	17.5428	20752428.	7.1883	0.3639	0.03960	0.1339	0.02000	5.2922	0.5760	5
28.623	33.8713	17.9596	17.9596	22260018.	7.4128	0.3666	0.03960	0.1349	0.02000	5.3314	0.5760	5
25.761	34.6307	18.3763	18.3763	23824166.	7.6381	0.3690	0.03960	0.1358	0.02000	5.3661	0.5760	5
22.899	35.3900	18.7931	18.7931	25443306.	7.8641	0.3710	0.03960	0.1365	0.02000	5.3961	0.5760	5
20.036	36.1494	19.2099	19.1785	27115758.	8.0906	0.3728	0.03960	0.1372	0.02000	5.4215	0.5760	5
17.174	36.9088	19.6266	17.1275	28820156.	8.3160	0.3739	0.03960	0.1376	0.02000	5.4386	0.5760	5
14.312	37.6681	20.0434	15.0765	30458276.	8.5332	0.3734	0.03960	0.1374	0.02000	5.4309	0.5760	5
11.449	38.4275	20.4602	13.0255	32123610.	8.7496	0.3725	0.03960	0.1371	0.02000	5.4179	0.5760	5
8.587	39.1869	20.8769	10.9744	33807708.	8.9649	0.3712	0.03960	0.1366	0.02000	5.3989	0.5760	5
5.725	39.9462	21.2937	8.9234	35503096.	9.1785	0.3695	0.03960	0.1360	0.02000	5.3737	0.5760	5
2.862	40.7056	21.7105	6.8724	37203268.	9.3903	0.3673	0.03960	0.1352	0.02000	5.3423	0.5760	5
0.000	41.4649	22.1272	4.8214	38893232.	9.5995	0.3646	0.03960	0.1342	0.02000	5.3034	0.5760	5

CLBOX1 FT	CLINT FT	CLINTP FT	LBOX FT	WBOX FT	TBOX FT	NJW	WEBSB FT	TORK FT-LBS	TTO IN	TBCOV IN
60.024	69.128	95.458	26.3302	20.2000	7.439	5	0.7106	18823984.0	0.0742	0.1236

WSHEAR LBS	WBEND LBS	WWING LBS	WSHBOX LBS	WBDBOX LBS	WTOBOX LBS	WWBOX LBS	WWINGT LBS	WPOD LBS	DELTIP FT
875.18	18812.62	39375.59	274.65	7947.85	1471.41	9693.90	49069.49	11072.50	8.312

CONTROL AREA FT2.	STRUCTURE AREA FT2.	SPLAN FT2.
1535.09	3450.32	5469.

Figure 17. PDCYL Wing Weight Output for 747-21P.

FUSE STAT FT	BENDING MOMENT FT LBS	THIC IN	SHELL STRESS PSI	EQUIV THICK IN	GAGE THICK IN	FRAME SPACE IN	NJ	SECTION AREA SQ FT	SHELL UNITWT LB/FT2	FRAME UNITWT	MAX BENDING
3.7528	4516.695	0.0000	44.5238	0.1448	0.0710	23797.0703	3	58.3945	2.1055	0.0000	MAN
7.5056	29328.754	0.0000	178.2442	0.1448	0.0710	5944.2905	3	94.7155	2.1055	0.0000	MAN
11.2584	87603.664	0.0000	401.2114	0.1448	0.0710	2640.8411	3	125.6875	2.1055	0.0000	MAN
15.0111	190409.281	0.0000	713.4453	0.1448	0.0710	1485.0968	3	153.6281	2.1055	0.0001	MAN
18.7639	347701.844	0.0000	1114.9587	0.1448	0.0710	950.2913	3	179.5111	2.1055	0.0002	MAN
22.5167	568694.500	0.0000	1605.7603	0.1448	0.0710	659.8342	3	203.8644	2.1055	0.0005	MAN
26.2695	872144.000	0.0000	2211.4465	0.1448	0.0710	479.1142	3	227.0152	2.1055	0.0010	MAN
30.0223	1293259.875	0.0000	2987.5078	0.1448	0.0710	354.6553	3	249.1838	2.1055	0.0020	MAN
33.7751	1802858.500	0.0000	3836.1211	0.1448	0.0710	276.1997	3	270.5282	2.1055	0.0037	MAN
37.5278	2408529.000	0.0000	4761.6157	0.1448	0.0710	222.5160	3	291.1660	2.1055	0.0061	MAN
41.2806	3117610.000	0.0000	5766.8906	0.1448	0.0710	183.7273	3	311.1883	2.1055	0.0095	MAN
45.0334	3937044.500	0.0000	7075.2378	0.1448	0.0710	149.7526	3	320.3114	2.1055	0.0147	MAN
48.7862	4870150.000	0.0000	8752.1152	0.1448	0.0710	121.0605	3	320.3114	2.1055	0.0225	MAN
52.5390	5917042.000	0.0000	10633.4785	0.1448	0.0710	99.6415	3	320.3114	2.1055	0.0332	MAN
56.2918	7077723.000	0.0000	12719.3301	0.1448	0.0710	83.3012	3	320.3114	2.1055	0.0476	MAN
60.0445	8352191.000	0.0000	15009.6689	0.1448	0.0710	70.5902	3	320.3114	2.1055	0.0662	MAN
63.7973	9740450.000	0.0000	17504.5000	0.1448	0.0710	60.5293	3	320.3114	2.1055	0.0901	MAN
67.5501	11718714.000	0.0000	21059.6289	0.1448	0.0710	50.3112	3	320.3114	2.1055	0.1304	MAN
71.3029	15602571.000	0.0000	28039.2813	0.1448	0.0710	37.7875	3	320.3114	2.1055	0.2311	MAN
75.0557	20633438.000	0.0000	37080.2188	0.1448	0.0710	28.5741	3	320.3114	2.1055	0.4042	MAN
78.8085	25873488.000	0.0000	46497.0820	0.1448	0.0710	22.7871	3	320.3114	2.1055	0.6356	MAN
82.5612	30384872.000	0.0000	47662.5430	0.1659	0.0813	25.4677	6	320.3114	2.4122	0.5829	MAN
86.3140	33229772.000	0.0000	48052.2500	0.1799	0.0882	27.4022	6	320.3114	2.6166	0.5462	MAN
90.0668	33470324.000	0.0000	48082.4258	0.1811	0.0888	27.5660	6	320.3114	2.6339	0.5433	MAN
93.8196	30972306.000	0.0000	47748.3359	0.1688	0.0828	25.8668	6	320.3114	2.4544	0.5750	MAN
97.5724	28304028.000	0.0000	47332.9063	0.1556	0.0763	24.0551	6	320.3114	2.2626	0.6129	MAN
101.3252	25749524.000	0.0000	46274.3086	0.1448	0.0710	22.8968	3	320.3114	2.1055	0.6295	MAN
105.0780	23308814.000	0.0000	41888.1211	0.1448	0.0710	25.2944	3	320.3114	2.1055	0.5158	MAN
108.8307	20981884.000	0.0000	37706.4102	0.1448	0.0710	28.0996	3	320.3114	2.1055	0.4180	MAN
112.5835	18768758.000	0.0000	33729.2148	0.1448	0.0710	31.4130	3	320.3114	2.1055	0.3344	MAN
116.3363	16843416.000	0.0000	30269.1953	0.1448	0.0710	35.0038	3	320.3114	2.1055	0.2693	LAN
120.0891	15216945.000	0.0000	27346.2754	0.1448	0.0710	38.7451	3	320.3114	2.1055	0.2198	LAN
123.8419	13674075.000	0.0000	24573.5938	0.1448	0.0710	43.1168	3	320.3114	2.1055	0.1775	LAN
127.5947	12214827.000	0.0000	21951.1875	0.1448	0.0710	48.2678	3	320.3114	2.1055	0.1417	LAN
131.3474	10839192.000	0.0000	19479.0430	0.1448	0.0710	54.3936	3	320.3114	2.1055	0.1115	LAN
135.1002	9547162.000	0.0000	17157.1445	0.1448	0.0710	61.7548	3	320.3114	2.1055	0.0865	LAN
138.8530	8338768.500	0.0000	14985.5488	0.1448	0.0710	70.7038	3	320.3114	2.1055	0.0660	LAN
142.6058	7213962.000	0.0000	12964.1660	0.1448	0.0710	81.7280	3	320.3114	2.1055	0.0494	LAN
146.3586	6172785.000	0.0000	11093.0723	0.1448	0.0710	95.5133	3	320.3114	2.1055	0.0362	LAN
150.1113	5215206.000	0.0000	9372.2129	0.1448	0.0710	113.0507	3	320.3114	2.1055	0.0258	LAN
153.8641	4341246.000	0.0000	7801.6255	0.1448	0.0710	135.8096	3	320.3114	2.1055	0.0179	LAN
157.6169	3550887.000	0.0000	6381.2769	0.1448	0.0710	166.0382	3	320.3114	2.1055	0.0120	LAN
161.3697	2837451.000	0.0000	5246.6328	0.1448	0.0710	201.9458	3	311.3084	2.1055	0.0079	LAN
165.1224	2213004.000	0.0000	4268.8013	0.1448	0.0710	248.2045	3	298.4142	2.1055	0.0050	LAN
168.8752	1666440.000	0.0000	3362.5671	0.1448	0.0710	315.0972	3	285.2738	2.1055	0.0030	LAN
172.6280	1307928.000	0.0000	2769.3157	0.1448	0.0710	382.5983	3	271.8658	2.1055	0.0019	BUM
176.3808	1530244.500	0.0000	3411.9824	0.1448	0.0710	310.5337	3	258.1649	2.1055	0.0028	MAN
180.1335	1753683.000	0.0000	4134.7847	0.1448	0.0710	256.2493	3	244.1414	2.1055	0.0038	MAN
183.8863	1890422.250	0.0000	4736.1792	0.1448	0.0710	223.7110	3	229.7597	2.1055	0.0047	MAN
187.6391	1945607.250	0.0000	5209.6304	0.1448	0.0710	203.3802	3	214.9767	2.1055	0.0054	MAN
191.3919	1924485.000	0.0000	5546.1831	0.1448	0.0710	191.0387	3	199.7393	2.1055	0.0056	MAN
195.1447	1832528.250	0.0000	5733.5396	0.1448	0.0710	184.7960	3	183.9802	2.1055	0.0056	MAN
198.8974	1675338.750	0.0000	5753.5972	0.1448	0.0710	184.1518	3	167.6125	2.1055	0.0051	MAN
202.6502	1458795.000	0.0000	5578.8437	0.1448	0.0710	189.9203	3	150.5197	2.1055	0.0043	MAN
206.4030	1188949.500	0.0000	5163.7246	0.1448	0.0710	205.1882	3	132.5389	2.1055	0.0032	MAN
210.1558	872269.500	0.0000	4426.6021	0.1448	0.0710	239.3564	3	113.4288	2.1055	0.0020	MAN
213.9085	515652.000	0.0000	3198.5554	0.1448	0.0710	331.2544	3	92.7996	2.1055	0.0009	MAN
217.6613	126475.500	0.0000	1041.0522	0.1448	0.0710	1017.7543	3	69.9322	2.1055	0.0001	MAN
221.4141	46821.000	0.0000	625.1013	0.1448	0.0710	1694.9822	3	43.1155	2.1055	0.0000	MAN
221.4141	45793.500	0.0000	611.3832	0.1448	0.0710	1694.9822	3	43.1155	2.1055	0.0000	NONE

1 STRUCTURAL WEIGHT SUMMARY

	(LBS)	FRACTION	WEIGHT (LBS/FT*FT)
SHELL	26671.41	0.0374	2.1409
FRAMES	1837.49	918.7455	0.1475
NONOP	0.00	0.0000	0.0000
SEC	0.00	0.0000	0.0000
TOTAL	28508.89	0.0400	2.2884
VOLPEN	0.00	0.0000	0.0000
GRANTOT	28508.89	0.0400	2.2884

Surface Area, SQF	12457.98
Volume Ratio	1.00000000
BODY WEIGHT	28508.89453125

Figure 18. PDCYL Fuselage Weight Output for 747-21P.

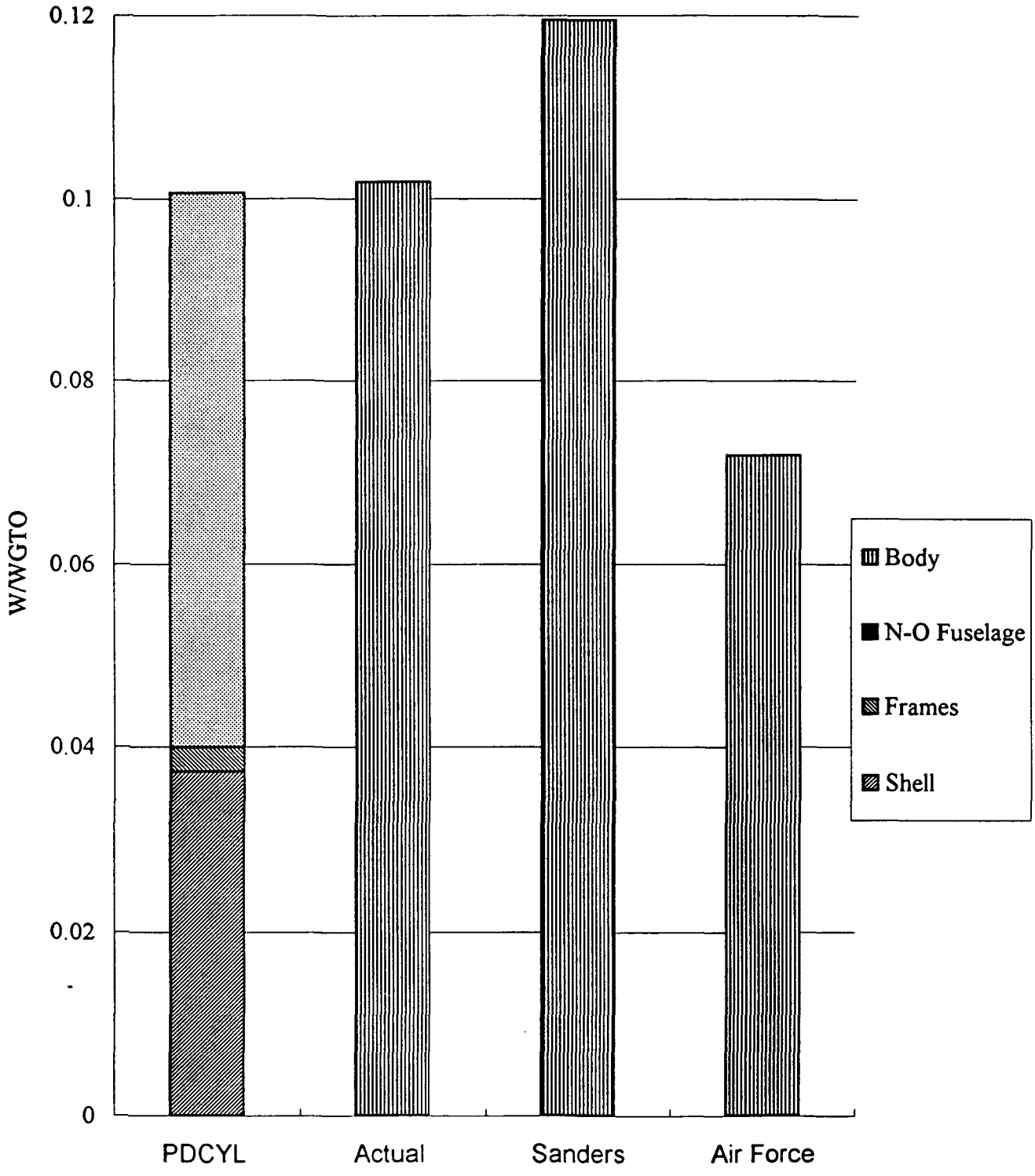

Figure 19a. Fuselage Weight Estimation Comparison for 747-21P.

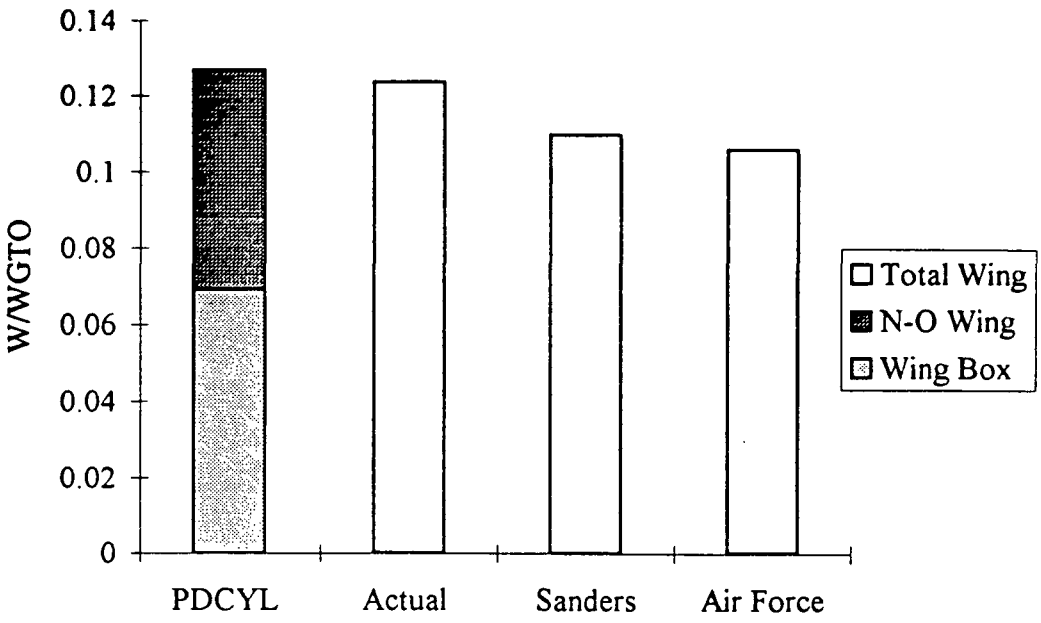

Figure 19b. Wing Weight Estimation Comparison for 747-21P.

APPENDIX B: High-Altitude Study

Description

A study was made to estimate the wing weight of a scaled version of an existing propeller-driven high-altitude drone aircraft. This aircraft, termed the Strato7, is modeled as an enlarged version of the existing Perseus-a3. PDCYL was used to validate the wing weight estimation returned by ACSYNT.

The wing of the Strato7 incorporates a single hollow, cylindrical carbon-fiber/epoxy spar placed at the leading edge. The strength of the cover is assumed negligible. No fuel is carried in the wing, while propulsion and landing gear are mounted on the fuselage. The layout of the Strato7 is shown in Figure 20.

Input

Fuselage weight estimation is not considered for the Strato7. An example of the ACSYNT input for the Strato7 wing weight estimation is shown in Figure 21. The corresponding PDCYLIN namelist for the case where the ratio of structural chord to total chord is 0.2 is shown in Figure 22.

Output

Wing weight as a function of the ratio of structural chord to total chord is shown in Figure 23. The wing weight estimated by ACSYNT is 789 pounds. PDCYL matches this wing weight when the ratio of structural chord to total chord is approximately 0.25. Non-optimum weight was not considered in this analysis. In order to estimate non-optimum weight, non-optimum factors would need to be recomputed for this type of aircraft.

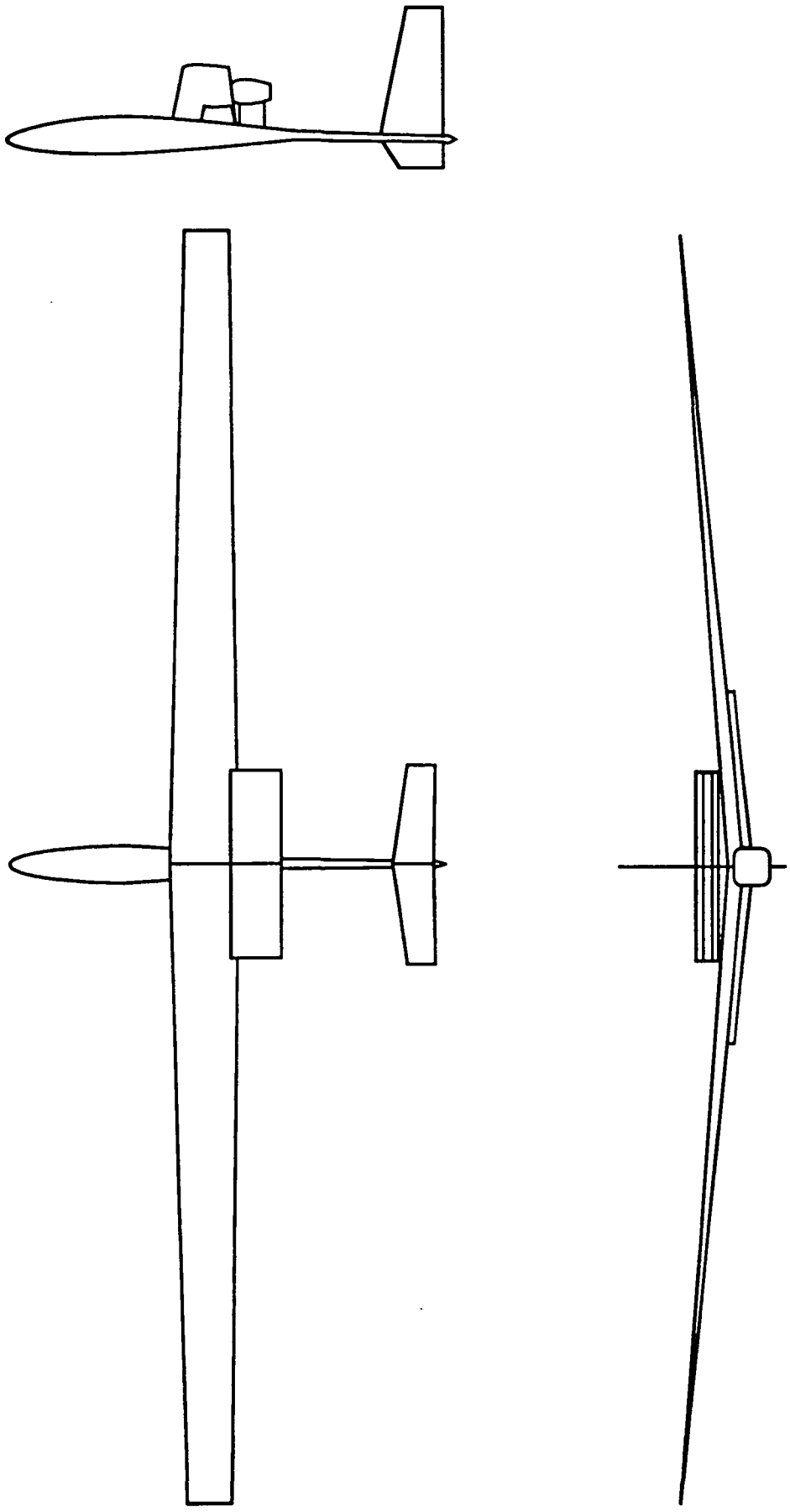

Figure 20. Strato7 Configuration.

```
RANSPORT
   4     2     2  570  570     0     0     0     2     1     7     0
 0.00010     0.6     10000.0
   1     2     3     6
   1     6
   1     6
** GEOMETRY ***
$FUS     BDMAX  = 3.00,       BODL   = 24.358,     FRAB   = 2.01
         FRN    = 2.15,       SFFACT = 1.082664,   ITAIL  = 1,
         OUTCOD = 3,          $END
$WING    AR     = 23.328,     AREA   = 500.00,     DIHED  = 5.0,
         FDENWG = 0.0,        LFLAPC = 0.00,       SWEEP  = 0.00,
         SWFACT = 1.0,        TAPER  = 0.695,      TCROOT = 0.14,
         TCTIP  = 0.14,       TFLAPC = 0.0,        WFFRAC = 0.0,
         XWING  = 0.5664,     ZROOT  = 1.00,       KSWEEP = 2,
         $END
$HTAIL   AR     = 5.96,       AREA   = 23.09,      SWEEP  = 5.00,
         SWFACT = 1.0,        TAPER  = 0.682,      TCROOT = 0.08,
         TCTIP  = 0.08,       XHTAIL = 1.25,       ZROOT  = 1.25,
         KSWEEP = 0,          SIZIT  = T,          HTFRAC = -0.20,
         CVHT   = -2.70560,   $END
$VTAIL   AR     = 3.08,       AREA   = 17.69,      SWEEP  = 5.00,
         SWFACT = 1.00,       TAPER  = 0.554,      TCROOT = 0.08,
         TCTIP  = 0.08,       VTNO   = 1.0,        XVTAIL = 1.39,
         YROOT  = 0.00,       ZROOT  = 1.0,        KSWEEP = 0,
         SIZIT  = T,          VTFRAC = -0.20,      CVVT   = -0.59909,
         CGM    = 0.40,       $END
$CREW    NCREW  = 0,          $END
$FUEL    DEN    = 63.78,      FRAC   = 1.00,       $END
$FPOD
  DIAM      =     2.,  LENGTH    =    2.,       X       =     0.592
  THETA     =     90.0,  SYMCOD    =     1,          SOD     =     -2,
 $END
ENGINE N      = 1,          $END
$$$$$$$$$$$$$$$$$$$$$$$$$$$$$$$$$$$$$$$$$$$$$$$$$$$$$$$$$$$$$$$$$$$$$$$$$$$$$$
$TRDATA  CRMACH = .40,     QMAX   = 70.45,  DESLF  = 2.5,     ULTLF  = 3.75,
         WFUEL  = 392.0,   WFEXT  = 0.0,    WFTRAP = 0.1,     FRFURE = 0.0,
         IPSTO1 = 5,       TIMTO1 = 0.0,    IPSTO2 = 2,       TIMTO2 = 1.0,
         IPSLND = 5,       MODLND = 7,      VMRGLD = 1.2,     WKLAND = 0.1,
         IBREG  = 0,       IENDUR = 0,      WCOMBP = 0.6,     MMPROP = 7,
         NCODE  = 0,       NCRUSE = 1,      RANGE  = 100.0,   LENVEL =.FALSE.,
         NLEGCL = 30,      NLEGLO = 4,      $END
        2
      MACH NO.    ALTITUDE      HORIZONTAL     NO.  VIND
HASE   START END  START  END     DIST  TIME    TURN  *G*S  WKFUEL M IP IX W B A P
------ ---- ---- ------ ------  ------ -----   ---- -----  ------ - -- -- - - - -
LIMB   .414   -1    100     -1     0.0   0.0    0.0    -1  1.0000 7 41  0 0 0 0 0
DITER  .400   -1  90000     -1     0.0  10.0    0.0   0.0  1.0000 7 21  0 0 0 0 0

**** AERODYNAMICS *****
$ACHAR   ABOSB=0.074, ALMAX=20.0, AMC=12.0, ALELJ=3, ISMNDR=0, SFWF=0.99,
         SMNSWP = 0.01, 0.10, 0.15, 0.20, 0.25, 0.30, 0.35, 0.40, 0.45, 0.51,
         CLOW   = 0.3821,0.3828,0.4266,0.4809,0.4849,0.4888,0.4946,0.5147,0.5502,0.5692
         CMO    = -.1591,-.1596,-.1531,-.1466,-.1502,-.1538,-.1581,-.1653,-.1749,-.1823
         $END
$AMULT   FCDW=1.1, $END
$ATRIM   FVCAM  = 0.9183,0.9244,0.9538,0.9196,0.9230,0.9276,0.9349,0.9345,0.9264,0.9247
         FLDM   = 1.0211,1.0254,1.0200,1.0139,1.0200,1.0232,1.0234,1.0205,1.0226,0.8790
         FLAPI  =  0.0,  0.0,  0.0,  0.0,  0.0,  0.0,  0.0,  0.0,  0.0,  0.0,
         ITRIM  =    1,    1,    1,    1,    1,    1,    1,    1,    1,    1,
         CGM=0.40, CFLAP=0.0, SPANF=0.0, IVCAM=1, ALFVC=5.0, $END
$ADET    ICOD=1, IPLOT=1, NALF=10, NMDTL=10,
         ALIN=    -6.8, 0.0,  1.0,  2.0,  4.0,  6.0,  8.0, 10.0, 12.0, 14.0,
         ALTV   = 22740.,37475.,50131.,61224.,71097.,79992.,86129.,90000.,
         SMN    =  0.085, 0.119, 0.161, 0.210, 0.266, 0.328, 0.379, 0.400,
         ISTRS=     0,    0,    0,    0,    0,    0,    0,    0,    0,    0,
```

```
        ITB=        0,     0,     0,     0,     0,     0,     0,     0,     0,     0,
        ITS=        0,     0,     0,     0,     0,     0,     0,     0,     0,     0,
        $END
$ADRAG  CDBMB=10*0.0,
        CDEXTR=10*0.0,
        CDTNK=10*0.00,
        $END
$ATAKE  DELFLD=0.0, DELFTO=0.0, DELLED=0.0, DELLTO=0.0, ALFROT=8.0, $END
$APRINT KERROR=2,    $END
park Ignition Internal Combustion Engine with Triple Turbocharging
$PCONTR HNOUT  =      0.,31001.,50131.,79992.,90000.,
        SMNOUT =     0.0, 0.085, 0.161, 0.328, 0.400,
        NOUTPT = 5,          $END
$PENGIN ENGNUM = 1,          NTPENG = 4,          ESZMCH = 0.00,
        ESZALT = 0.,         XNMAX  = 7200.0,     HPENG  = 115.0,
        SWTENG = 6.0,        HCRIT  = 90000.,     FSFC   = 1.0,
        $END
$PROP   AF     = 125.0,      BL     = 2,          CLI    = 0.5,
        DPROP  = 17.88,      FPRW   = 0.087437,   FTHR   = 1.0,
        NTPPRP = 12,         PSZMCH = 0.00,       PSZALT = 0.,
        $END
$PGEAR  GR     = 7.43,       ETR    = .95,        FGRW   = 0.2476234,
        GRSND  = 14.86,      $END
$PENGNC XLENG  = 1.5,        RLENG  = 1.0,        DIA1   = 1.0,
        FT     = 0.0,        FRPN   = 1.0,        FRBT   = 2.0,
        NBDFT  = 0.3,        ANACHP = 0.,         DQ     = 0.024,
        $END
RANSPORT
** WEIGHTS ***
$OPTS   WGTO = 3000.0, KERROR = 2,
        SLOPE(1)  = 0.47970,   TECHI(1)  =    0.85,
        SLOPE(2)  = 0.97945,   TECHI(2)  =    0.85,
        SLOPE(3)  = 0.64225,   TECHI(3)  =    0.85,
        SLOPE(4)  = 0.85841,   TECHI(4)  =    0.85,
        SLOPE(6)  = 0.70145,   TECHI(6)  =    0.85,
        SLOPE(7)  = 0.85396,
        SLOPE(8)  = 0.55290,   TECHI(8)  =    0.85,
        SLOPE(9)  = 1.89582,   TECHI(9)  =    0.85,
        SLOPE(10) = 1.49618,
        SLOPE(11) = 0.19543,
        SLOPE(12) = 0.48091,
        SLOPE(13) = 3.68569,
        SLOPE(16) = 0.02254,
        SLOPE(17) = 1.0,
        KWING     =   6,
        KBODY     =   3,
        $END
$FIXW   WE        = 757.5,
        WFEQ      =  0.,
        WFS       =  0.,
        WPL       =  0.,
$END
```

Figure 21. ACSYNT Input for Strato7.

```
$PDCYLIN

      PS=1.,          TMGW=.05,       EFFW=.605,
      EFFC=1.108,     ESW=12.9E06,    FCSW=75000.,     DSW=0.058,
      KDEW=1.0,       KDFW=1.0,
      ISTAMA=2,       CS1=0.01,       CS2=0.75,

      CLAQR=.001,     IFUEL=1,        CWMAN=1.0,       CF=6.25E-05,

      CKF=5.24,       EC=2.00,        KGC=.368,        KGW=.505,

      FTST = 4*58500.,8*0.,           FTSB = 4*58500.,8*0.,
      FCST = 4*54000.,8*0.,           FCSB = 4*54000.,8*0.,
      EST = 4*10.70E06,8*0.,          ESB = 4*10.70E06,8*0.,
      EFT = 4*30.0E06,8*0.,           EFB = 4*30.0E06,8*0.,
      DST = 4*.101,8*0.,              DSB = 4*.101,8*0.,
      DFT = 4*.292,8*0.,              DFB = 4*.292,8*0.,
      TMGT = 4*.03,8*0.,              TMGB = 4*.03,8*0.,
      KDE=0.9,                        KDF=0.8,
      CLBR1=1.1,      ICYL = 1,

      KCONT = 12*4,   KCONB = 12*4,

      AXAC=0.,        CBUM=1.0,       CLAN=0.93,
      CMAN=1.0,       ILOAD=3,        PGB = 12*11.5,   PGT = 12*11.5,
      WFBUMP=0.001,   WFLAND=0.9,

      WTFF=0.07,

      VSINK=10.0,     STROKE=1.0,     CLRG1=.395,      CLRG2=0.5,
      WFGR1=0.0031,   WFGR2=0.0058,   IGEAR=1,         GFRL=0.001,
      CLRGW1=0.20,    CLRGW2 = 0.0,

      ITAIL=1,

      ISCHRENK=1,     ICOMND=1,       WGNO=1.00,       SLFMB=1.2,
      WMIS=0.,        WSUR=0.,        WCW=1.0,         WCA=0.0,
      NWING=40,

$END
```

Figure 22. PDCYLIN Namelist Input for Strato7.

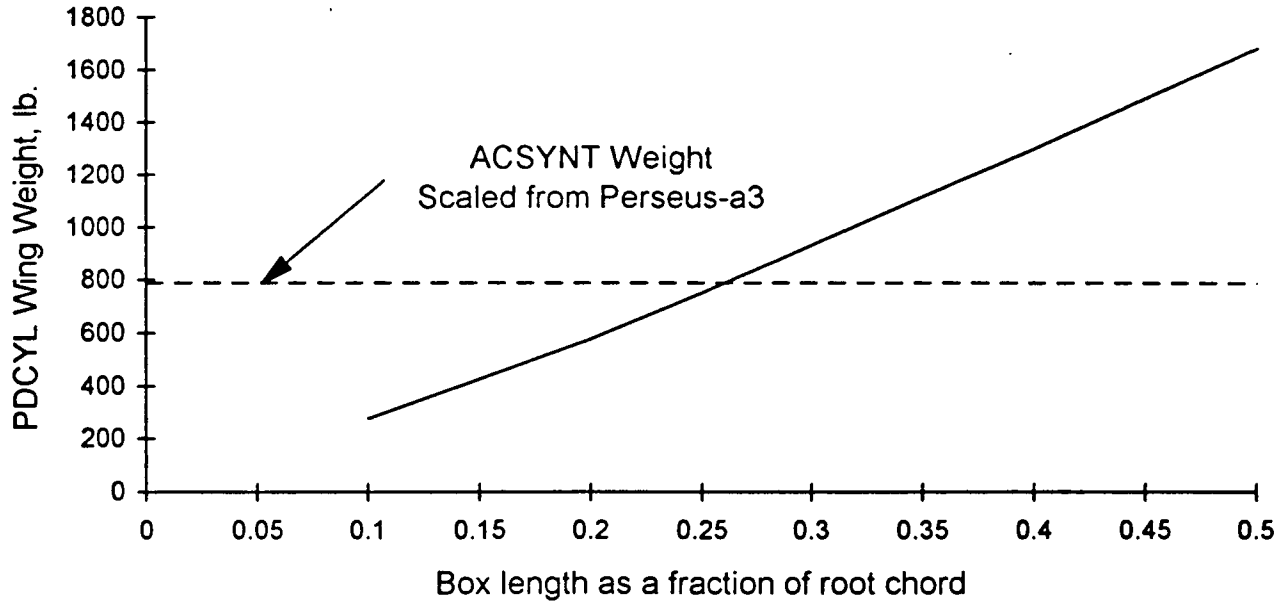

Figure 23. Strato7 Wing Weight as a Function of Structural Box Length.